RESEARCH REPORT NUMBER OU-AMNE-78-12

EXPERIMENTAL INVESTIGATION OF SOLAR HEATING OF BRIDGE DECKS

BY J. E. FRANCIS, T. J. LOVE, F. O. CALVERT, L. P. YAO, & A. H. ZARGAR

UNIVERSITY OF OKLAHOMA

AEROSPACE, MECHANICAL & NUCLEAR ENGINEERING

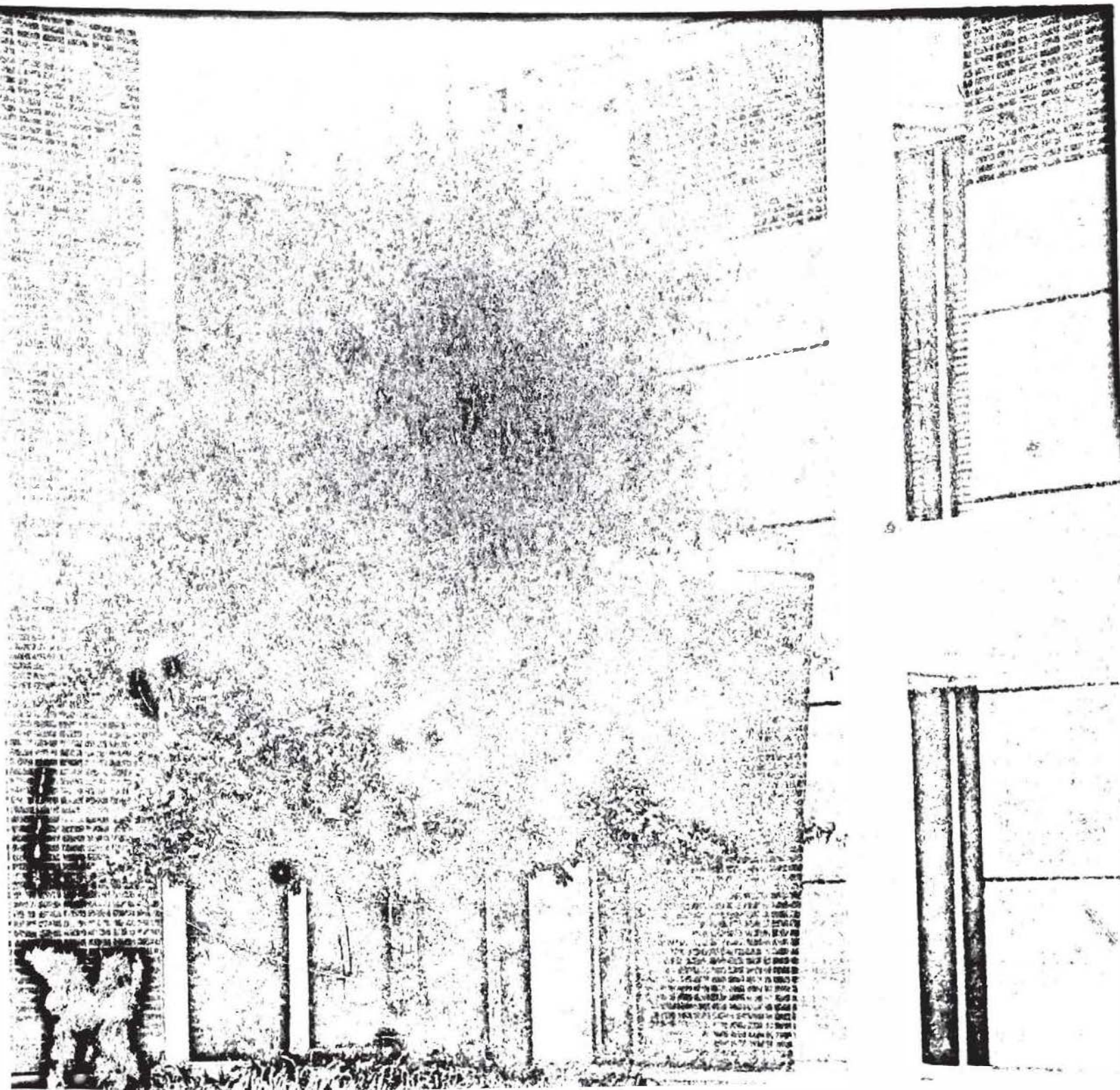

Final Report
ODOT Study 77-08-2
ORA 158-631

EXPERIMENTAL INVESTIGATION OF SOLAR HEATING OF BRIDGE DECKS

Prepared By

J. E. Francis, Professor AMNE

T. J. Love, George Lynn Cross Research Professor and Halliburton Professor AMNE

F. O. Calvert, Professor Environmental Design

L. P. Yao, Research Assistant AMNE

A. H. Zargar, Research Assistant AMNE

Submitted To

The Oklahoma Department of Transportation

From The

Office of Research Administration
University of Oklahoma
Norman, Oklahoma

December 1978

TECHNICAL REPORT STANDARD TITLE PAGE

1. Report No.	2. Government Accession No.	3. Recipient's Catalog No.
ODOT 77-08-2		

4. Title and Subtitle
Experimental Investigation of Solar Heating of Bridge Decks

5. Report Date
October 1978

6. Performing Organization Code
ORA-158-631

7. Author(s)
J. E. Francis, T. J. Love, F. O. Calvert, L. P. Yao and A. H. Zargar

8. Performing Organization Report No.

9. Performing Organization Name and Address
University of Oklahoma
865 Asp
Norman, OK 73019

10. Work Unit No.

11. Contract or Grant No.
77-08-2

12. Sponsoring Agency Name and Address
The Department of Transportation
Research Division
200 N.E. 21
Oklahoma City, OK 73105

13. Type of Report and Period Covered
Type A
4/1/77 to 6/30/79

14. Sponsoring Agency Code

15. Supplementary Notes
Performed in cooperation with the Federal Highway Administration

16. Abstract

The addition of monomers or the inclusion of wax within highway bridge decks are two methods being used to prevent salt penetration during winter deicing. Both of these methods require the addition of heat until the upper two inches of bridge deck reaches from 160-190 F. This study investigated the potential for using solar energy as a means of providing the required heat. The bridge was modeled analytically and the time varying temperature distribution was determined for both a flat plate type cover collector and focusing tracking solar collection schemes. The models indicated the flat plate approach for typical summer conditions in Oklahoma was at best marginal but that the focusing collector scheme did show promise for providing the required heat. Both models suffered from lack of accurate thermal properties data for the concrete. Experimental studies were conducted on a simulated bridge deck using flat plate covers and Northrup focusing Fresnel Lens collectors. Neither scheme was able to provide the desired temperatures. A major difficulty encountered was the design of an appropriate heat exchanger to transfer the collected energy from the heat transfer fluid to the bridge deck. Several different designs were tested, but none of the methods used would provide the desired bridge deck temperatures for the collector area used. The collectors did not perform up to their expectations.

17. Key Words	18. Distribution Statement
Solar, Bridge Deicing, Temperature Distribution	This document is available through the National Technical Information Service, Springfield, Virginia 22161

19. Security Classif. (of this report)	20. Security Classif. (of this page)	21. No. of Pages	22. Price
unclassified		110	

Form DOT F 1700.7 (8-69)

TABLE OF CONTENTS

LIST OF TABLES

LIST OF ILLUSTRATIONS

LIST OF SYMBOLS

A	Area
c_p	Specific heat at constant pressure
D	Tilt angle in degrees
d	Dust factor
F	Function
h	Heat transfer coefficient
hc	Convective heat transfer coefficient
h_{wind}	Convective heat transfer coefficient related to the wind effect on the flat plate
K	Length extincion coefficient
k	Thermal conductivity
L	Thickness of bridge deck, actual path of the radiation through medium
m	Mass
n	Index of refraction
N	Number of glass cover
$\dot{Q}$	Rate of heat flow
q"	Heat flux
R	Thermal contact resistance
s	Shade factor
T	Temperature
T_{amb}	Ambient air temperature

T_{avg}	Temperature of solar collector, fluid, heat exchanger and piping system
T_{sky}	Effective sky temperature
t	Time
U_t	Overall heat transfer coefficient
V	Wind velocity
x,y,z	Space coordinates in the rectangular coordinate system

GREEK

α	Absorptance
ε	Emittance
η	Efficiency
θ	Angle between surface normal and beam radiation
ρ	Reflectance
σ	Stefan-Boltzman Constant
τ	Transmittance
ω	Angular frequency

SUBSCRIPTS AND SUPERSCRIPTS

a	Absorption, ambient
b	Bottom
d	Diffuse
g	Glass
i	Nodal location
L	Loss
m	Mean
n	Time interval

o	Initial
P	Plate
r	Radiation, reflection
R	Released
s	Sky
t	Top
u	Useful

SOLAR HEATING OF HIGHWAY BRIDGE DECKS

CHAPTER I

INTRODUCTION

Currently the Oklahoma Department of Highways is investigating two methods of protecting bridge decks from prevention of salt penetration during winter deicing which may cause corrosion of bridge reinforcing steel and decrease the life span of the bridge. These two methods require the use of monomers which polymerize and seal the concrete or using wax to internally seal the bridge deck. Both of these methods require the application of heat to the bridge deck until the concrete is heated to temperatures from 160°F - 190°F at a depth of approximately two inches. Gas fired heaters and electrical heating blankets are means of achieving the desired temperatures, however, these are quite expensive and require a considerable expenditure of energy. The present study is designed to evaluate the use of solar energy for this application.

Compared with the other energy sources, like fossil fuels, nuclear energy etc., solar energy is one of the most dilute and intermittent forms and therefore requires different methods of collection. Modified flat plate type and concentrating type solar collectors are studied for the purpose of heating highway bridge decks. The study is divided into two phases as follows.

PHASE I - ANALYTICAL STUDY

A. FLAT PLATE

1. Blackened bridge surface without a glass cover.
2. Blackened bridge surface with a single glass cover.
3. Blackened bridge surface with, two glass covers.

B. CONCENTRATING COLLECTORS

Northrup collectors with tube-in-sheet type heat exchangers and an area ratio of 1, 1-1/2, 2, and 2-1/2.

PHASE II - EXPERIMENTAL STUDY

A. FLAT PLATE

Blackened bridge surface with a single glass cover.

B. CONCENTRATING COLLECTORS

Northrup collectors with tube-in-sheet type heat exchangers and an area ratio of 2.

This study was sponsored by The Oklahoma Department of Transportation. It is hoped that the study will be a contribution to the prevention of highway bridge deterioration caused by the salt penetration during winter deicing.

CHAPTER II

MATHEMATICAL MODEL

A representation of a lateral cross section of a bridge is shown in Fig. 2.1. In this diagram, the traffic flow is in the z direction, perpendicular to the page. The y direction is parallel to the surface of the bridge. Compared with the dimensions in z and y directions of the bridge, the x dimension of the bridge is very small. Therefore, the models used in this study were all one-dimensional transient models.

Governing Differential Equation

$$\frac{\partial^2 T}{\partial x^2} = \frac{1}{\alpha}\frac{\partial T}{\partial t} \tag{2.1}$$

where α = thermal diffusivity $= \frac{k}{\rho c_p}$

ρ = density

c_p = specific heat at constant pressure

k = thermal conductivity

T = temperature

t = time

Initial Condition

Since the governing equation is of the first order with respect to time, only one initial condition is required.

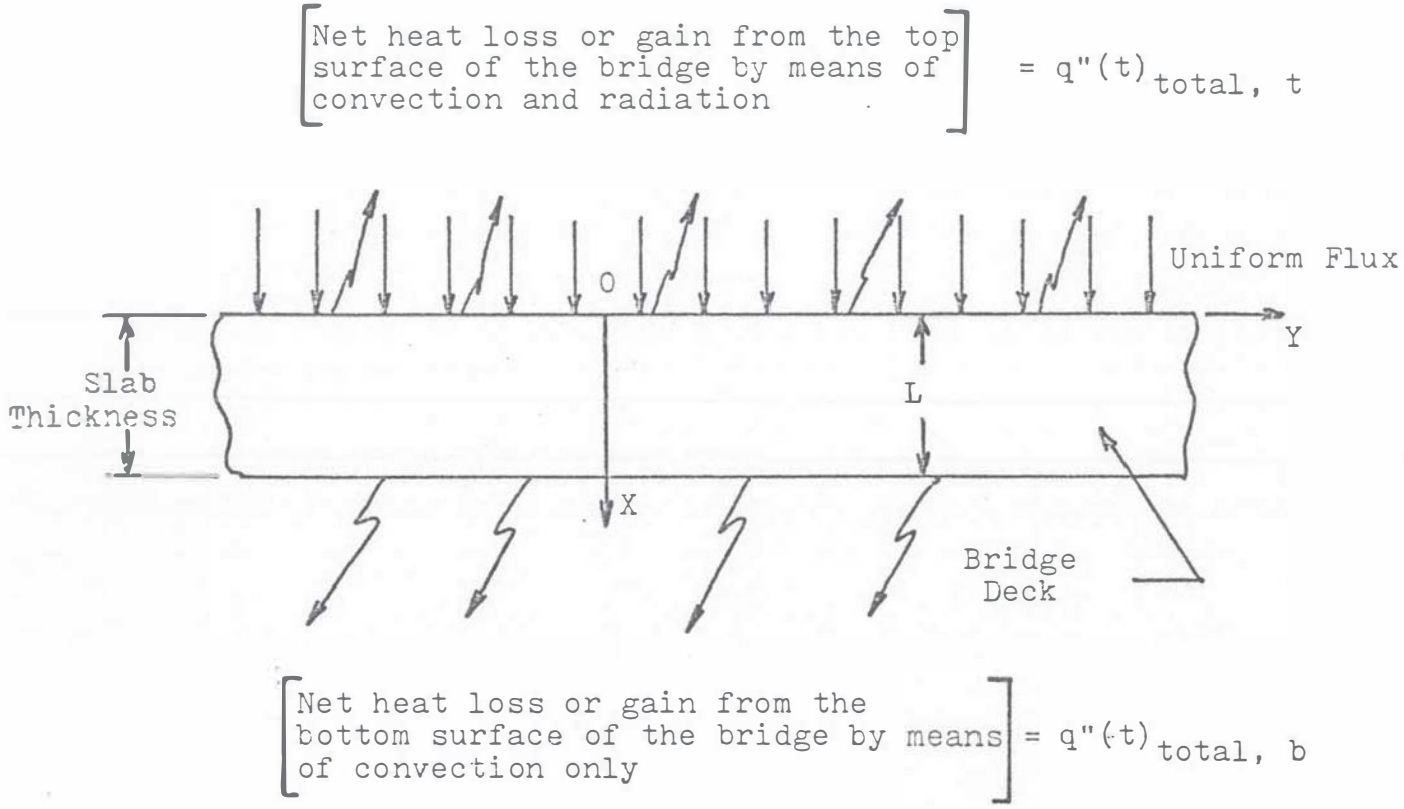

Fig. 2.1. Model for bridge deck.

This is

$$T = F(x) \text{ for } t = 0 \text{ in } 0 \leq x \leq L \tag{2.2}$$

where $F(x)$ specifies the bridge's initial temperature distribution.

Boundary Conditions

Since the governing equation is of the second order with respect to x coordinate, a proper solution requires two boundary conditions in the x direction.

(I) $$-k \frac{\partial T}{\partial x} = q''(t)_{\text{total, t}} \text{ at } x = 0, \text{ for } t > 0 \tag{2.3}$$

(II) $$-k \frac{\partial T}{\partial x} = q''(t)_{\text{total, b}} \text{ at } x = L, \text{ for } t > 0 \tag{2.4}$$

where L = thickness of the bridge deck

$q''(t)_{\text{total,t}}$ = heat loss or gain from bridge by means of convection and radiation from top surface

$q''(t)_{\text{total,b}}$ = heat loss or gain from bridge by means of convection only.

An Explicit Method of Finite Differencing

The governing differential equation of a one dimensional transient heat conduction problem can be expressed in the finite-difference form by using an explicit method. The x and t domains are divided into small intervals of Δx and Δt so that

$$x = n\Delta x, \quad n = 0, 1, 2, \ldots N \text{ with } L = N\Delta x$$

$$t = i\Delta t, \quad i = 0, 1, 2, 3, \ldots$$

Then, the temperature $T(x,t)$ at a location x and a time t is denoted by the symbol T_n^i, that is

$$T(x,t) = T(n\Delta x, i\Delta t) = T_n^i$$

The second derivative of temperature with respect to x, at a position $n\Delta x$ and time $i\Delta t$, is represented in the finite - difference form as

$$\left.\frac{\partial^2 T}{\partial x^2}\right|_{n,i} = \frac{T^i_{n-1} + T^i_{n+1} - 2T^i_n}{(\Delta x)^2} \qquad (2.5)$$

where T^i_{n-1} and T^i_{n+1} are the two neighboring points of the node T^i_n and all of which are evaluated at the time $i\Delta t$.

The first derivative of temperature with respect to the time variable t at a poistion $n\Delta x$ and a time $i\Delta t$ is represented by

$$\left.\frac{\partial T}{\partial t}\right|_{n,i} = \frac{T^{i+1}_n - T^i_n}{\Delta t} \qquad (2.6)$$

substituting equation (2.5) (2.6) into (2.1), the finite - difference form of the time - dependent heat-conduction equation becomes

$$\frac{1}{\alpha}\,\frac{T^{i+1}_n - T^i_n}{\Delta t} = \frac{T^i_{n-1} + T^i_{n+1} - 2T^i_n}{(\Delta x)^2} \qquad (2.7)$$

which can be rearranged to

$$T^{i+1}_n = rT^i_{n-1} + (1-2r)T^i_n + rT^i_{n+1} \,,$$

$$n = 1, 2, 3, \ldots N-1 \ldots \qquad (2.7a)$$

where $r = \dfrac{\alpha\Delta t}{(\Delta x)^2} = F_o$

the solution of this equation is stable if the value of the parameter r is chosen as $0 < r \leq \frac{1}{2}$.

By central differencing, the boundary conditions can be written in finite-difference form as follows

(I) $$- k \frac{(T_1^i - T_{-1}^i)}{2\Delta x} = q^i_{\text{total, t}} \tag{2.8}$$

$$T_{-1}^i = T_1^i + \frac{2q^i_{\text{total, t}}\Delta x}{k} \tag{2.8a}$$

Substitution of (2.8a) into (2.7a) yields

$$T_0^{i+1} = T_0^i + 2r(T_1^i - T_0^i + \frac{q^i_{\text{total, t}}\Delta x}{k})$$

$$\text{at} \quad n = 0 \tag{2.8b}$$

(II) $$- k \frac{(T_{N+1}^i - T_{N-1}^i)}{2\Delta x} = q^i_{\text{total, b}} \tag{2.9}$$

$$T_{N+1}^i = T_{N-1}^i - \frac{2q^i_{\text{total, b}}\Delta x}{k} \tag{2.9a}$$

Substitution of (2.9a) into (2.7a) yields

$$T_N^{i+1} = T_N^i + 2r(T_{N-1}^i - T_N^i - \frac{q^i_{\text{total, b}}\Delta x}{k})$$

$$\text{at} \quad n = N \tag{2.9b}$$

The initial condition can be written as:

$$T_n^0 = F(n\Delta x), \quad n = 0, 1, 2, \ldots N \quad \text{for} \quad i = 0 \tag{2.10}$$

Due to the non-homogeneous boundary conditions occurring for this one dimensional transient problem, the exact solution is difficult to solve. Therefore, the numerical method of explicit finite-difference technique is adopted to solve this problem.

CHAPTER III

ANALYTICAL STUDY

Before the final model was determined for the experimental study, two computer programs were designed using the explicit finite differencing technique, for the purpose of feasibility studies. The first computer program was solved to study the bridge's thermal response with the different top surface boundary conditions of: (1) A blackened top bridge surface without glass cover, (2) A blackened top bridge surface with single glass cover (3) A blackened top bridge surface with two glass covers. Typical plots of these different boundary conditions are presented in Figure 3.1 through Figure 3.18. To summarize the results of these plots, Figure 3.19 shows the effect of number of covers, wind, solar flux and specific heat on the maximum temperature attained at 2" depth. It also shows that under optimal conditions such as: low specific heat (0.15, for a dry concrete condition), low wind velocity, high ambient air temperature etc., these temperatures may be increased, however, the temperatures are still very marginal to achieve the required bridge heating.

The second computer program was designed to investigate the usage of solar concentrating collectors. The collector we chose to model for this study was a commercially available Fresnel lens trough collector manufactured by Northrup Corporation. To model the focusing collector we selected 1200 ft^2 of the bridge deck and used solar data for 32° North Latitude on

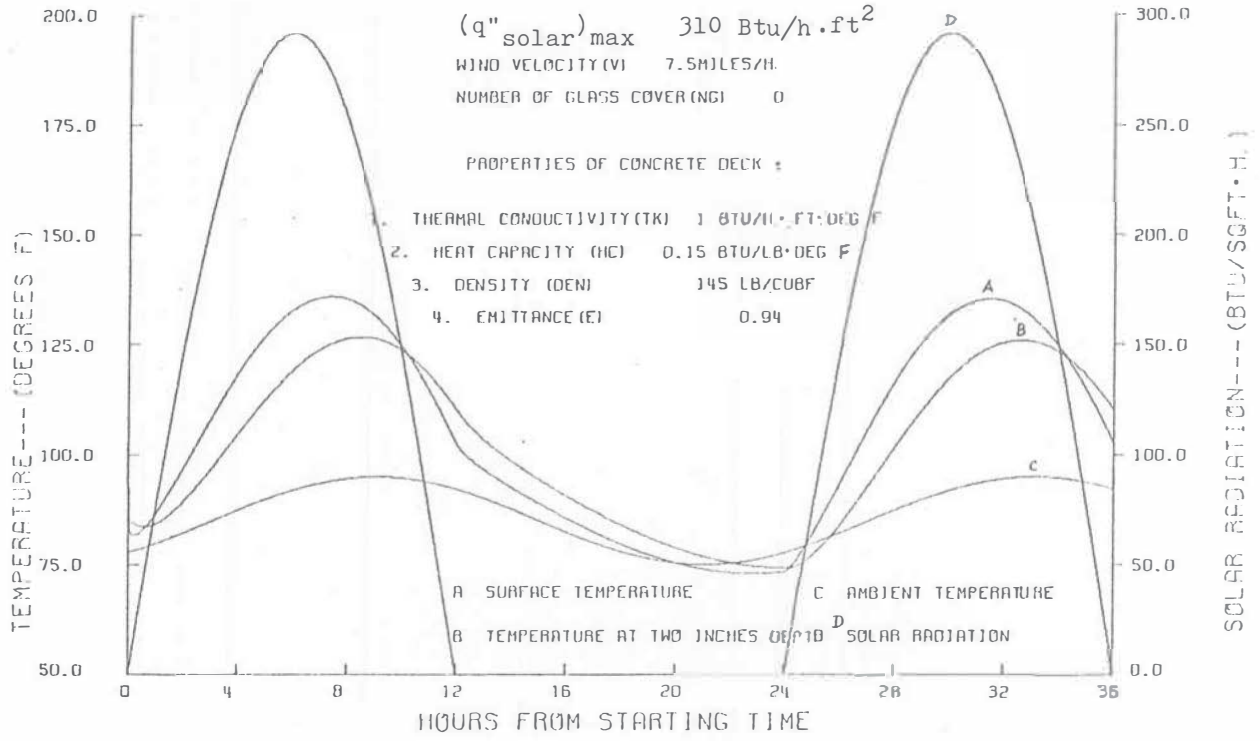

Fig. 3.1. Sensitivity study of the bridge thermal response (c_p=0.15 Btu/lb.^{o}F, v=7.5 mph, $(q"_{solar})_{max}$ = 310 Btu/h.ft^2).

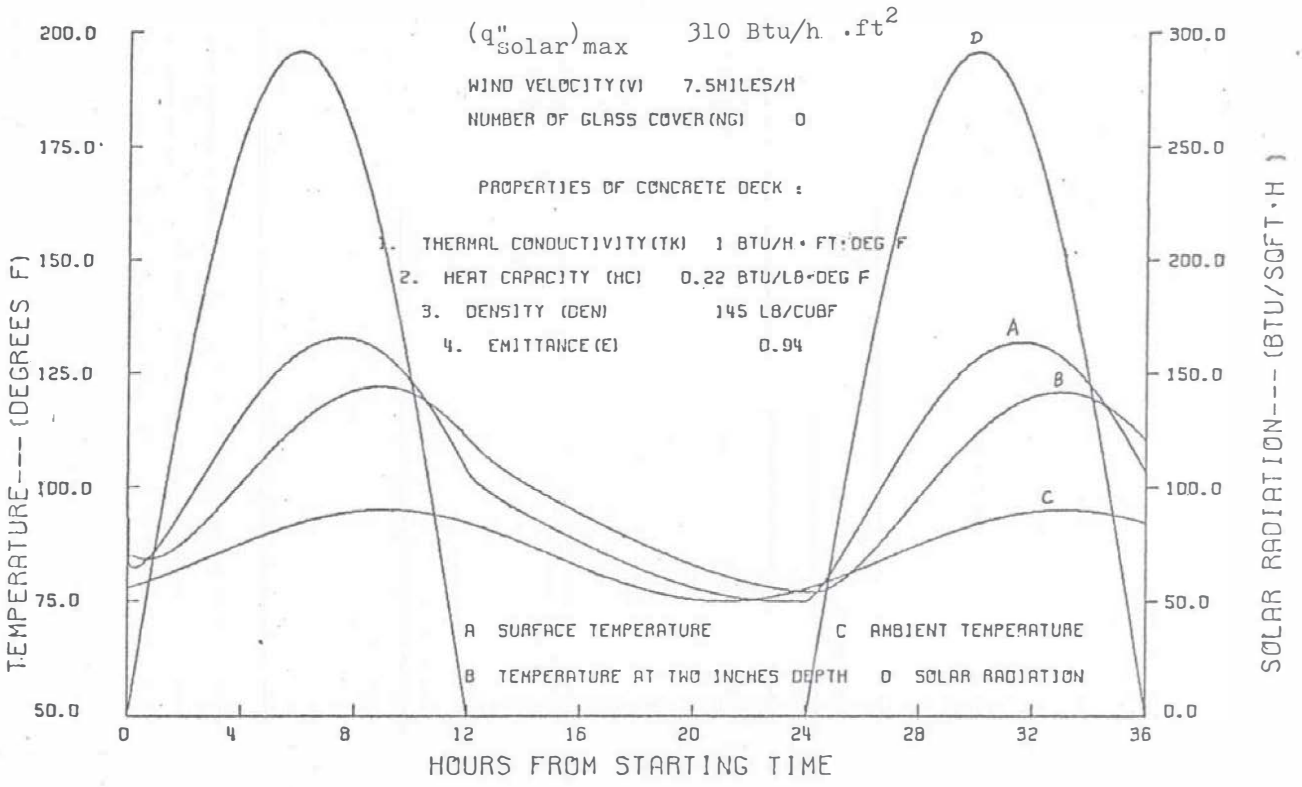

Fig. 3.2. Sensitivity study of bridge thermal response (c_p = 0.22 Btu/lb.^{o}F, v = 7.5 mph, $(q''_{solar})_{max}$ = 310 Btu/h.ft^2).

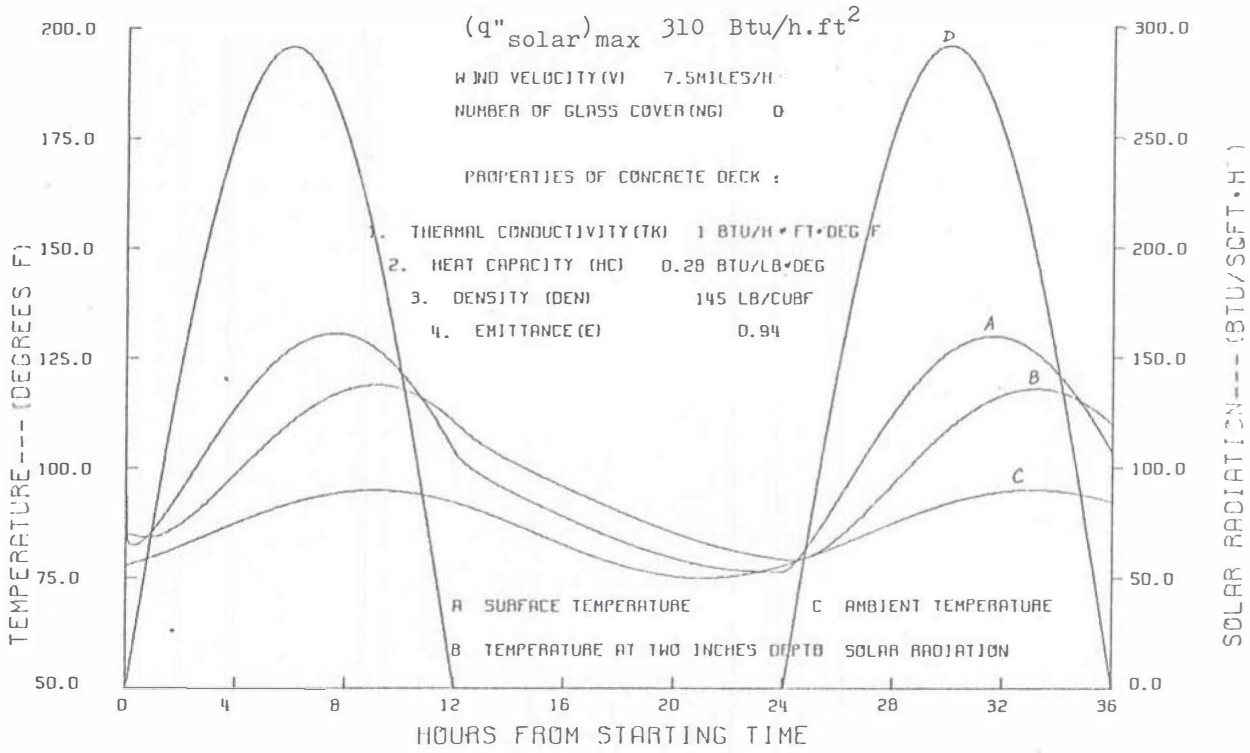

Fig. 3.3. Sensitivity study of bridge thermal response (c_p=0.28 Btu/lb.^oF, v=7.5 mph, $(q"_{solar})_{max}$ = 310 Btu/h.ft^2).

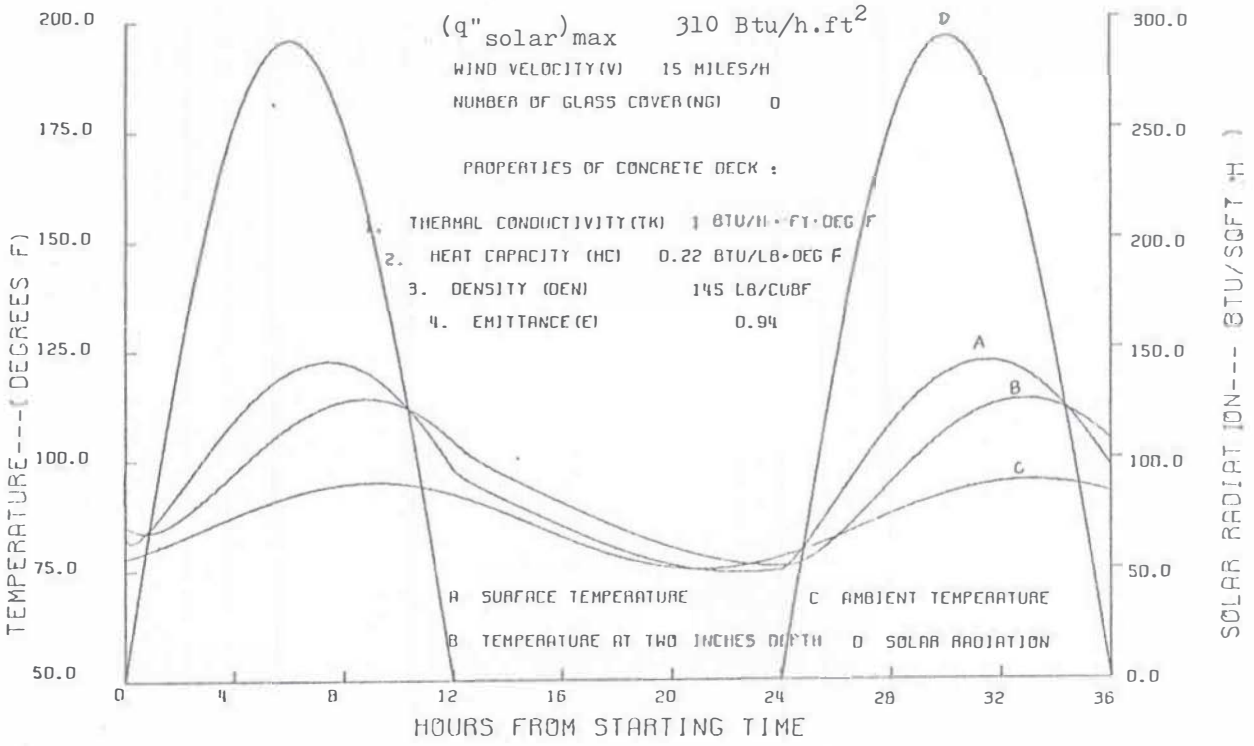

Fig. 3.4. Sensitivity study of bridge thermal response (c_p=0.22 Btu/lb.^{o}F, v=15 mph, $(q''_{solar})_{max}$ = 310 Btu/h . ft^2).

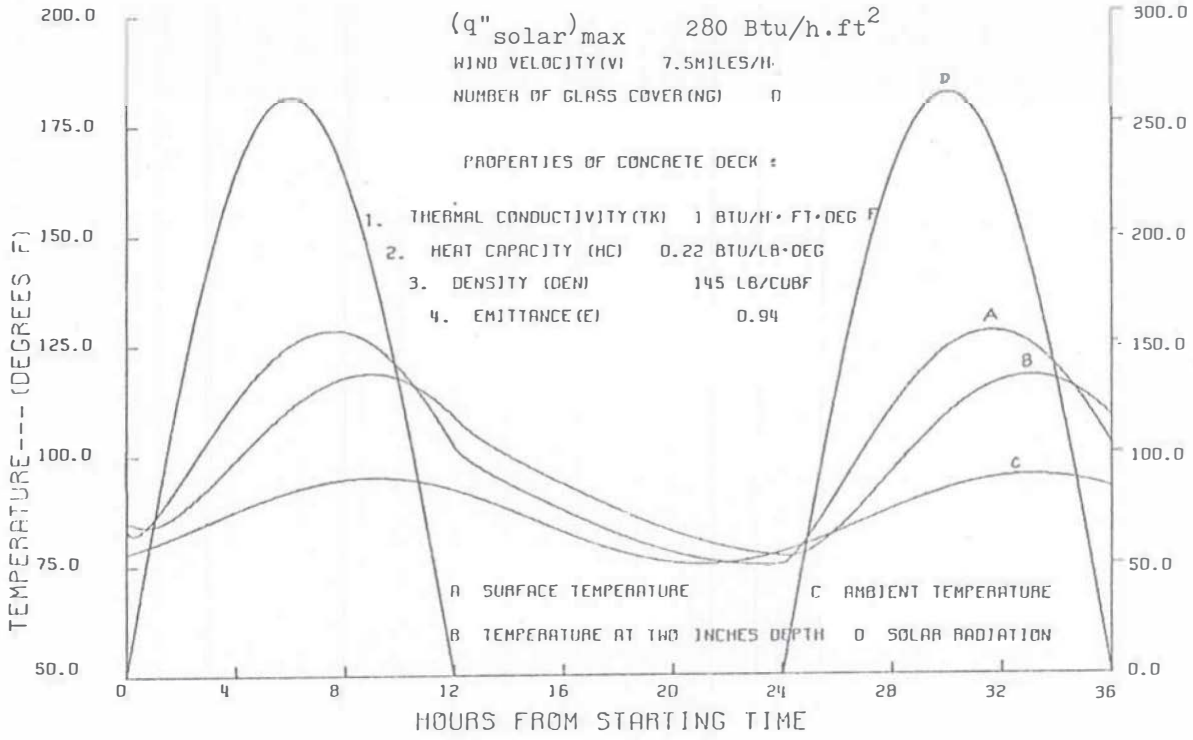

Fig. 3.5. Sensitivity study of bridge thermal response (c_p=0.22 Btu/lb.^oF, v=7.5 mph, $(q"_{solar})_{max}$ = 280 Btu/h .ft^2)..

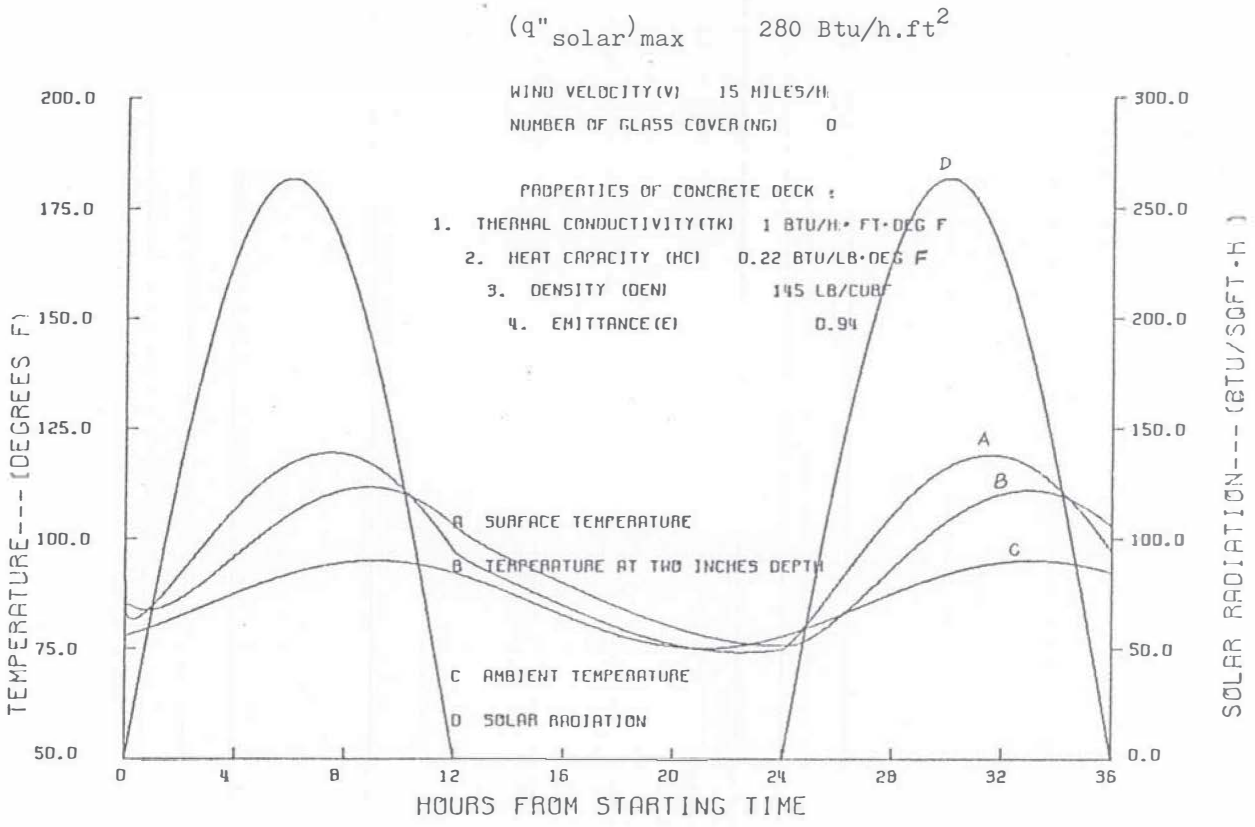

Fig. 3.6. Sensitivity study of bridge thermal response (c_p=0.22 Btu/lb.^oF, v=15 mph, $(q"_{solar})_{max}$ =280 Btu/h.ft^2).

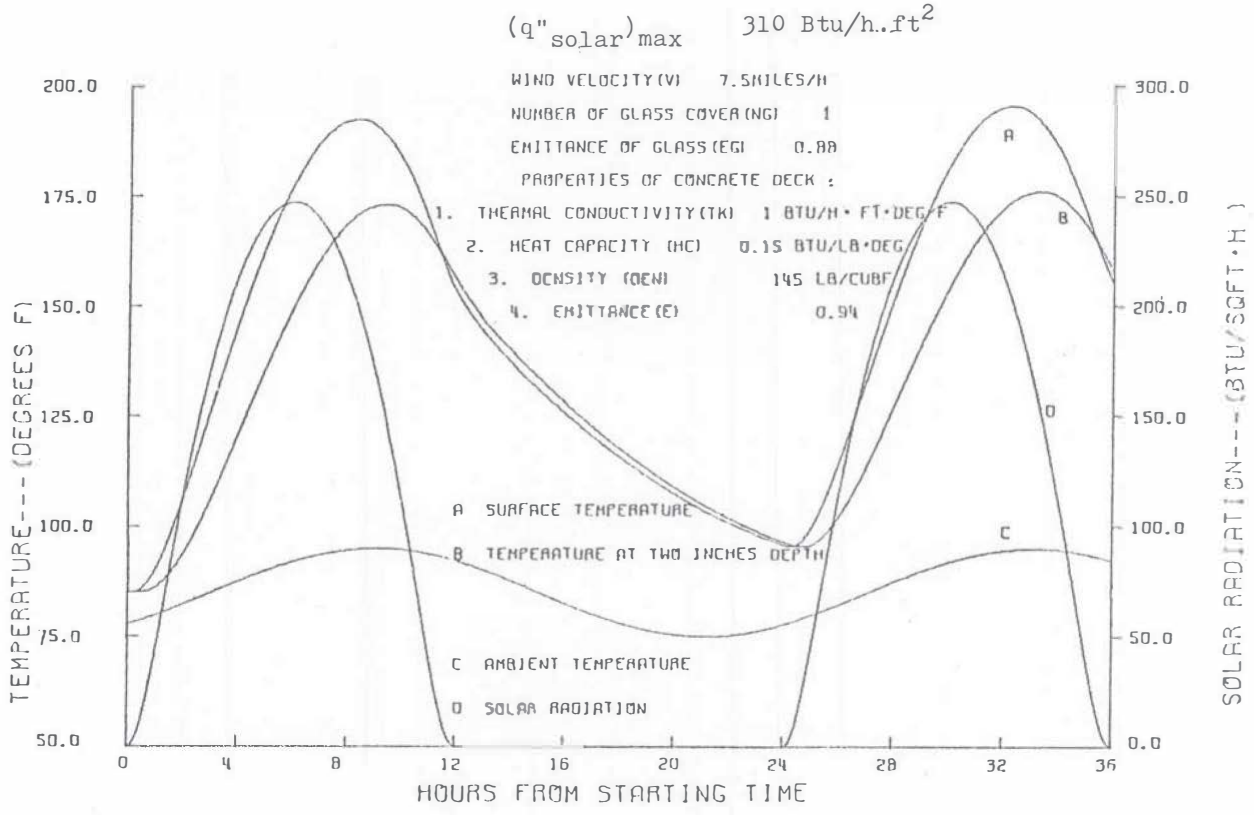

Fig. 3.7. Sensitivity study of bridge thermal response, one cover (c_p=0.15 Btu/lb.^{o}F, v=7.5 mph, $(q''_{solar})_{max}$ = 310 Btu/h.ft^2).

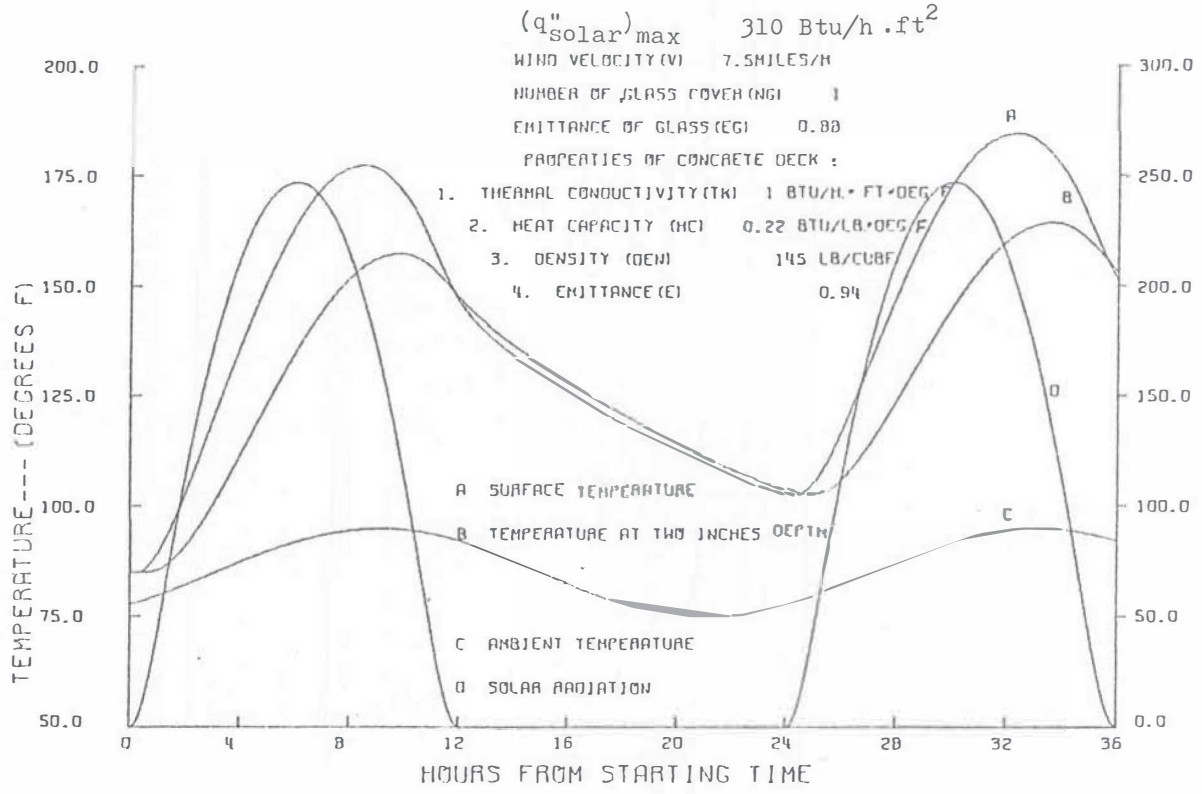

Fig. 3.8. Sensitivity study of bridge thermal response, one cover (c_p=0.22 Btu/lb ^{o}F, v=7.5 mph, $(\dot{q}''_{solar})_{max}$ = 310 Btu/h.ft^2).

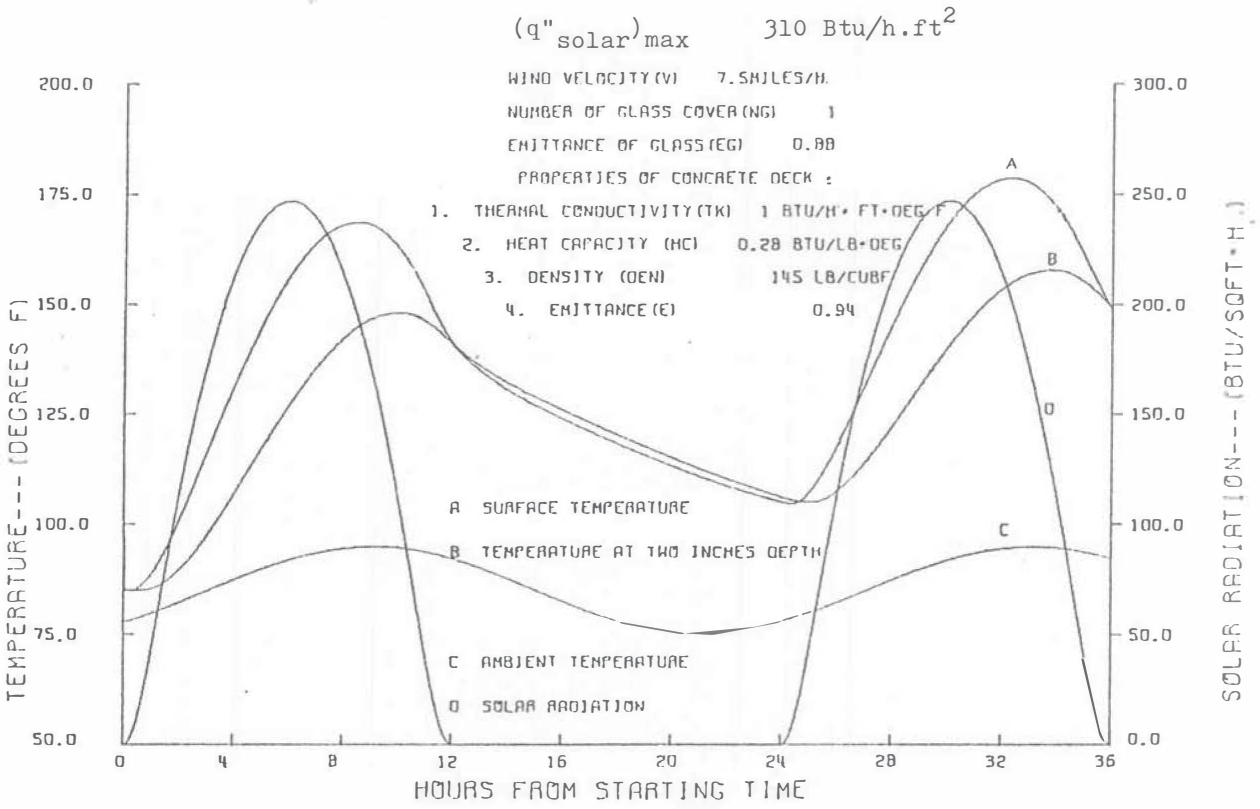

Fig. 3.9. Sensitivity study of bridge thermal response, one cover (c_p=0.28 Btu/lb·^{o}F, v=7.5 mph, $(q"_{solar})_{max}$ = 310 Btu/h.ft^2).

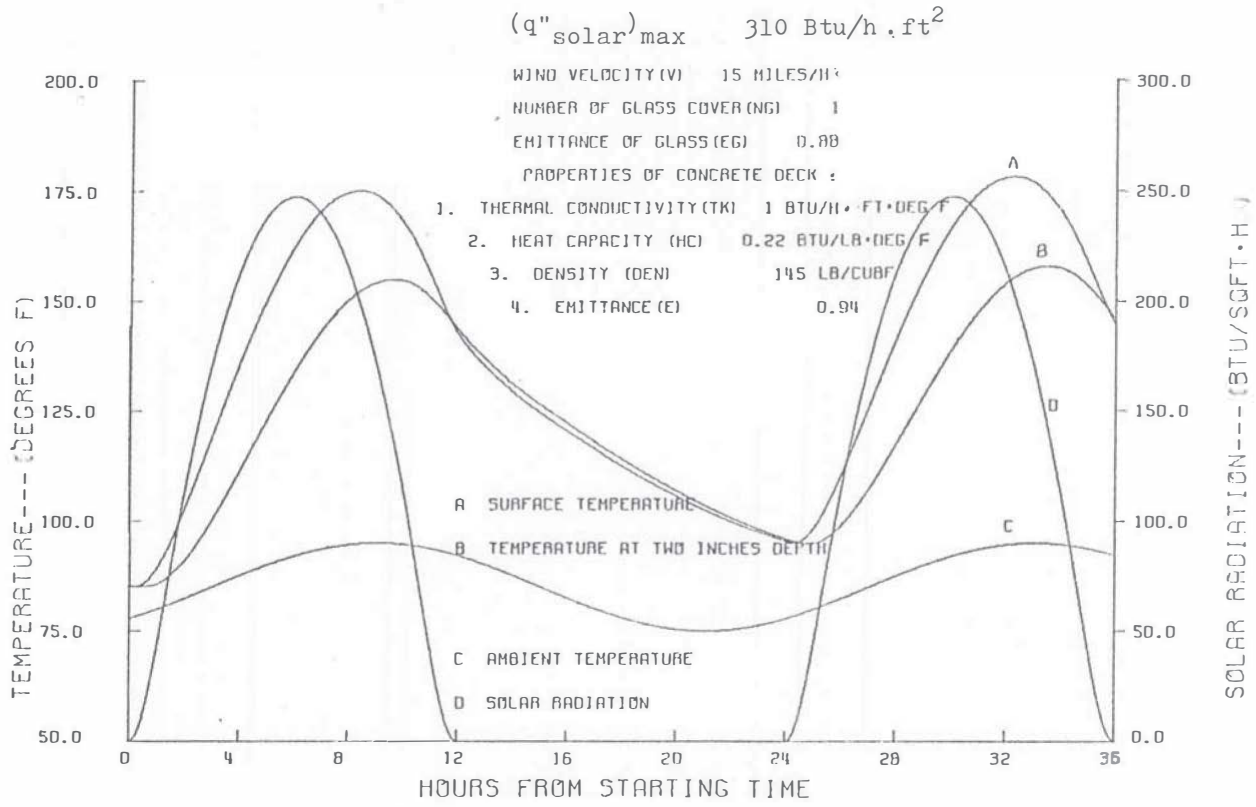

Fig. 3.10. Sensitivity study of bridge thermal response, one cover (c_p=0.22 Btu/lb.$^{\circ}$F, v=15 mph, $(q''_{solar})_{max}$ = 310 Btu/h.ft^2).

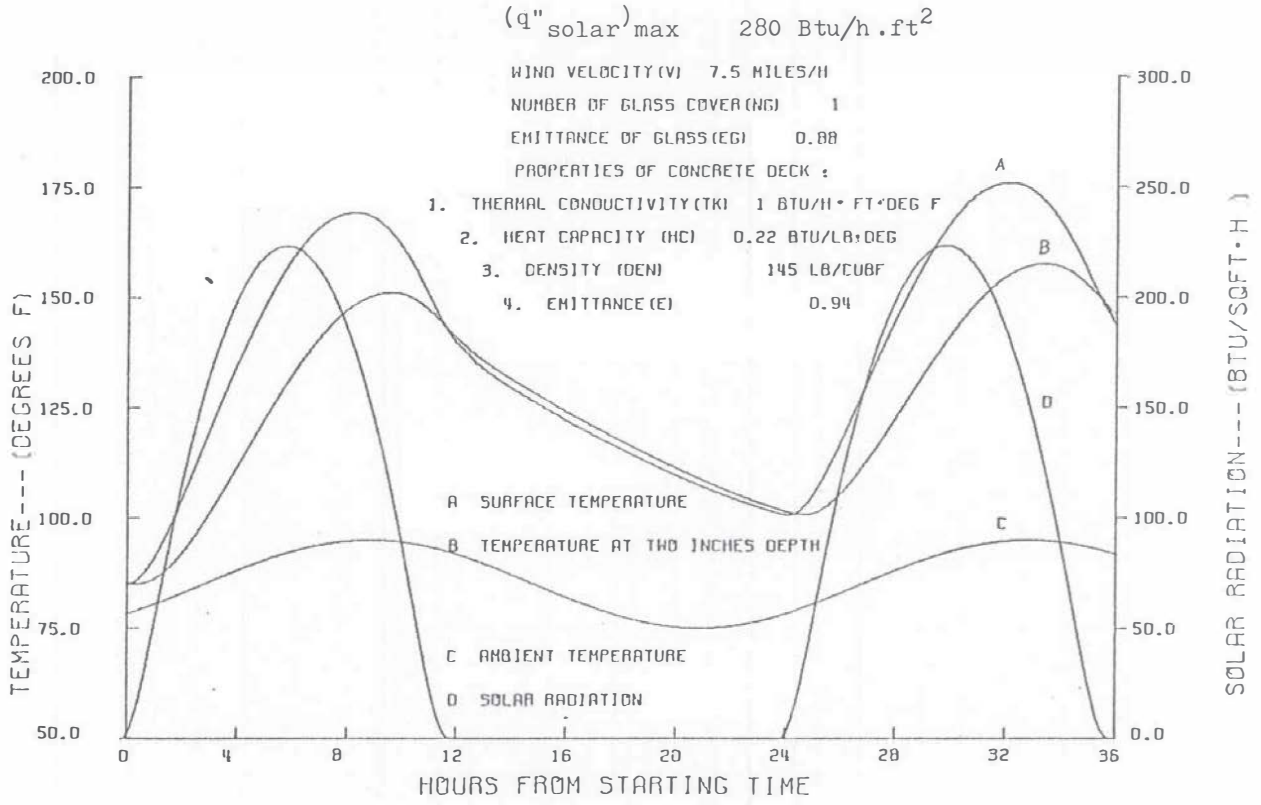

Fig. 3.11. Sensitivity study of bridge thermal response, one cover (c_p=0.22 Btu/lb·^{o}F, v=7.5 mph, $(q"_{solar})_{max}$ = 280 Btu/h.ft^2).

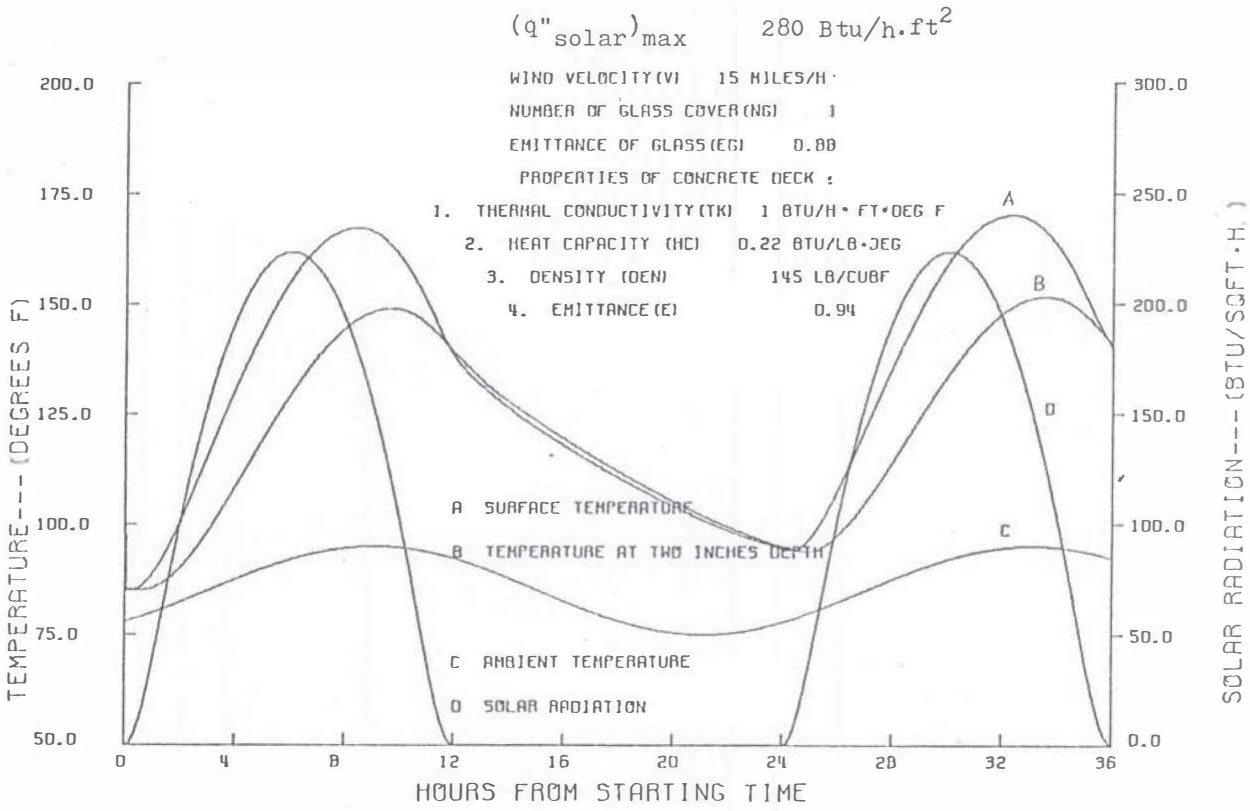

Fig. 3.12. Sensitivity study of bridge thermal response, one cover (c_p=0.22 Btu/lb·^{o}F, v=15 mph, $(q"_{solar})_{max}$ = 280 Btu/h.ft^2).

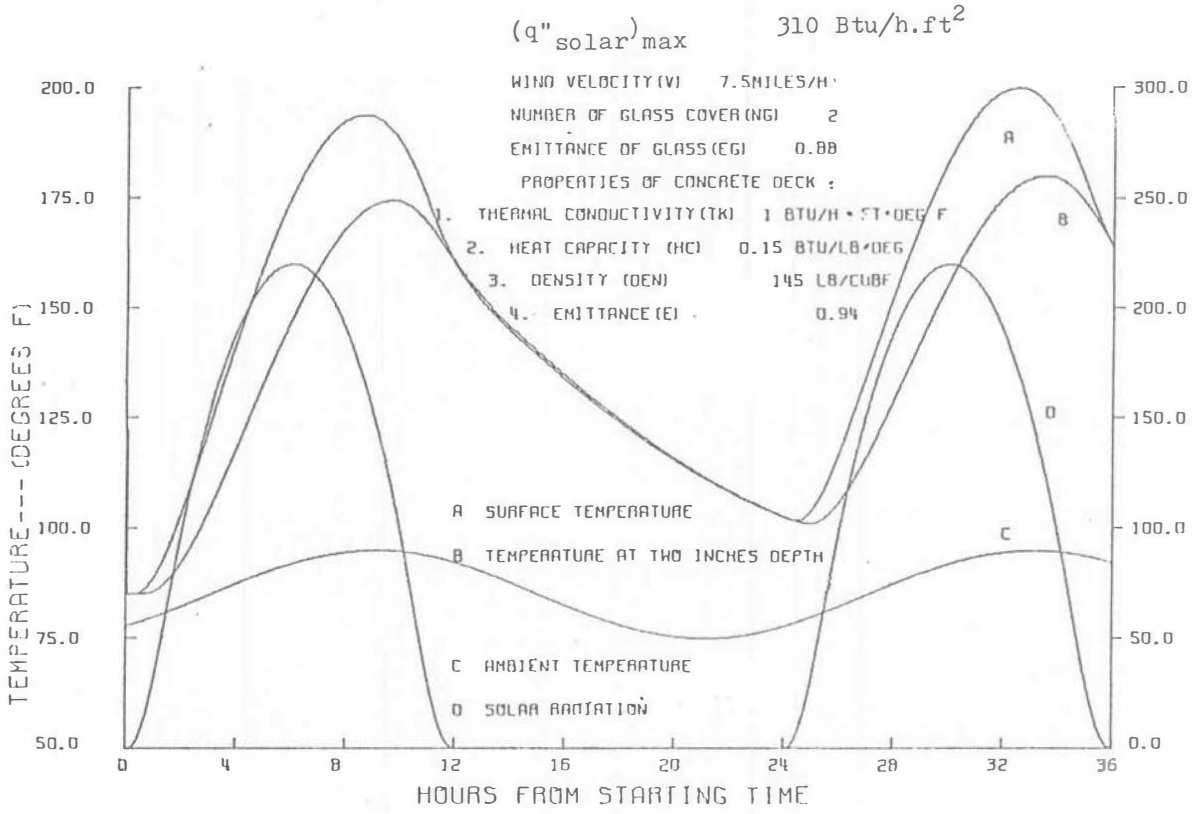

Fig. 3.13. Sensitivity study of bridge thermal response, two covers (c_p=0.15 Btu/lb·^{o}F, v=7.5 mph, $(q"_{solar})_{max}$ = 310 Btu/h. ft^2).

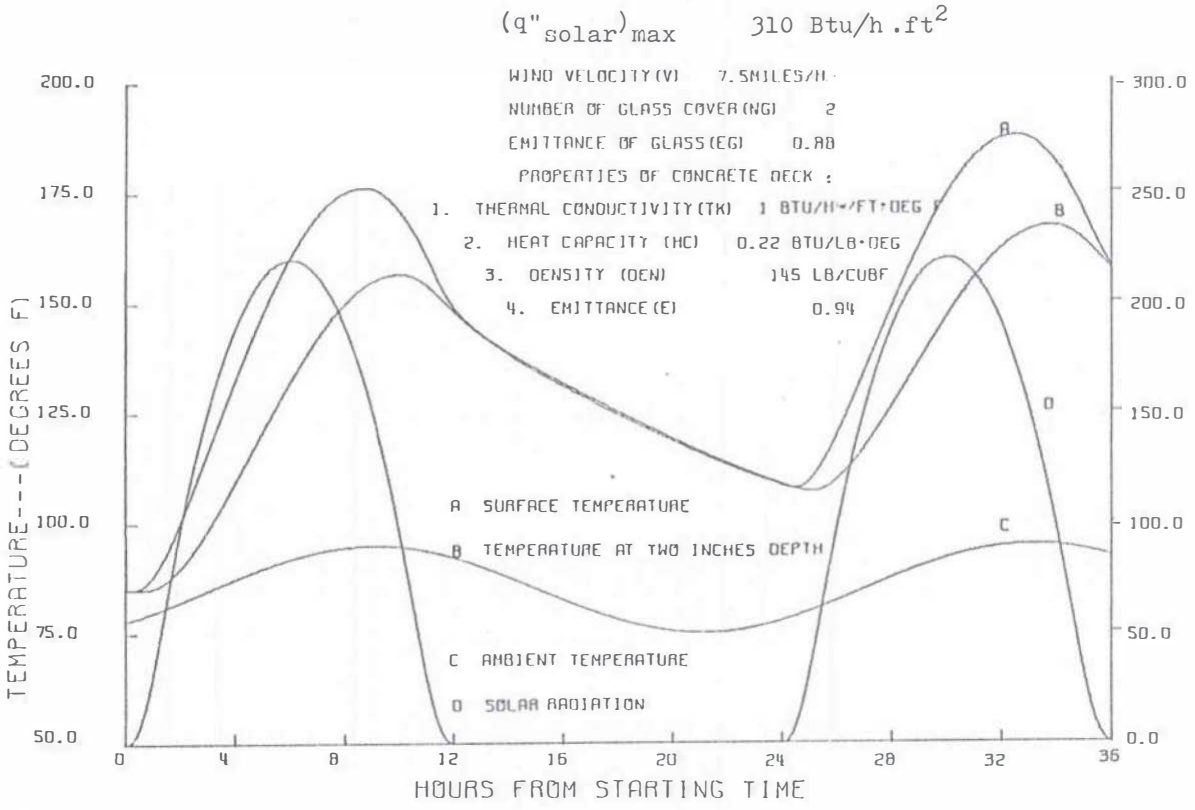

Fig. 3.14. Sensitivity study of bridge thermal response, two covers (c_p=0.22 Btu/lb·^{o}F, v=7.5 mph, $(q"_{solar})_{max}$ = 310 Btu/h.ft^2).

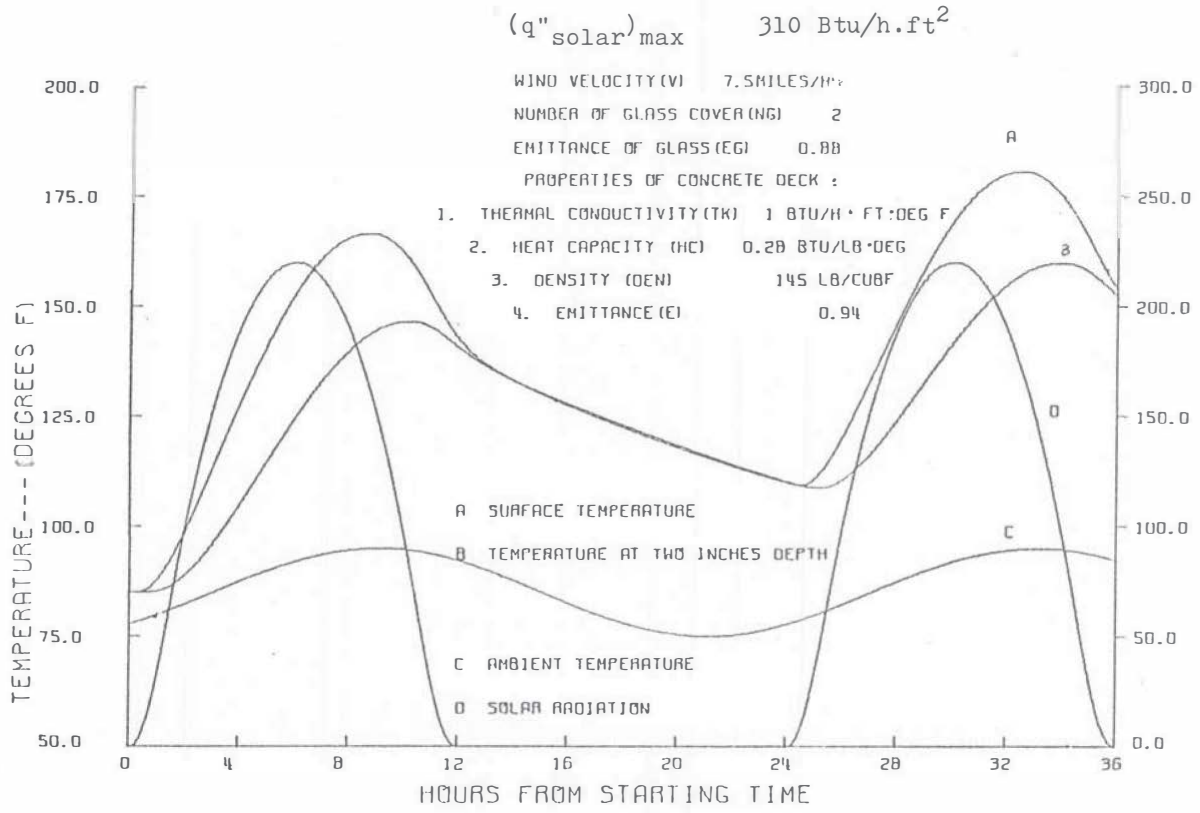

Fig. 3.15. Sensitivity study of bridge thermal response, two covers (c_p=0.28 Btu/lb·^{o}F, v=7.5 mph, $(q''_{solar})_{max}$ = 310 Btu/h.ft^2).

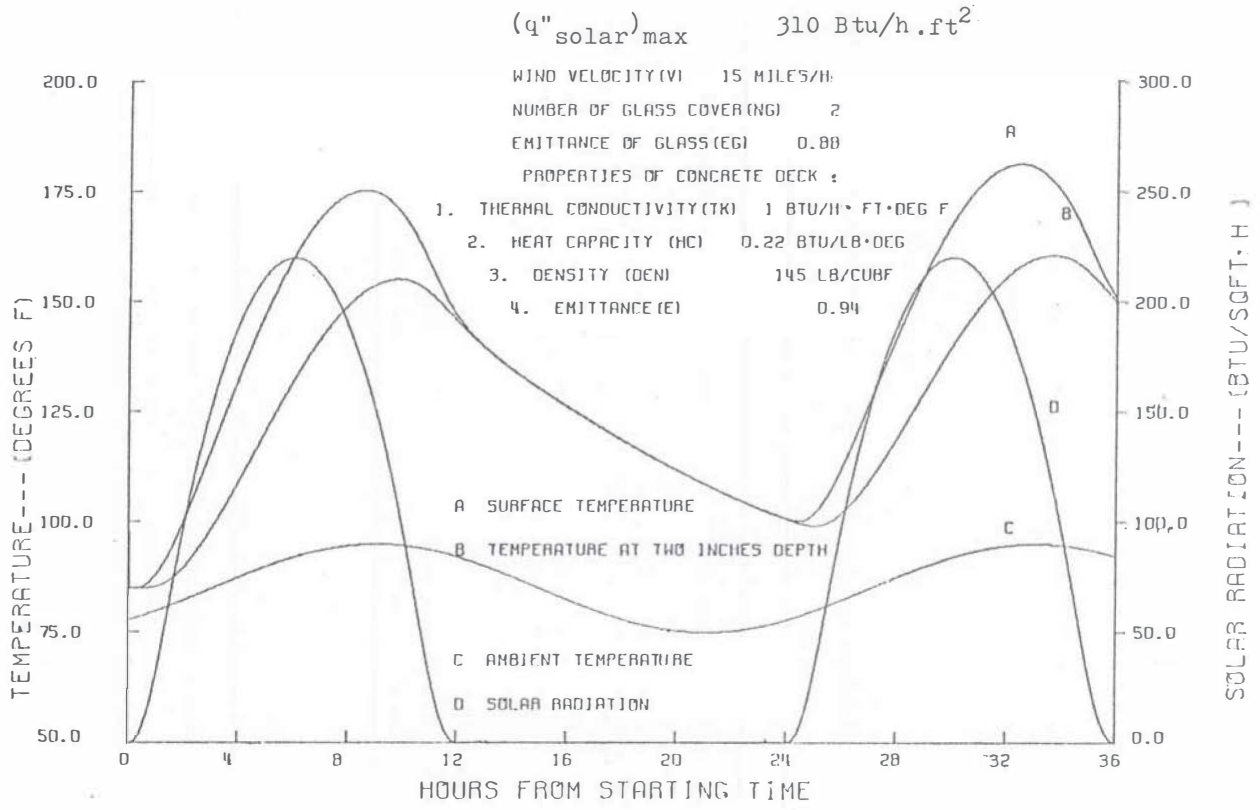

Fig. 3.16. Sensitivity study of bridge thermal response, two covers (c_p=0.15 Btu/lb.^{o}F, v=15 mph, $(q''_{solar})_{max}$ =310 Btu/h.ft^2).

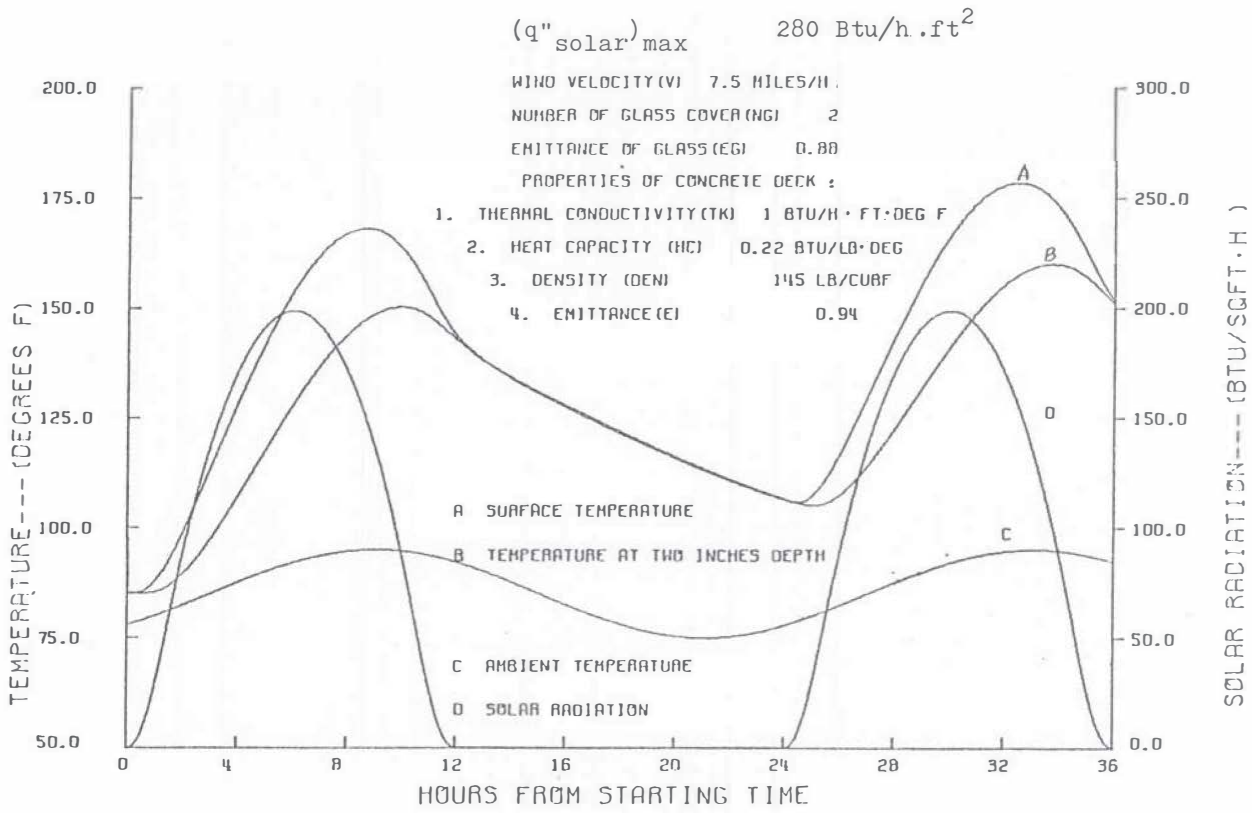

Fig. 3.17. Sensitivity study of bridge thermal response, two covers (c_p= 0.22 Btu/lb·^{o}F, v=7.5 mph, $(q"_{solar})_{max}$= 280 Btu/h.ft^2).

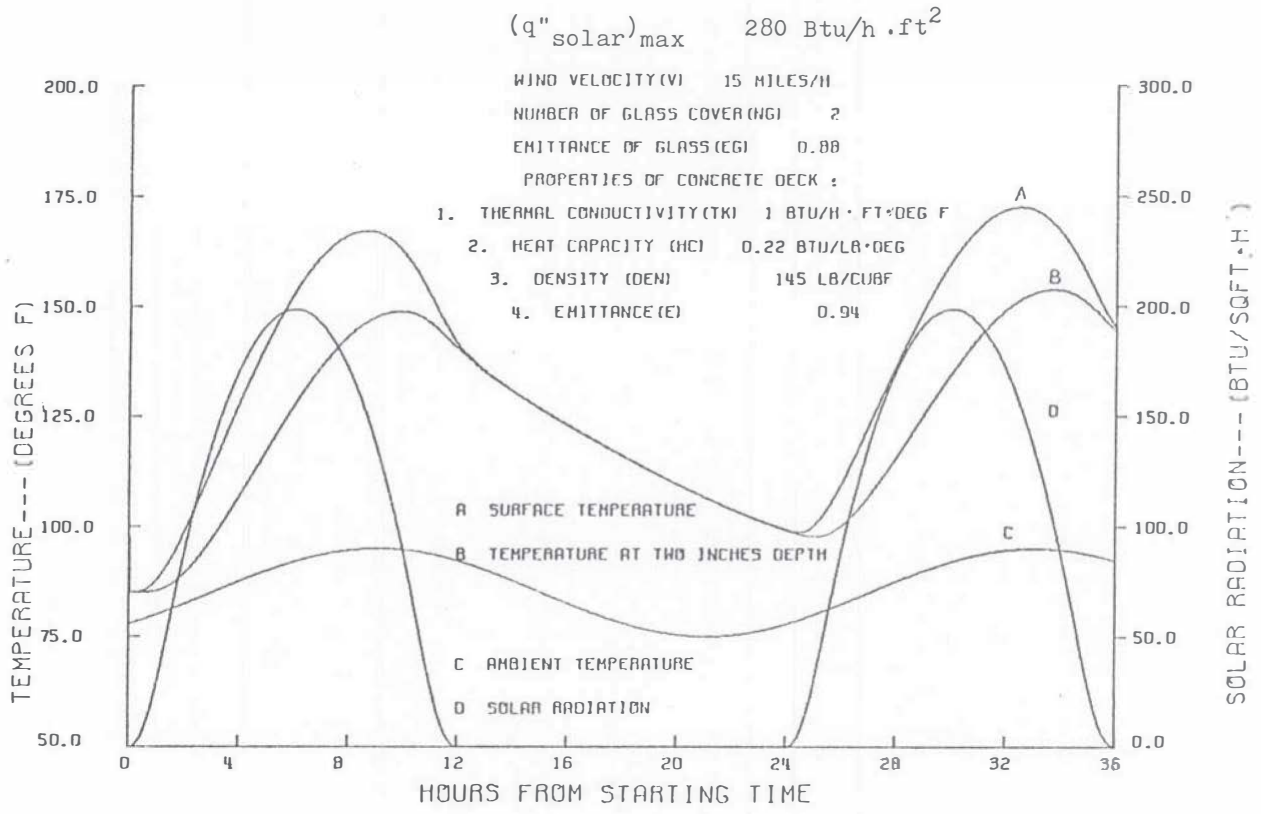

Fig. 3.18. Sensitivity study of bridge thermal response, two covers (c_p=0.22 Btu/lb·^{o}F, v= 15 mph, $(q''_{solar})_{max}$ = 280 Btu/h..ft^2).

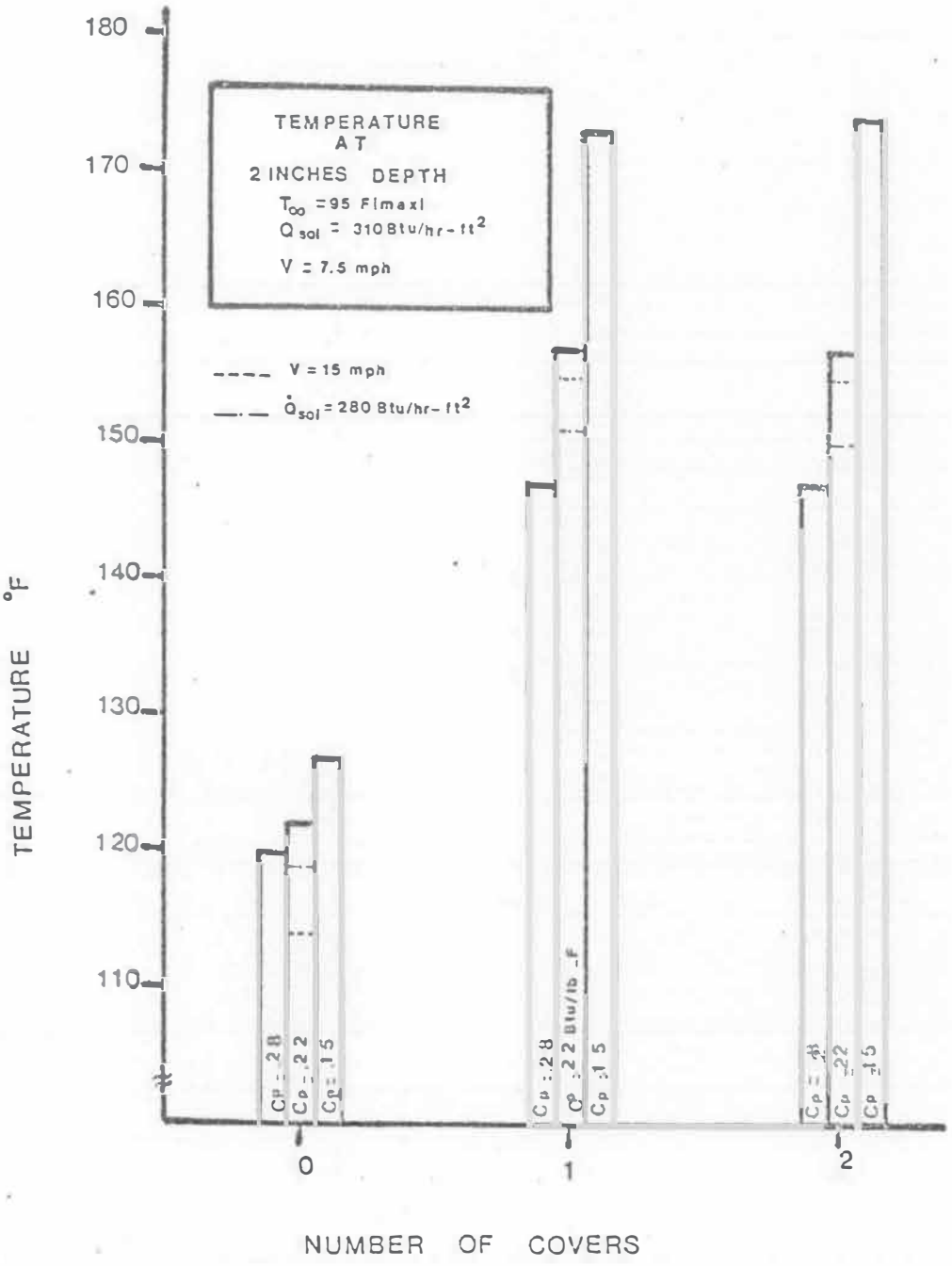

Fig. 3.19. Summarized result of the sensitivity analysis

July 21 [1, 2]. The ambient temperature was modeled in the same manner as the first computer program which will be discussed later. The surface of the bridge deck was assumed to be in contact with an isothermal heat exchanger. Since a minimum amount of fluid is desirable, the model did not allow for any storage. The mass of heat transfer fluid and heat exchanger was taken to be 17552 lbm. This was based on the assumption of approximately 14.63 lbm of heat exchanger and fluid per ft^2 of bridge deck. This number was considerably greater than the value actually used in the experiments. Computer runs were also made with different values of contact resistance. The fluid and collector were treated as a bulk system, and the solar heat gain and the calculated heat transfer from the fluid to the slab were used in the thermal balance of the collector and fluid system. In all cases the collector and fluid system were assumed to have thermal losses of 10% of the total energy absorbed. The varying collector efficiency was determined from a graph published by Northrup Corporation and reproduced as Figure 3.20. Typical results of this study are presented in Figure 3.21 through 3.27. The contact resistance was assumed to be negligible. These figures show the effect of different specific heats and area ratio on the temperature at the two inch depth. The area ratio is defined as the ratio of collector area to bridge deck surface (heat exhanger) area. These results show the concentrating collector system to be promising. The temperature at 2 inch depth should reach 160°F with the area ratio = 2 system in a period of approximately 5 hours.

The detailed simulations and different boundary conditions for these mathematical computer models are discussed as follows.

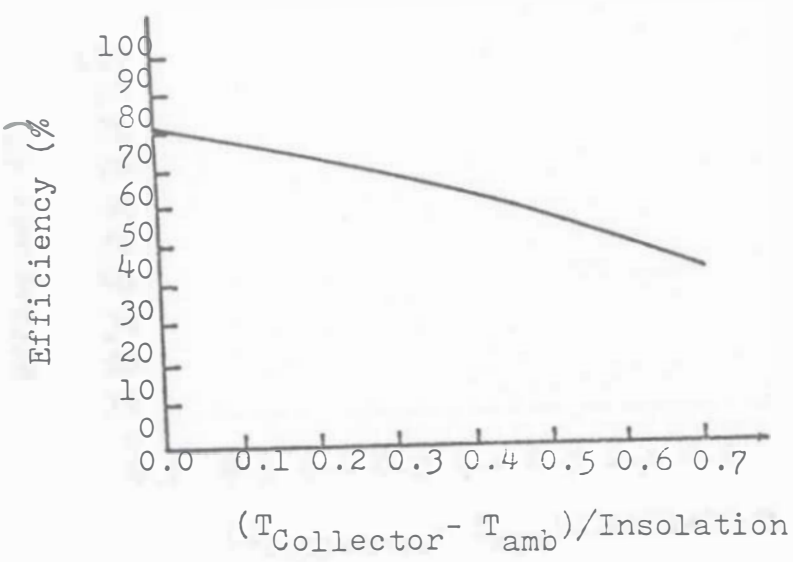

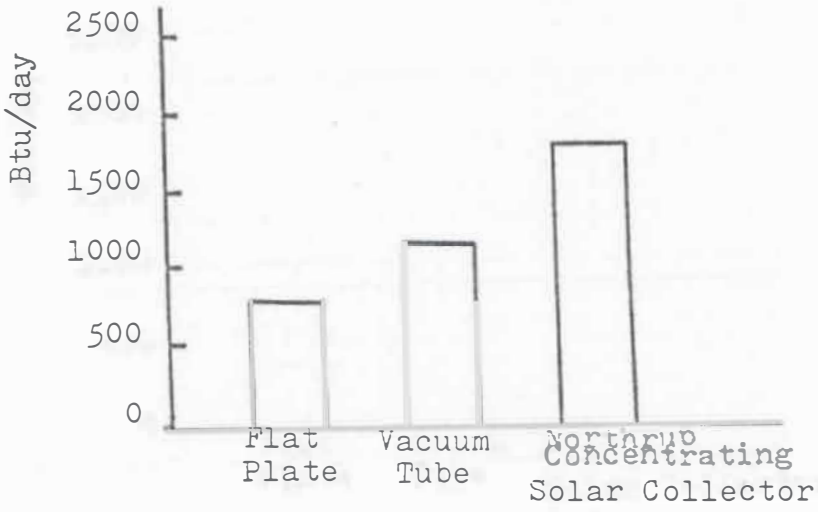

Fig. 3.20. Upper: Efficiency curve of Northrup concentrating solar collector.

Lower: Comparison of different collector performance.

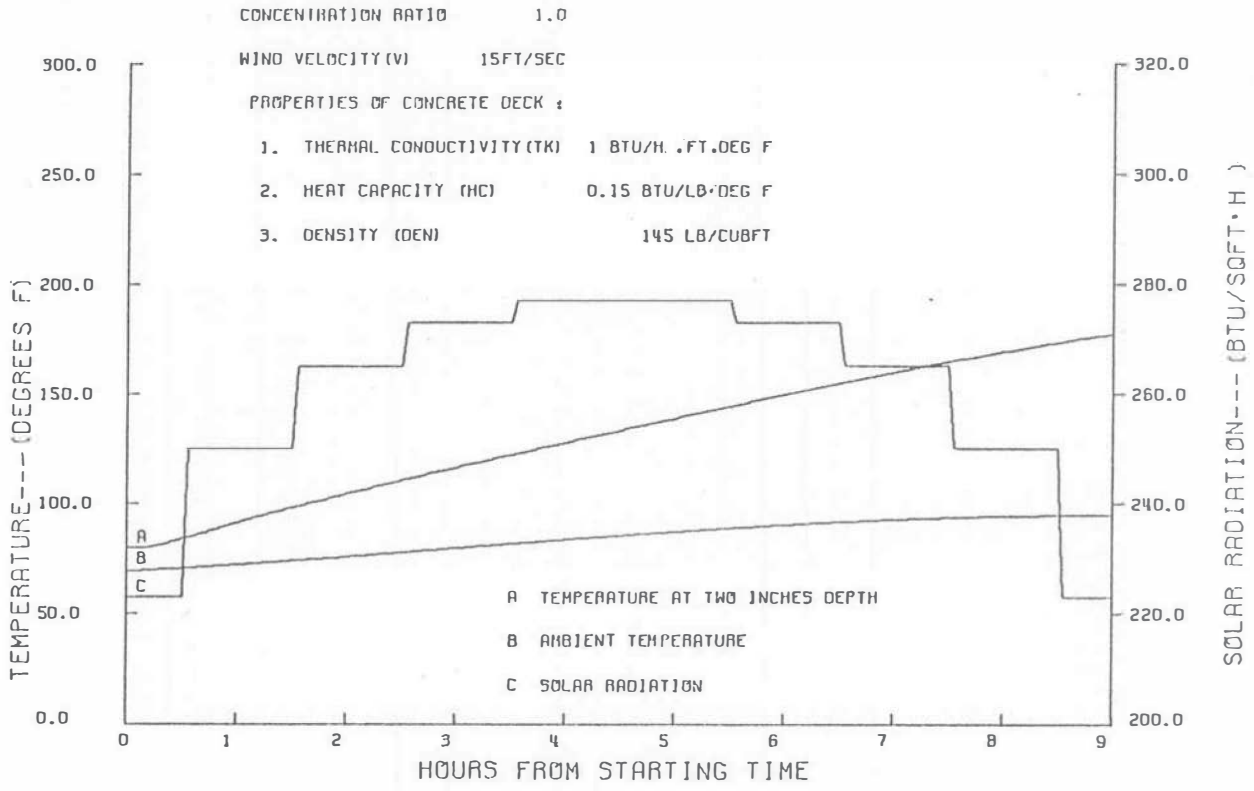

Fig. 3.21. Bridge thermal response study with focusing solar collector (c_p=0.15 Btu/lb.^{o}F, Area ratio =1.0).

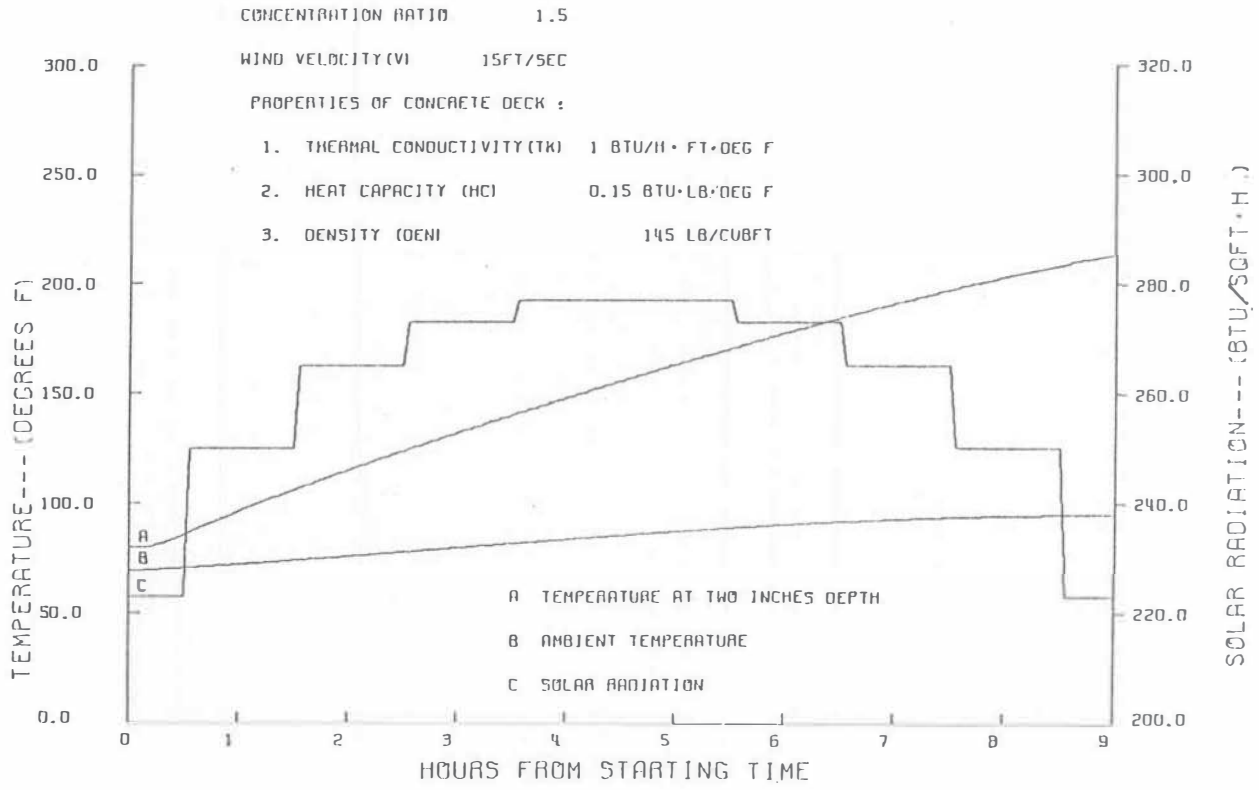

Fig. 3.22. Bridge thermal response study with focusing solar collector (c_p=0.15 Btu/lb.^{o}F, Area ratio= 1.5).

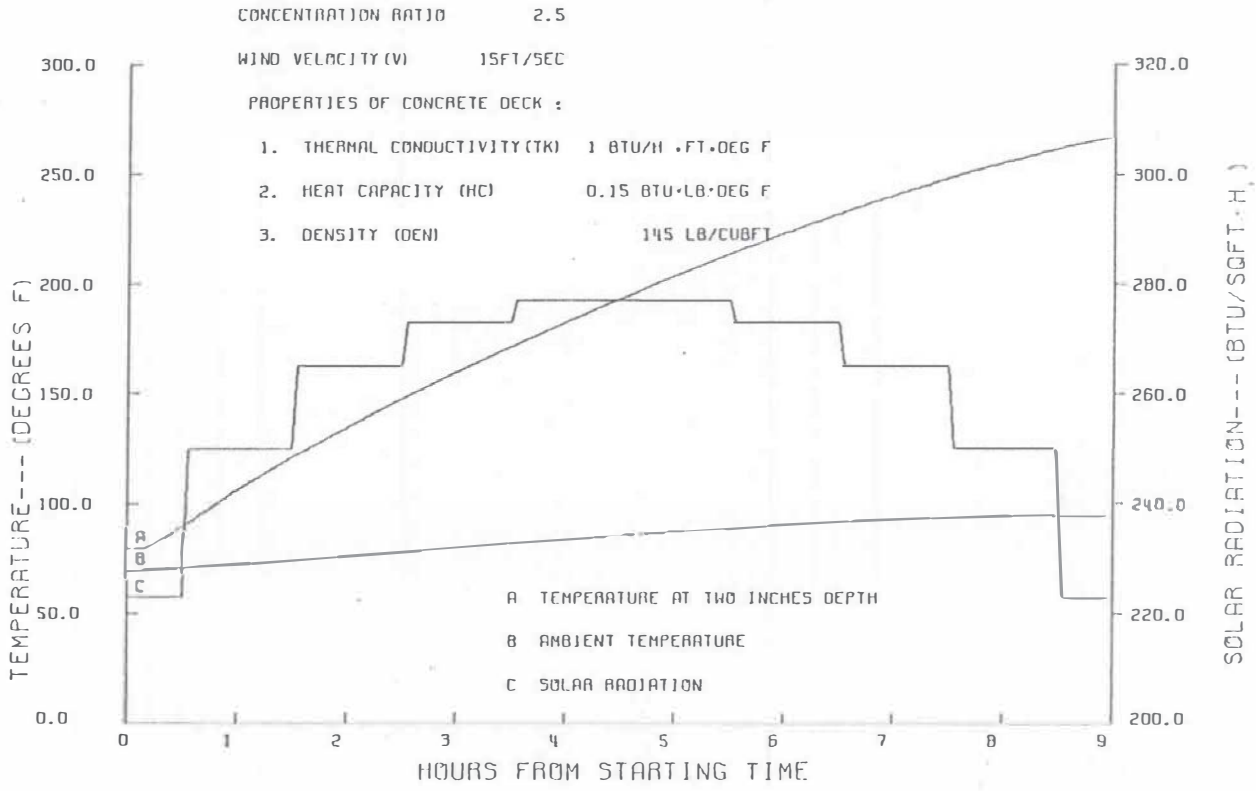

Fig. 3.23. Bridge thermal response study with focusing solar collector (c_p=0.15 Btu/lb.^{o}F, Area ratio=2.5).

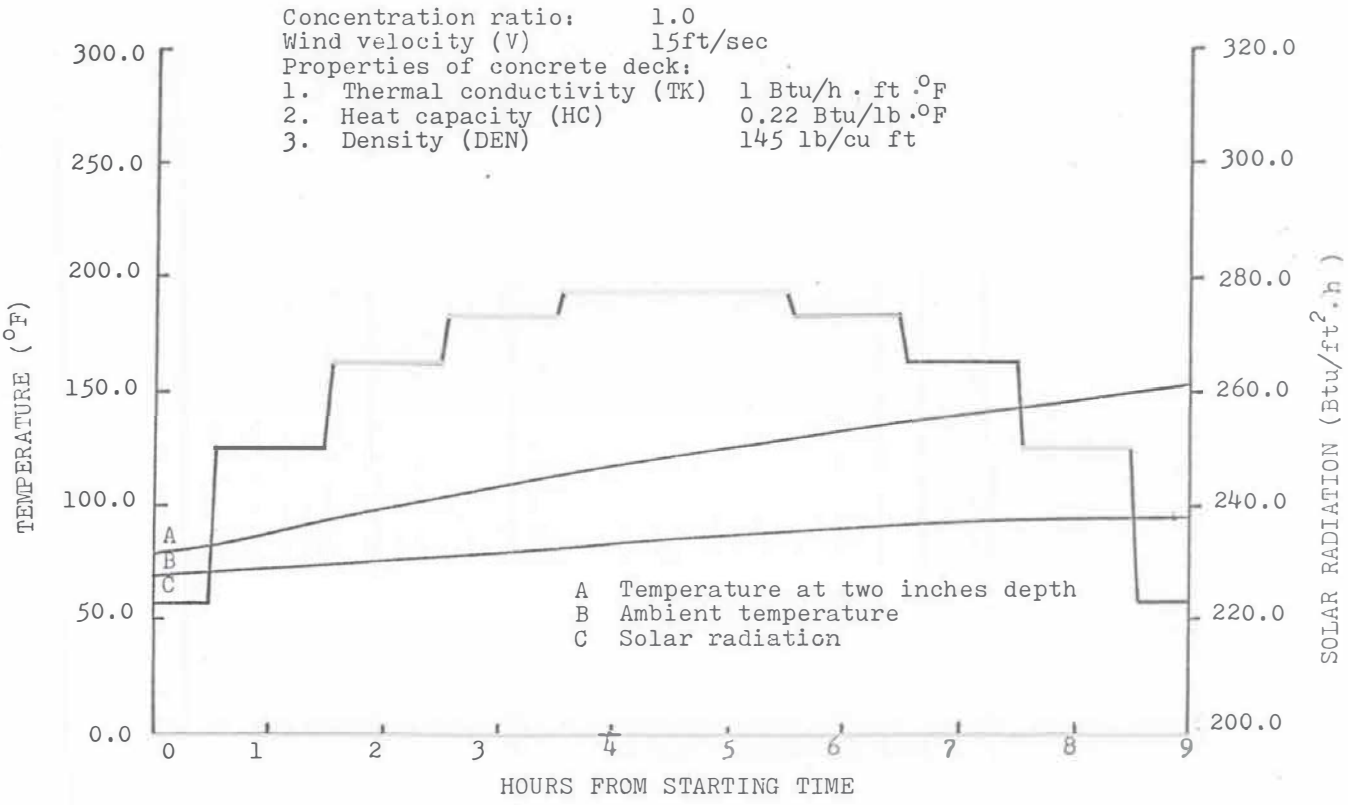

Fig. 3.24. Bridge thermal response study with focusing solar collector (c_p=0.22 Btu/lb·°F, Area ratio=1.0).

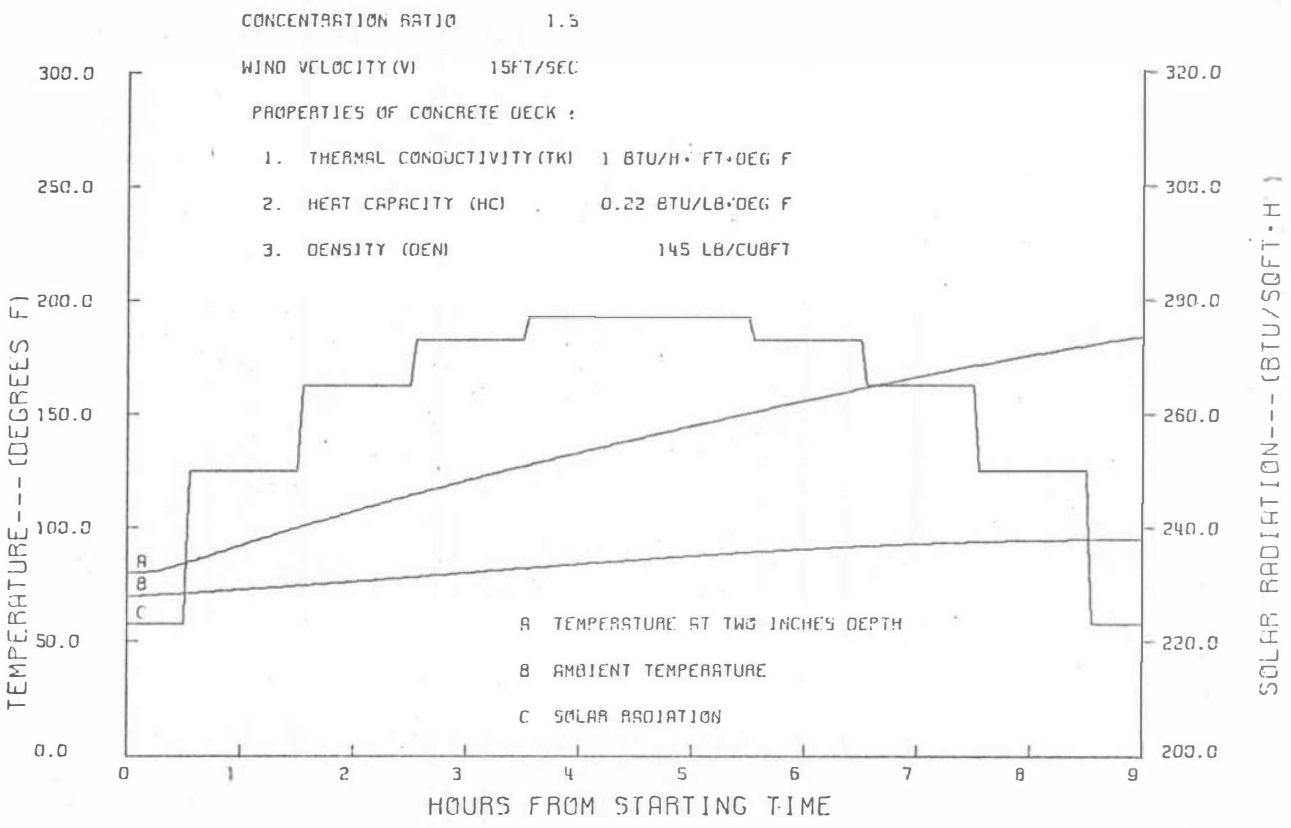

Fig. 3.25 Bridge thermal response study with focusing solar collector (c_p = 0.22 Btu/lb·°F, Area ratio=1.5).

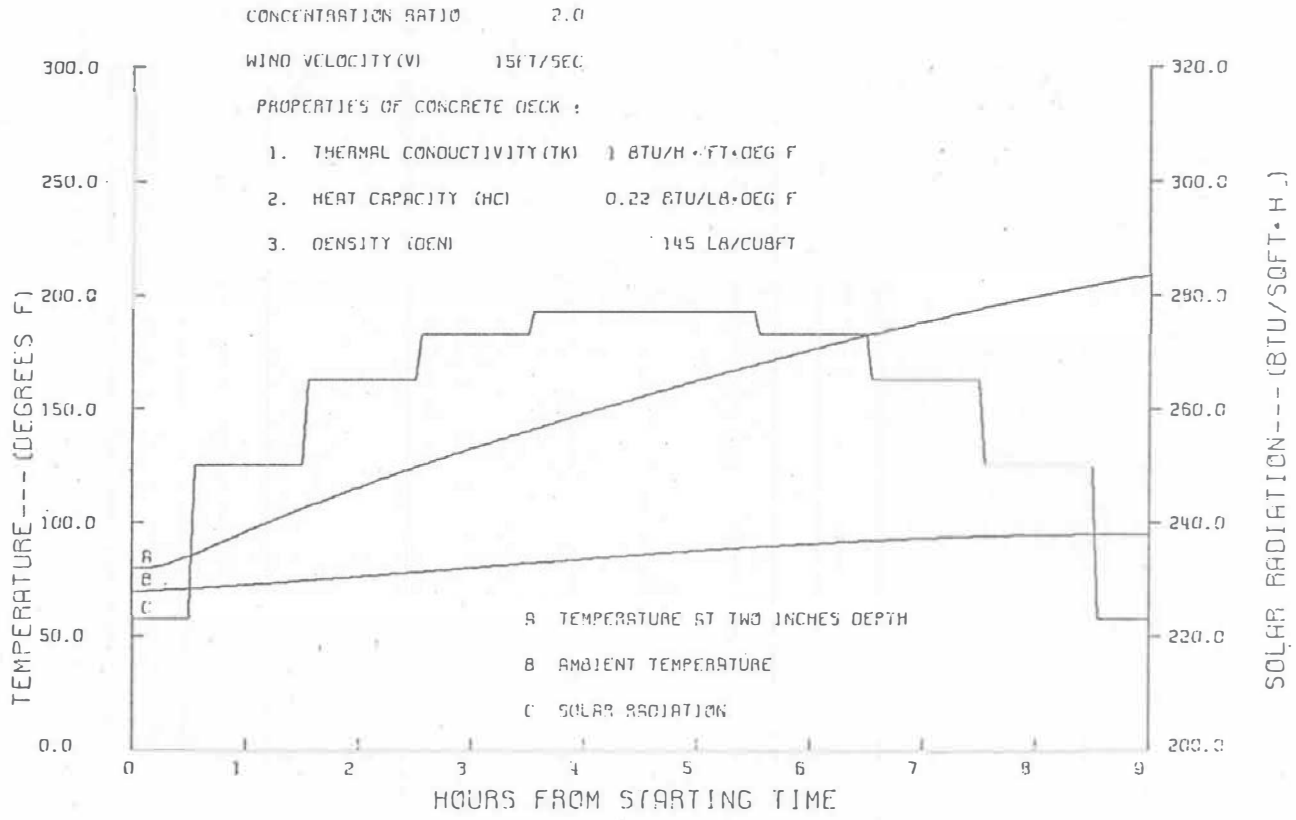

Fig. 3.26. Bridge thermal response study with focusing solar collector (c_p=0.22 Btu/lb.^{o}F, Area ratio = 2.0).

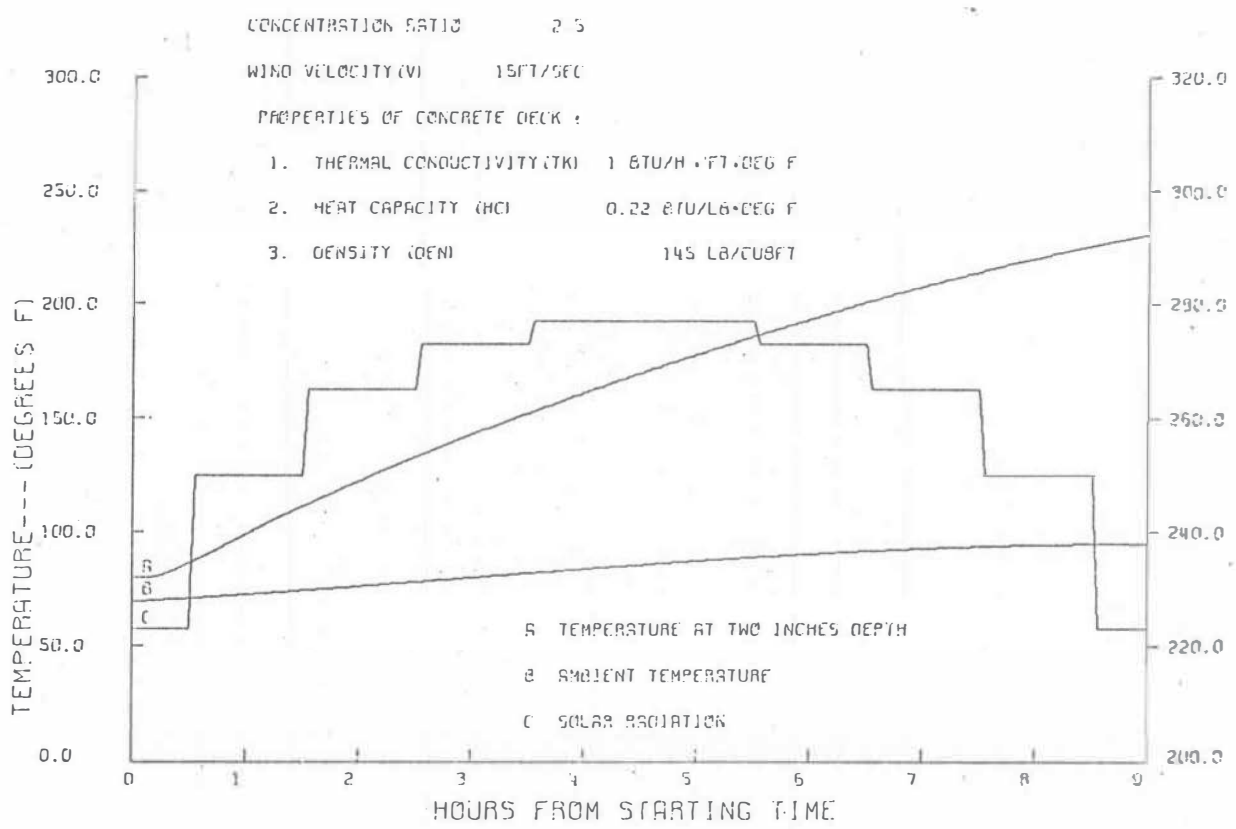

Fig. 3.27. Bridge thermal response study with focusing solar collector (c_p = 0.22 Btu/lb·°F, Area ratio = 2.5).

Weather Simulation

The analytical transient heat transfer study of these bridge models can be greatly affected by the climatic data in many ways, such as: ambient air temperature, solar flux and wind velocity, etc.

The simulation of ambient air temperature and solar insulation made in this analytical study are shown in Fig. 3.28.

The incident solar radiation was modeled as sinusoidally varying in time and was represented by

$$q''_{solar} = q''_o \text{ Sin } \omega t$$

where q''_o in this study were 310 Btu per $h \cdot ft^2$ and 280 Btu per $h \cdot ft^2$ which are representative for Oklahoma in the summer. The value of ω was $\pi/12$ where 12 denotes 12 hours of sunlight.

The ambient temperature was varied by the representation $T_{amb} = T_o + 15 \text{ Sin}\omega(t - t_o)$ where the value of t_o was taken to be 3. This allowed the air temperature to lag the solar flux by 3 hours. Various ambient air temperatures were simulated in order to show the effect of different air temperatures. A typical summer ambient temperature was chosen as $T_{amb} = 80 + 15 \text{ Sin } [\frac{\pi}{12}(t - 3)]$, which allowed for a range from a minimum 65° at night to a maximum of 95° in the day time. Time zero is considered to be 6:00 a.m.

The effect of varying wind velocity was also accounted for in the convective heat transfer coefficient used in calculation of heat losses. Wind velocity in the simulation was assumed to be a constant all through the day. Therefore, the convective heat transfer coefficient used in the calculation was a constant instead of a function of time, and the actual unsteady nature of the wind has been neglected. The variation in wind

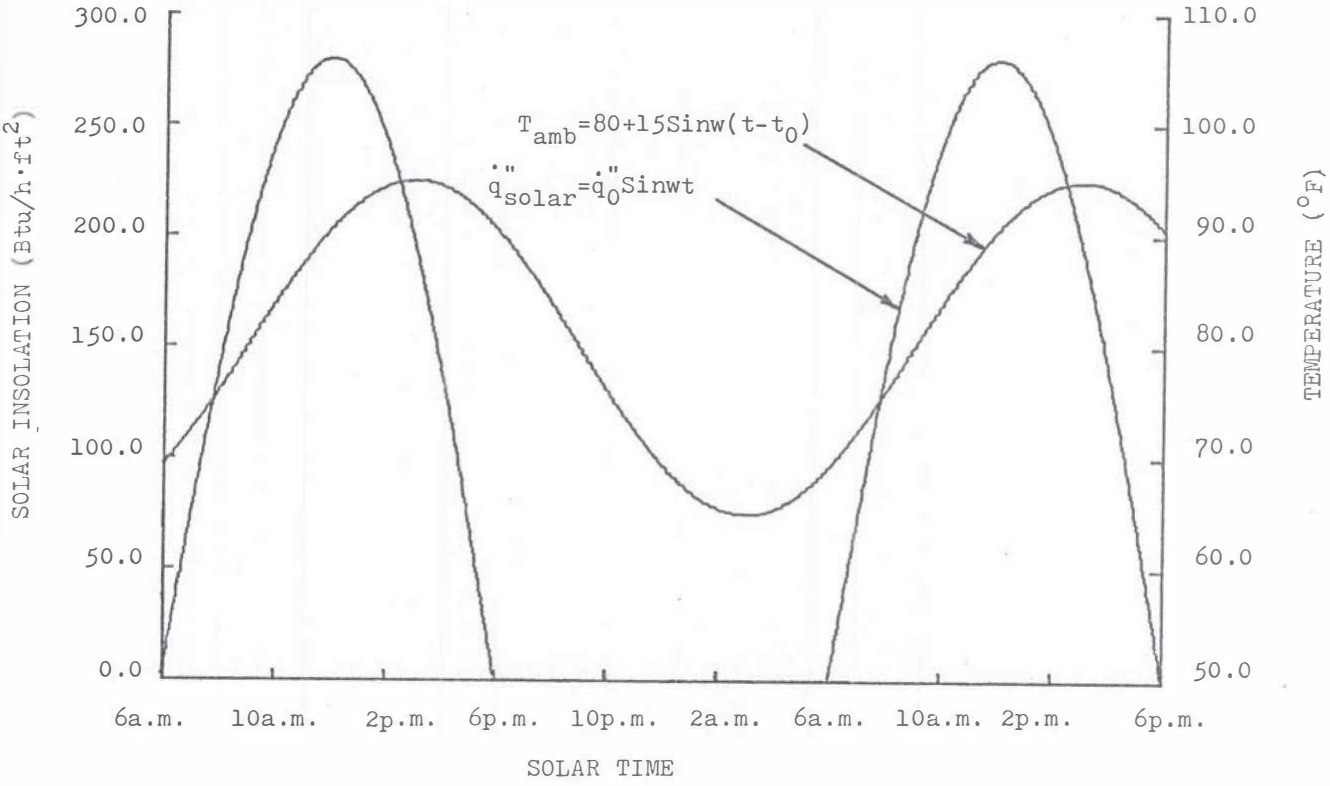

Fig. 3.28. Simulation of ambient air temperature and solar insolation.

velocity did have appreciable effect for no cover condition but as expected the effect was much less when covers were incorporated.

The heat loss from flat plates exposed to outside winds are found from a dimensional expression given by McAdams [3] which relates the heat transfer coefficient in W/m^2 °C to the wind speed in m/s

$$h_{wind} = 5.7 + 3.8V \tag{3.1}$$

The sky can be considered as a blackbody at some equivalent sky temperature so that the actual net radiation between a flat plate facing the sky and the sky can be expressed by

$$q''_{pS} = \varepsilon_p \sigma(T_p^4 - T_{sky}^4) \tag{3.2}$$

where

ε_p = flat plate emissivity

σ = Stefan-Boltzmann constant

T_{sky} = effective sky temperature

T_p = flat plate temperature

The equivalent blackbody sky temperature of equation (3.2) accounts for the fact that the atmosphere is not at a uniform temperature and that the atmosphere radiates only in certain wavelength bands. The atmosphere is essentially transparent in the wavelength region from 8 to 14 μm while outside the "window" the atmosphere has radiating bands covering much of the infrared spectrum. Several relations for clear skies have been proposed to relate T_{sky} to other measured meterological variables. Swinbank [4] relates sky temperatures to the local air temperature in the simple relationship.

$$T_{sky} = 0.0552\ T_{amb}^{1.5}$$

where T_{sky} and T_{amb} are both in degrees Kelvin.

Physical Properties of Concrete

Wide variations in reported properties were listed in Table 3.1 which shows a typical range of property values as reported in the literatures [5, 6, and 7]. These variations may cause large differences between the results for computer analysis and experimental analysis if we choose values of concrete physical properties in our computer program, which are different from the actual model. Therefore, a sensitivity analysis relative to these properties was made.

Variations in concrete density, thermal conductivity and specific heat were studied by means of the computer runs. The sensitivity analysis showed specific heat to be the prime consideration. The variations in the amount of moisture in the concrete would cause a great change in property values. It should be noted that since the specific heat of water is unity, the amount of moisture present in the slab will drastically affect the temperature achieved.

A brief analysis indicates that the effect of the steel reinforcing rod will be negligible since the density-specific heat product is not greatly different than that for concrete. This is especially true since the steel is more than 2" from the surface. Near the edges there is the possibility that the steel may afford a path for the removal of heat from the slab which would cause lower temperatures to be reached; however, the cross-section area of the steel is small relative to the concrete and the area-thermal conductivity factor assures that this effect will be small.

TABLE 3.1

PHYSICAL PROPERTIES OF CONCRETE

Thermal Conductivity (Btu/hr·ft·°F)		Density (lbm/ft^3)		Specific Heat (Btu/lbm·°F)		Literature Source
Unimpregnated Concrete	Polymer Impregnated Concrete	Unimpregnated Concrete	Polymer Impregnated Concrete	Unimpregnated Concrete	Polymer Impregnated Concrete	
1.24		134.78		0.31		5
0.54		140		0.21		6
1.332	1.265	144.6	148.9	0.241	0.220	7

Model I Flat Plate Studies

1. Blackened Bridge Surface Without Cover

This study was made to analyze the thermal response of the highway bridge model. During the day time, the top surface of the bridge will receive the incident solar radiation, also it will have convective heat loss to the ambient cooler air and the long wave radiation loss to the sky. The surroundings at the bottom side of the bridge have approximately the same temperature as the bottom bridge surface, therefore the long wave radiation from the bottom side to these surroundings can be neglected. Also there is no incident solar energy. Therefore, the radiative heat transfer from the bridge's underside is assumed to be negligible and the bottom heat loss was assumed to be by convection only. The net heat gain or loss on both sides of this model can be shown as:

$$q''(t)_{total,\ t} = \alpha q''_o \sin \omega t - \varepsilon\sigma[T^4(t) - T^4_{sky}(t)] - hc_1\,[T(t) - T_{amb}(t)]\ ,\ \text{at } x = 0 \qquad (3.3)$$

$$q''(t)_{total,\ b} = hc_2[T(t) - T_{amb}(t)],\ \text{at } x = L \qquad (3.4)$$

where

α = concrete absorptivity

ε = concrete emissivity

σ = Stefan-Boltzmann constant

$= 0.1714\ (10^{-8})\ \dfrac{Btu}{hr \cdot ft^2 \cdot R^4}$

T_{amb} = ambient air temperature (°R)

T_{sky} = effective sky temperature (°R)

hc_1 = convective heat transfer coefficient of top surface ($\frac{Btu}{hr \cdot ft^2 \cdot F}$)

hc_2 = convective heat transfer coefficient of bottom surface, ($\frac{Btu}{hr \cdot ft^2 \cdot F}$)

Thermal responses of this model are shown by means of the computer plots in Figure 3.1 through Figure 3.6. These results indicate that the top 2" temperature will not be heated to the desired 160 °F.

2. Single and Double Covers

An alternative method derived from the flat plate solar collector is shown in Figure 3.29 with a single transparent cover on top of the bridge surface. The transparent cover over the bridge surface reduces greatly the convective and the radiative heat losses in the same manner as storm windows in a home or the well known green house effect.

The scheme of double covers on top of the bridge surface may reduce more heat losses but it also reduces transmission of incident solar radiation. The directional transmittance of the covers is shown in Figure 3.30. Studies were made of the thermal responses of the bridge model with one or two glass covers on the top. The result shows that the temperature increase is very small. Figure 3.19 shows that it is not necessary to add another cover for such a small improvement.

The analytical method as outlined by Duffie and Beckman [8] was incorporated into a computer program designed to calculate the net heat absorbed with one or two covers on top of the bridge surface. The net heat gain or loss at the bottom surface is calculated in the same manner as in the previous discussion of the flat plate without cover. The only difference will be

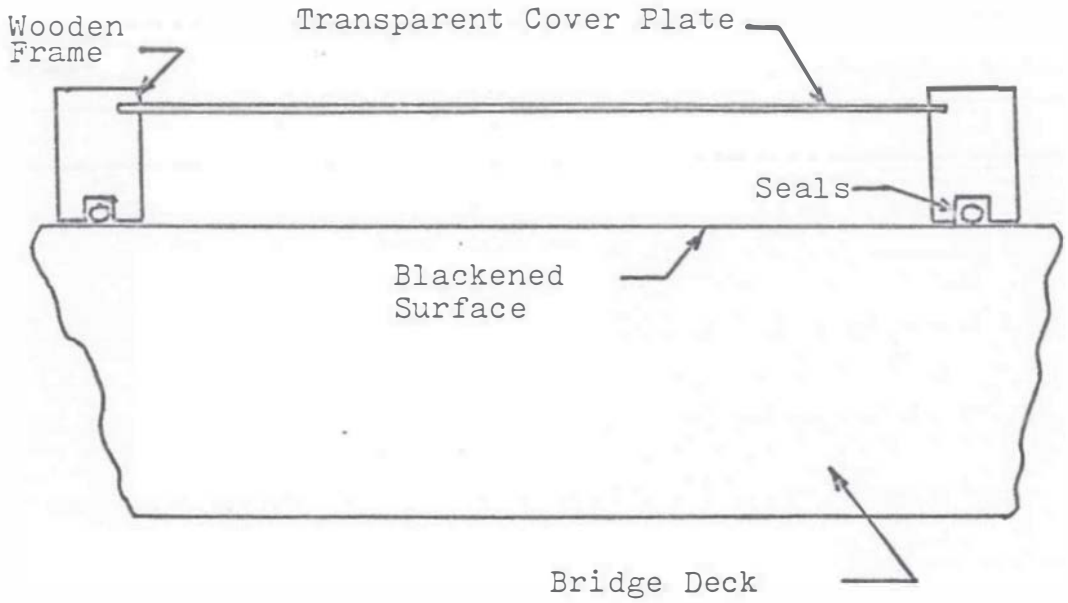

Fig. 3.29. Flat Plate Solar Collector

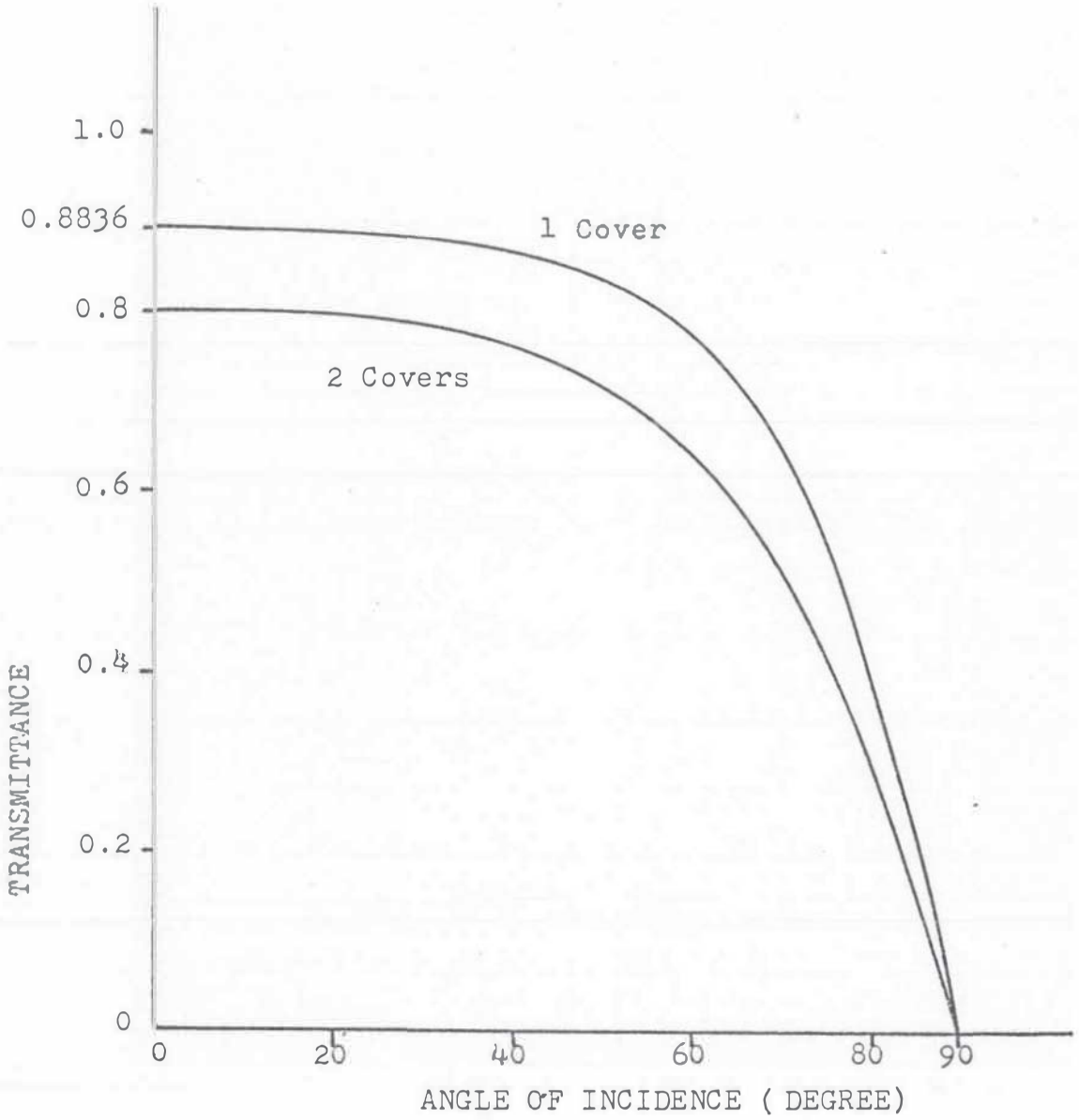

Fig. 3.30. Directional Transmittance of Cover Glass.

the top boundary condition. Due to the transparent cover, the losses from the top can be greatly reduced. But the cover also can cause a decreasing amount of transmission of incident solar radiation due to the reflection and absorption of the cover. Therefore the net energy absorption is calculated by means of the following equations:

for $\theta_1 \neq 0$

$$\rho_1 = \frac{\tan^2(\theta_2 - \theta_1)}{\tan^2(\theta_2 + \theta_1)} \tag{3.5}$$

$$\rho_2 = \frac{\sin^2(\theta_2 - \theta_1)}{\sin^2(\theta_2 + \theta_1)} \tag{3.6}$$

where

ρ_1 = polarized reflectance component in the plane perpendicular to the interface that contains the incident ray.

ρ_2 = polarized reflectance component in the direction perpendicular to the above-mentioned plane.

θ_1 = angle of incidence

θ_2 = angle of refraction

The angle θ_1 and θ_2 are related to the indices of refraction by Snell's law

$$\frac{n_1}{n_2} = \frac{\sin \theta_2}{\sin \theta_1} \tag{3.7}$$

n_1 = refractive index of medium 1

n_2 = refractive index of medium 2

Transmittance through N covers can be represented as:

$$\tau_r(\theta_1) = \frac{1}{2}\left[\frac{(1-\rho_2)}{1+(2N-1)\rho_2} + \frac{(1-\rho_1)}{1+(2N-1)\rho_1}\right] \quad (3.8)$$

where

$\tau_r(\theta_1)$ = transmittance due to reflection for the incident angle θ_1.

N = number of transparent covers.

$$\tau_a(\theta_1) = e^{-NKL/\cos\theta_2} \quad (3.9)$$

where

τ_a = transmittance concerning only the absorpiton

K = extinction coefficient

L = actual path of the radiation through the medium

A special case for radiation at normal incidence, both θ_1 and θ_2 are zero.

$$\rho = \left(\frac{n_1 - n_2}{n_1 + n_2}\right)^2 \quad (3.10)$$

$$\tau_r(0) = \left[\frac{1-\rho}{1+(2N-1)\rho}\right] \quad (3.11)$$

$$\tau = \tau_r \tau_a \quad (3.12)$$

where

τ = transmittance for both reflection and absorption

$$(\tau\alpha) = \frac{\tau\alpha}{1-(1-\alpha)\rho_d} \quad (3.13)$$

where

$(\tau\alpha)$ = Transmittance - absorptance product

ρ_d = diffuse reflectance which can be estimated by using the specular reflection of the cover system at an incident angle of 60°.

$$q''_{u(t)} = (q''_o \text{ Sin } \omega t)(\tau\alpha)(1 - d)(1 - s) \qquad (3.14)$$

$q''_{u(t)}$ = useful solar flux absorbed

d = dust factor

s = shade factor

An empirical equation for U_t was developed by Klein (1973), referenced from [8], following the basic procedure of Hottel and Woertz [9], which can be applied to calculate the energy losses due to convection and the radiation through a transparent cover,

$$U_t = \left\{ \frac{N}{(344/T_p)[(T_p - T_a)/(N + f)]^{0.31}} + \frac{1}{h_w} \right\}^{-1} + \frac{\sigma(T_p + T_a)(T_p^2 + T_a^2)}{[\varepsilon_p + 0.0425N(1 - \varepsilon_p)]^{-1} + [(2N + f - 1)/\varepsilon_g] - N} \qquad (3.15)$$

U_t = overall heat transfer coefficient at 45° collector tilted angle

N = number of glass covers

$f = (1.0 - 0.04\, h_w + 5.0 \times 10^{-4}\, h_w^2)(1 + 0.058N)$

ε_g = emittance of glass (0.88)

ε_p = emittance of plate

$T_a = T_{amb}$ (°K)

T_p = plate tempearture (top surface temperature °K)

h_w = wind heat transfer coefficient from equation (3.1)

An equation used to interpolate for other plate emittance and for the tilted angle of the plate was proposed by Klein as:

$$\frac{U_t\ (D)}{U_t(45)} = 1 - (D - 45)(0.00259 - 0.00144\ \varepsilon_p) \qquad (3.16)$$

where

D = the tilt angle in degrees

Therefore, the losses from the top surface can be represented as:

$$q''_L\ (t) = U_L(t)[T(t) - T_{amb}\ (t)] \qquad (3.17)$$

The net energy gain or loss from the top surface can be shown as:

$$q''\ (t)_{total,\ t} = q''_u\ (t) - q''_L\ (t) \qquad (3.18)$$

Model II. Focusing Collector

As a result of the flat plate studies, we conclude that the incident solar flux absorbed by the bridge surface with this simple model is not sufficient to heat the bridge to the desired temperature. A method that can provide a higher energy flux to the bridge surface must be made to achieve the required heating. One way that this can be achieved with solar energy is to use a solar focusing collector, heat exchanger system.

The focusing collectors utilize optical system reflectors or refractors, to increase the intensity of solar radiation which is absorbed. Therefore, higher temperatures will be achieved by the focusing collector and this higher temperature energy can be more readily used with a heat exchanger to heat up the bridge to the desired temperature. A concept as shown in Figure 3.31 was designed to achieve this purpose. The solar collector, fluid, heat exchanger, and piping system were treated as a lumped system at temperature T^i_{avg}, where i indicates a certain time interval i. An amount of energy $(\dot{Q}^i_{useful})\ (\Delta t)$ is absorbed by solar collector, $(\dot{Q}^i_R)\ (\Delta t)$ is the energy released from the heat exchanger to the slab

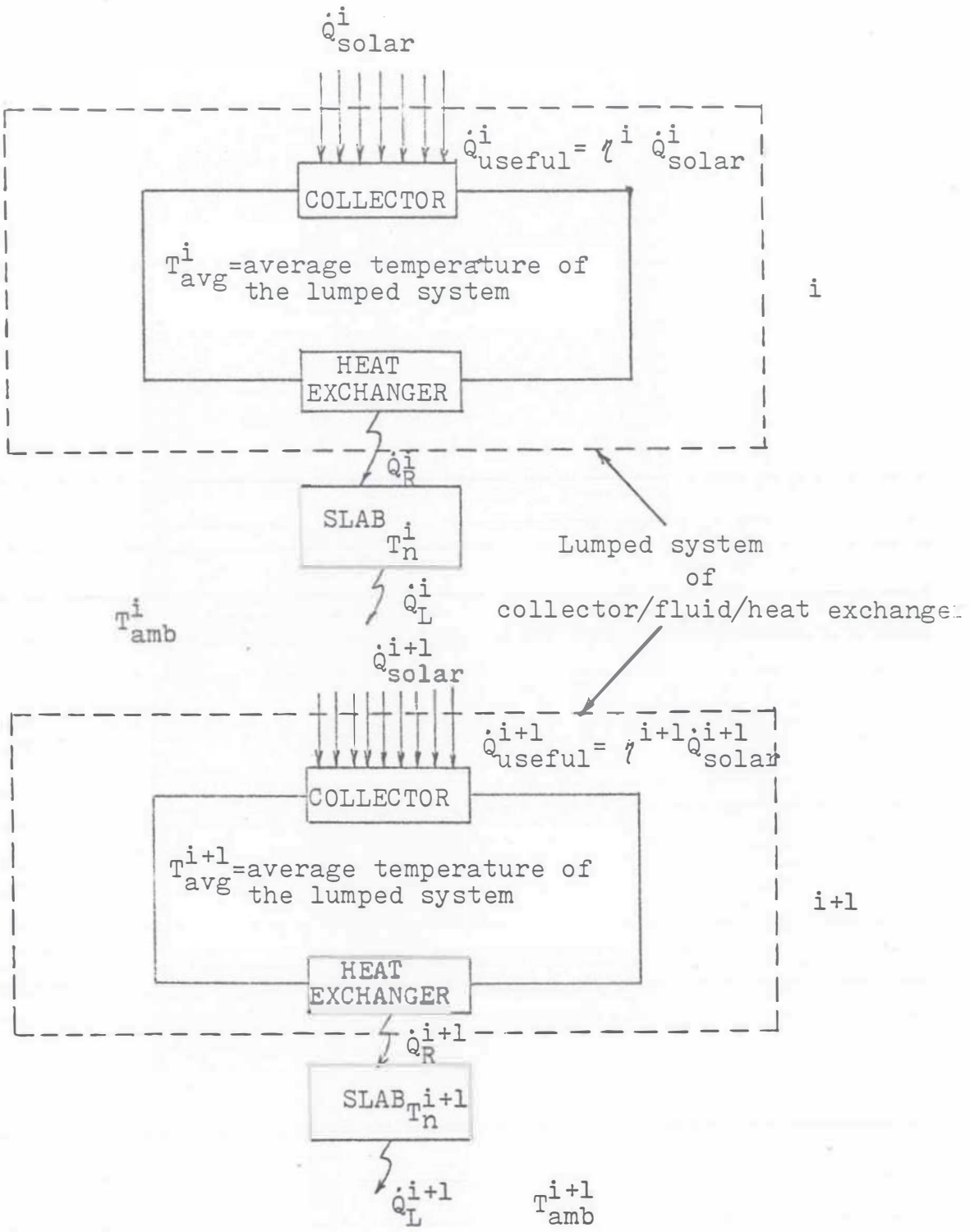

Fig. 3.31 Lumped system of collector/fluid/heat exchanger at time interval i+1 and i respectively.

during time interval $(i - 1)$ to i. The remaining energy $(\dot{Q}^i_{useful} - \dot{Q}^i_R)(\Delta t)$ will be stored to increase the lumped system to the temperature T^{i+1}_{avg} (T_{avg} at time interval $(i + 1)$). An energy balance was made for the slab system so that the amount of energy $(\dot{Q}^i_R)(\Delta t)$ absorbed by the slab minus the energy $(\dot{Q}^i_L)(\Delta t)$ lost from the slab to the surroundings by heat convection in time interval $(i - 1)$ to i can be stored in the slab to raise the slab temperature from T^{i-1}_n, where n indicates the temperatures at different depths of the slab, to the temperatures of T^i_n. The mathematical model can be arranged as:

$$(mc_p)_{sys}(T^{i+1}_{avg} - T^i_{avg}) = (\dot{Q}^i_{useful} - \dot{Q}^i_R)(\Delta t) \qquad (3.19)$$

where

$(mc_p)_{sys}$ = mass-specific heat product of the whole lumped system

$$\dot{Q}^i_{useful} = (\eta^i)(\dot{Q}^i_{solar}) \qquad (3.20)$$

where

η^i = the efficiency of the solar collector at time interval i.

$$\dot{Q}^i_R = \frac{\rho cA}{\Delta t}\left(\int_o^L T^i_N\, dx - \int_o^L T^{i-1}_N\, dx\right) + \dot{Q}^i_L \qquad (3.21)$$

where ρ - Density of concrete slab

c - Specific heat of concrete slab

L - Thickness of concrete slab

$$\dot{Q}^i_L = (hc_2)(A)(T^i_N - T^i_{amb}) \qquad (3.22)$$

where

hc_2 = bottom convective heat transfer coefficient

A = area of slab

T_N^i = bottom surface temperature at time interval i.

From equation (3.19)

$$T_{avg}^{i+1} = T_{avg}^{i} + (\dot{Q}_{useful}^{i} - \dot{Q}_R^i)\,\Delta t/(mc_p)_{sys} \tag{3.23}$$

The temperature difference between heat exchanger and slab surface can be determined if the contact resistance between them and the amount of heat released from the heat exchanger is known. The equation for contact resistance can be written as follows:

$$R^{i+1} = \frac{F_{avg}^{i+1} - T_o^{i+1}}{\dot{Q}_R^{i+1}} = \frac{\Delta T^{i+1}}{\dot{Q}_R^{i+1}} \tag{3.24}$$

where

R^{i+1} = Contact resistance

$$\Delta T^{i+1} = T_{avg}^{i+1} - T_o^{i+1} \tag{3.25}$$

Then, the top boundary temperature at time (i + 1) interval can be expressed as:

$$T_o^{i+1} = T_{avg}^{i+1} - \Delta T^{i+1} \tag{3.26}$$

where

T_o^{i+1} = top surface temperature at time interval (i + 1)

An idealized assumption was made that the temperature ranges for T_{avg}^{i+1} and T_o^{i+1} will not be too large and the heat released from heat exchanger is a constant, then ΔT^{i+1} can be treated as a constant that can be programmed in the computer program in order to investigate the bride thermal response. The values of 0°F and 20°F were assumed as

ΔT^{i+1} in the computer program. The results indicate that the slab temberature at 2" depth from the top will reach 160°F in less than 9 hours, (with area ratio = 2 system). The results are shown on Figures 3.21 to 3.27.

CHAPTER IV

EXPERIMENTAL STUDY

Experiments were conducted on the North Campus at the AMNE research center of the University of Oklahoma, Norman. The temperature profiles of the concrete slab bridge model were measured during tests involving several different heat exchanger concepts which incorporated two Northrup focusing solar collectors, piped in parallel, and also with the single covered blackened surface of the bridge model.

The reason for introducing focusing solar collectors to heat up the bridge is to deliver the heat into the slab at a higher temperature.

More detailed descriptions concerning these models and the results are discussed in the following chapters.

Description of Apparatus

A bridge model was designed according to the drawing furnished by the Oklahoma Highway Department, drawing No. PCB-42.75-1. A Section as shown in Fig. 4.1 was chosen for this model. To simulate the bridge, a slab 57" by 47" by 8" thick was poured on forms such that the completed bridge deck rested on concrete block piers 4' high along the 47" edges. The bridge had rebar steel inserted according to the bridge specifications.

Copper-constantan thermocouples were placed in the center of the slab and at the edge locations as indicated in Fig. 4.2. In order to

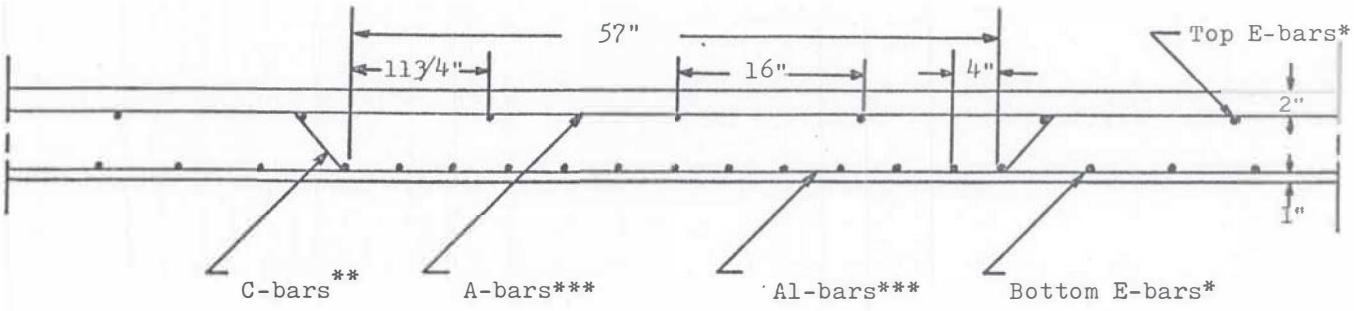

* E Bars, ½" Dia. (3 top E bars, 11 bottom E-bars), 46" long.

** C-bars, 5/8" Dia. (4 pieces), 56" long.

*** A-bars and Al-bars, 3/4" Dia., (4 pieces) and 3/4" Dia, (5 pieces) respectively, 56 " long.

Fig. 4.1 . Cross Sectional view of highway bridge.

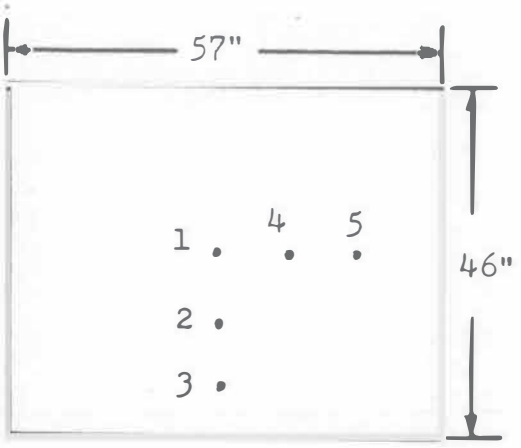

Figure 4.2 Locations of all the thermocouples inside the slab.

LOCATION 1 (CENTER OF SLAB)

Thermocouples	Depth (inches)
1	surface
2	$\frac{1}{2}$
2	1
2	$1\frac{1}{2}$
3	2
1	3
1	4
1	7

LOCATIONS 2, 3, 4, AND 5

Thermocouples	Depth (inches)
1	surface
1	1
1	2

insure the thermocouples were in the proper location, the following procedure was followed. Copper tubing 1/8" dia. was cut to 10" lengths. Holes for thermocouples were drilled in the bottom of the concrete form and the copper tubes were positioned over these holes. As shown in Fig. 4.3. The thermocouples were inserted in the tubes to the proper depth in the bridge. As the concrete was poured and reached the 8" level, the tubes were removed upward with a gentle vibratory motion to insure that the concrete settled around the thermocouple. This procedure was followed in order to be certain that no aggregate was directly above a thermocouple which might cause the thermocouple to settle to a lower position.

After the bridge deck had cured for about a week, the forms were removed but the concrete was covered with a plastic sheet. The slab was then exposed to the summer sun for several days in order to remove the moisture.

Two of the Northrup focusing collectors were purchased for this experimental study. The collector is 1' wide by 10' long for an effective area of 9.72 ft^2 as shown in Appendix A. The target tube is 2" wide and has a black chrome selective absorber coating with : $\alpha = 0.93$, $\varepsilon = 0.12$ or $\alpha/\varepsilon = 7.75$. The tracking unit is rated at 2.59 °/min or 10.21 times sun speed with an accuracy of $\pm$ 0.20°. The published efficiency of the tracker is shown in Fig. 3.20. The purchase price for these units was:

collectors	$154.00 each
tracker	$284.72 each
frame	$ 67.26

A special aluminium steel frame was constructed to hold the collectors. The frame is mounted on casters for easy moving and has an adjustable rear

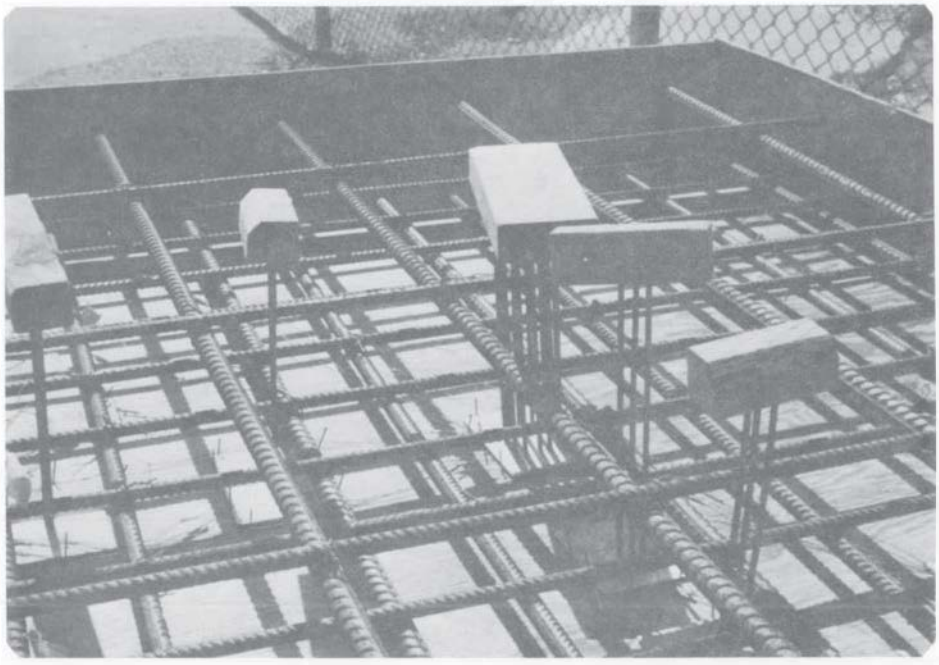

Fig. 4.3. Thermocouples in the tubes to the proper depth. Steel rebars inserted at different levels and locations.

Fig. 4.4. After concrete was poured on forms and surface being levelled.

height from 69" to 103". The front height of the frame is 9". This is sketched in Fig. 4.5. The adjustable height allows for positioning the collector at angles with the horizon ranging from 19.28° to 40.6°. A Viking pump series 432 FH with nominal rating of approximately 3 gallons per minute at 1800 rpm was incorporated in the circuit. The pump was calibrated with scale and stop watch, and the calibration shows that the pump in this circuit delivered between 3.2 - 3.3 gallons per minute with the Mobiltherm 603 fluid in the circuit. All piping was covered with 1½ fiberglass insulation (k = 0.275 Btu in·per h·ft^2· F) as shown in Fig. 4.6. A one gallon expansion tank was placed in the system to allow for volumetric expansion of the heat transfer fluid during heating. Copper-Constantan thermocouples were located in the piping as indicated in Fig. 4.7. The heat transfer fluid chosen was the mobiltherm 603 used in the analytical study. The specifications for this fluid are shown in Fig. 4.8. The fluid was chosen since we intended to utilize high temperatures, but the acutal results never achieved the desired temperatures. A Bell and Gosset flow indicator was placed in the system to give an indication of flow rate and to insure air entrainment was not present. Several heat exchanger concepts were evaluated.

1. The first exchanger design was made with 1/8" steel plate and 1/2" by 1/2" square tubing in a serpentine pattern as shown in Fig. 4.9. Calculations based on 1.5 gallons per minute flow rate through the tubes indicated a mean heat transfer coefficient of h_m = 58.6 Btu per h·ft^2· F. The heat exchanger was placed on the bridge deck and the top of the heat exchanger was covered with 6" of 700 series (high temperature) fiberglass insulation board (k = 0.375 Btu in·per h·ft^2· F), as shown in Fig. 4.10.

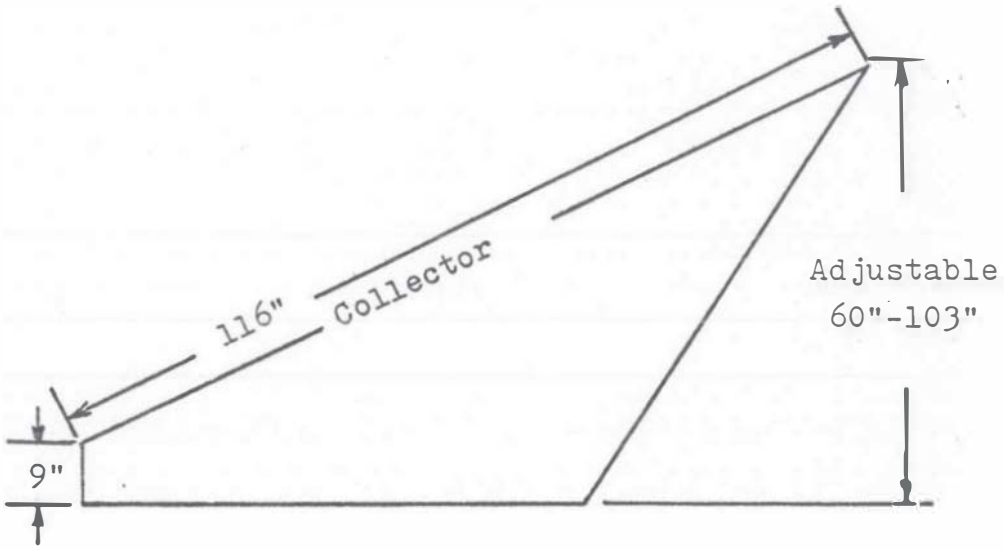

Fig. 4.5 Scheme of Solar Collector Frame.

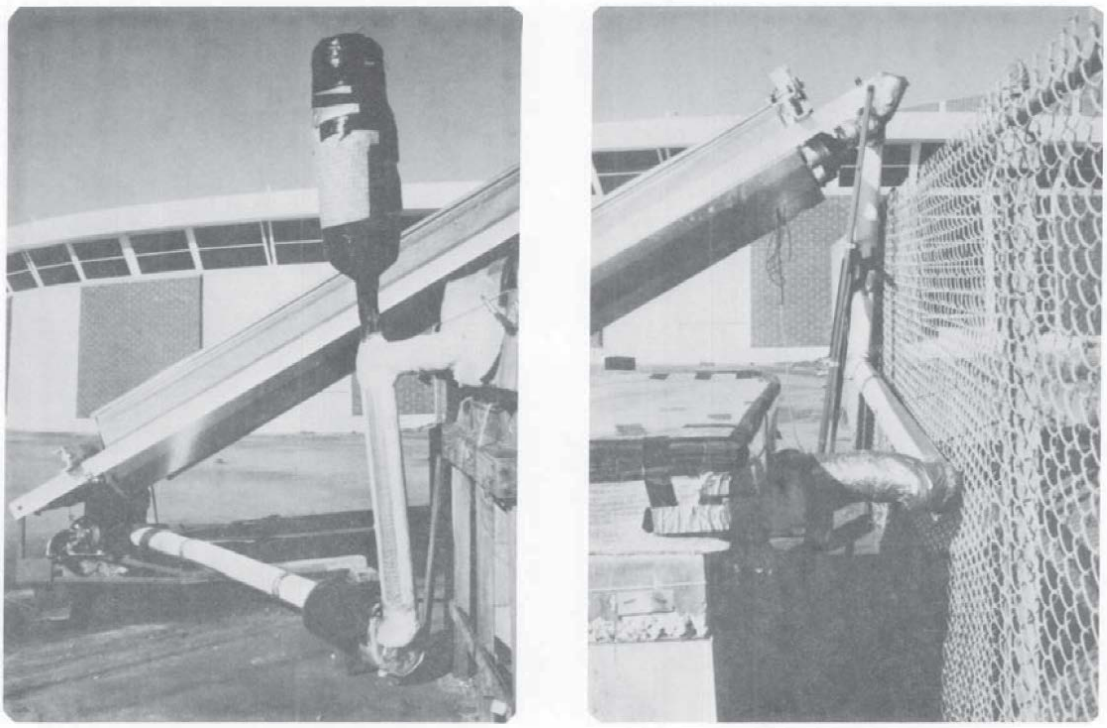

Fig. 4.6. Left side: Insulated pipe from heat exchanger to the pump.

Right side: Insulated pipe from solar collector to the heat exchanger.

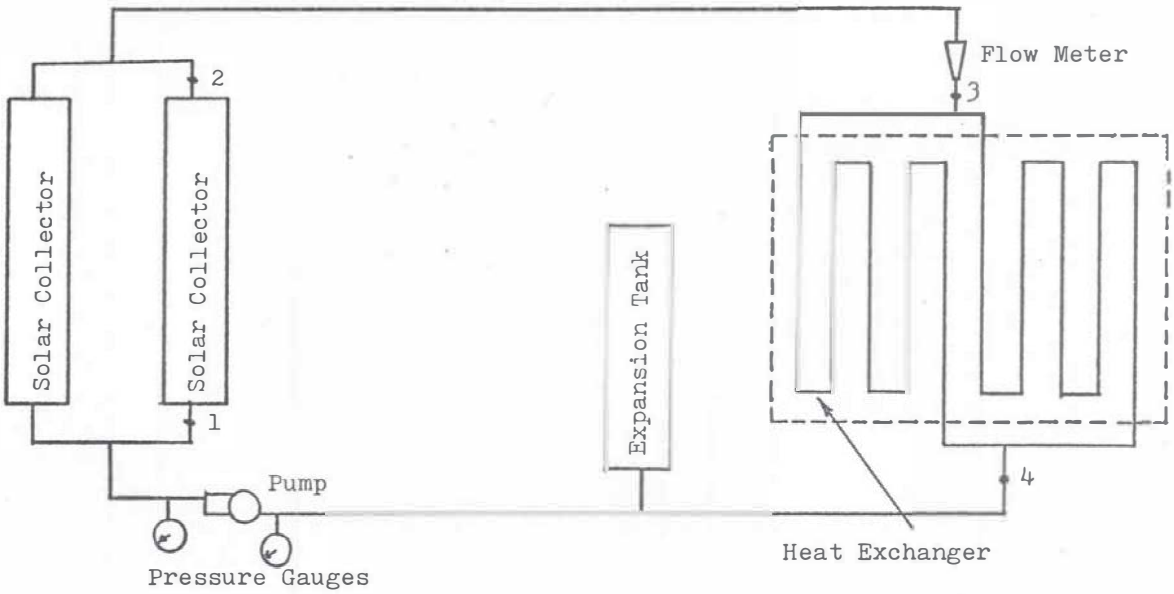

Thermocouples Locations: 1 - Solar collector inlet
2 - Solar collector outlet
3 - Heat exchanger inlet
4 - Heat exchanger outlet

Fig. 4.7. Thermocouple locations of solar collector and heat exchanger system

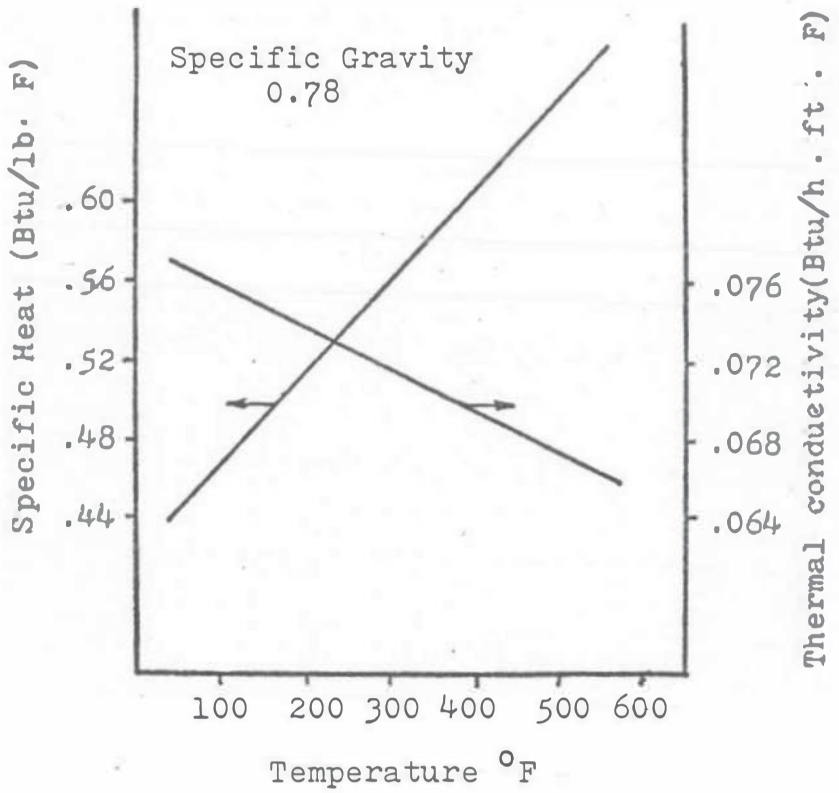

Fig. 4.8. Thermal properties of Mobiltherm 603.

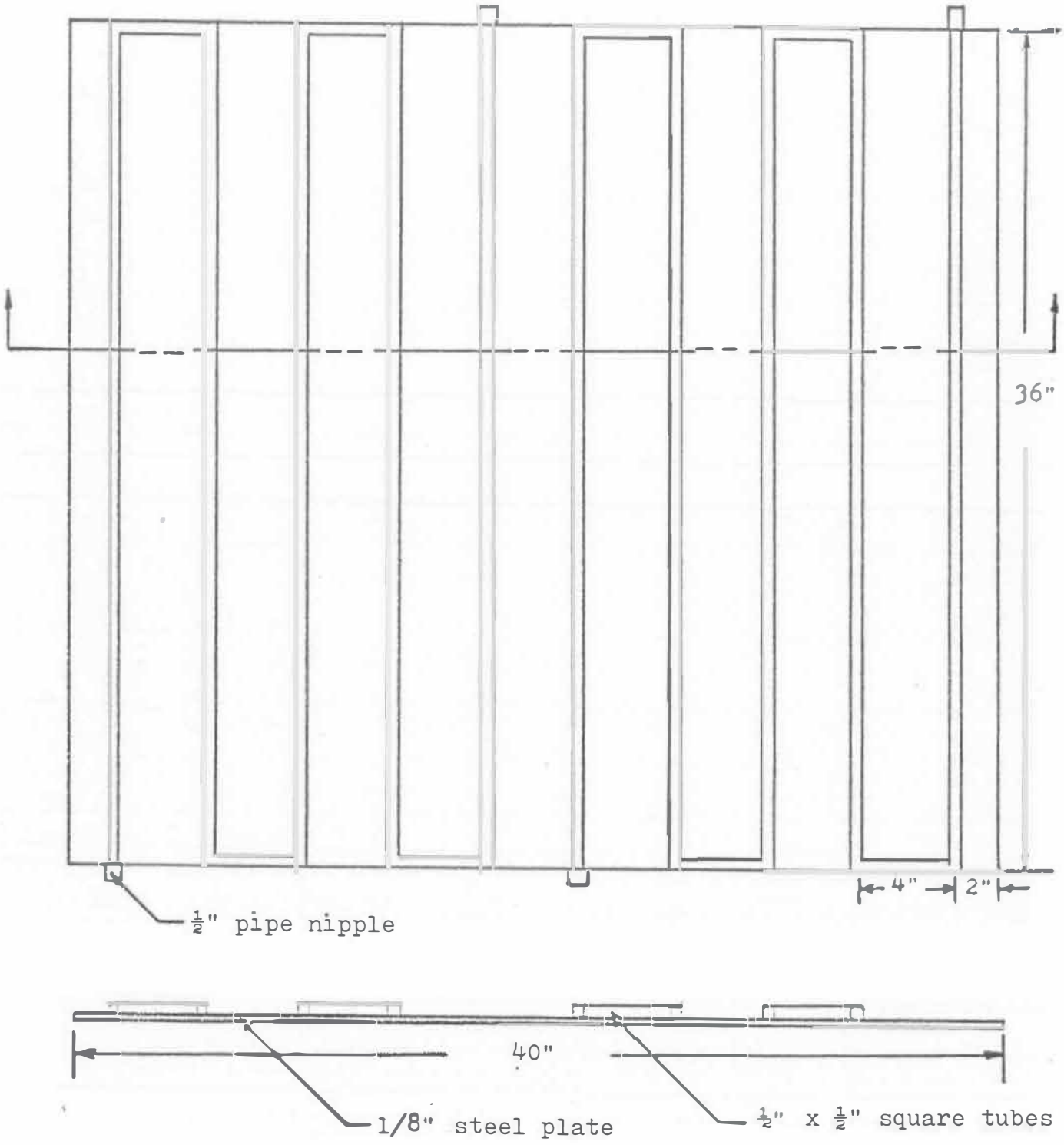

Fig.4.9. Tube in sheet type heat exchanger.

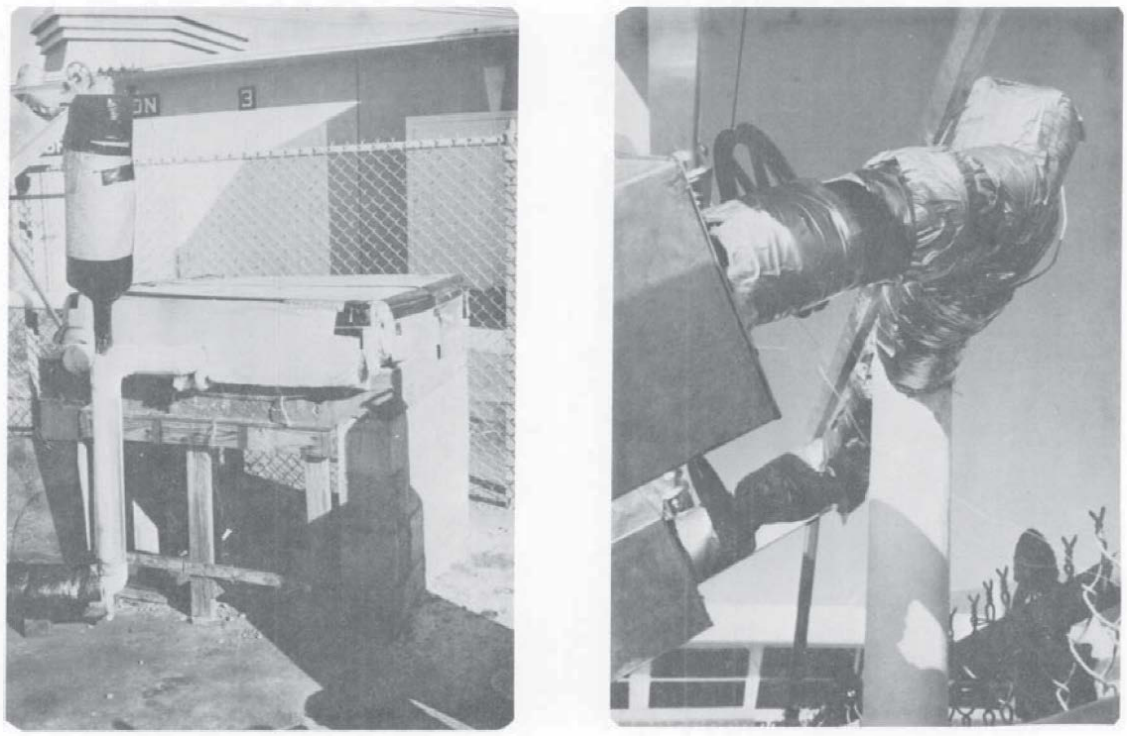

Fig. 4.10. Left side : Outlet end of heat exchanger, where the top surface and the edges were covered with fiberglass board insulation. The expansion tank as shown was also well insulated with fiberglass sheet.

Right side: Outlet end of solar collector where the S shaped copper tubes were insulated with fiberglass sheet.

2. The second heat exchanger is a modification of the first heat exchanger. Instead of putting fiberglass insulation on the top of it, a glass cover designed as shown in Fig. 4.11 was positioned on top of the heat exchanger, so that the heat exchanger will function as a solar absorbing plate which can therefore absorb more solar energy than the first concept, and will be able to deliver more energy to the bridge slab.

3. A final concept as shown in Fig. 4.12, is a pooled oil concept intended to reduce the thermal contact resistance between the heat exchanger and the surface of bridge slab. The contact resistance was one of the major problems for the bridge heating with the first and second concepts of the heat exchanger.

The tracking system, bridge deck and the first heat exchanger were completed and put into operation in late summer of 1977. At this time we experienced leaks in the quick connect swivels provided with the Northrup collectors and poor tracking caused by poorly aligned copper "S" shaped connecting tubes. After elimination of leaks, and realignment of copper tubes we began to take data, however, we experienced difficulty in keeping both collectors focused while tracking. This seems to be a problem inherent in the steel cable drive used with the trackers. For large systems this is not a serious problem because one or two collectors in forty does not make an appreciable difference. However, for our system with only two collectors this was totally unacceptable. Only with careful adjustments

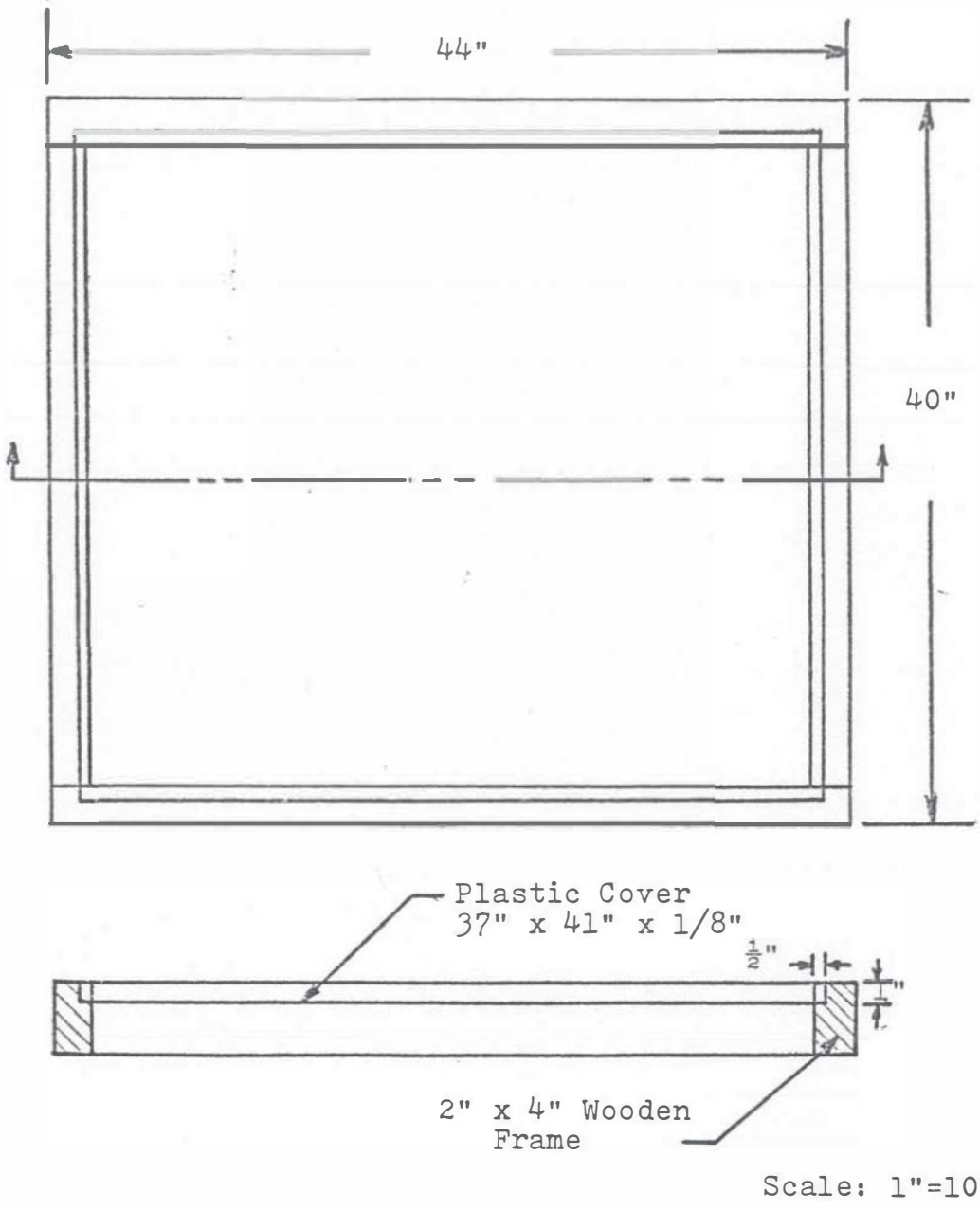

Fig. 4.11. Scheme of single glass cover

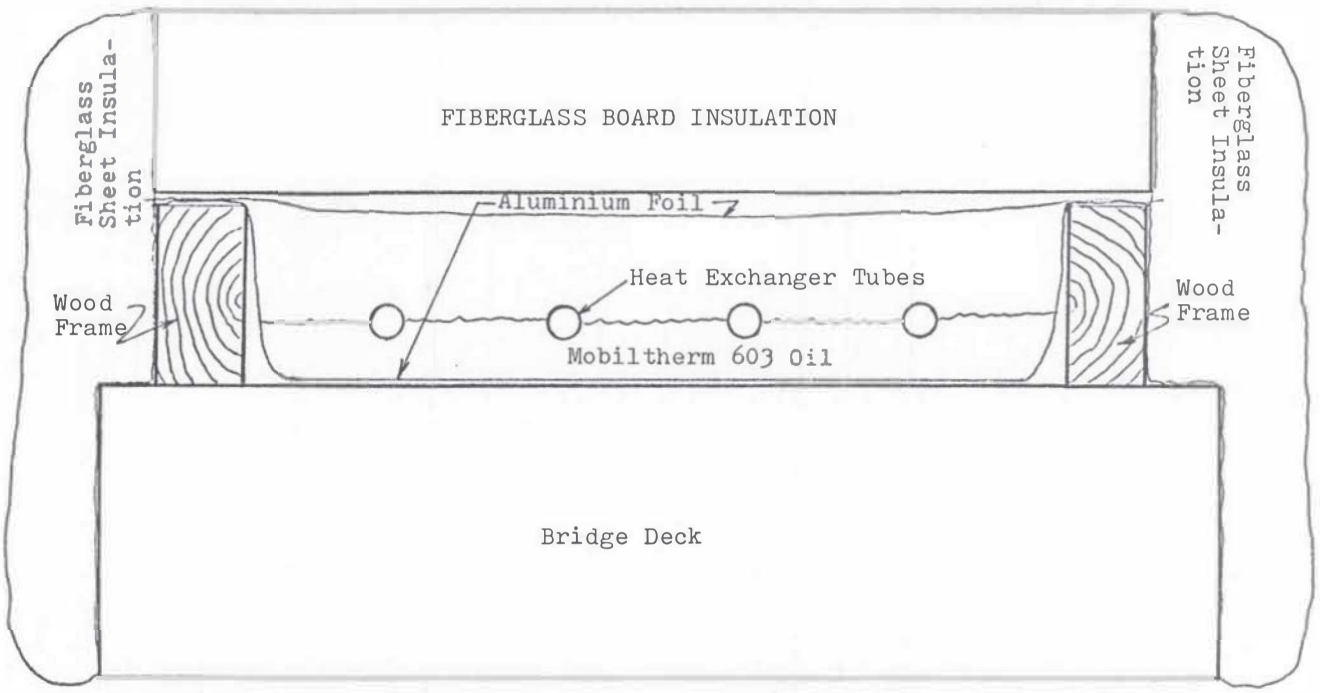

Figure 4.12. Copper Tubes embedded in oil type heat exchanger.

and constant surveillance were we able to keep both collectors forcused. At this time the daily weather involved a great deal of intermittant cloud cover. The system tracked nicely when there was no cloud cover, however, with the intermittant clouds the tracker would stop while the cloud passed between the sun and collector and then start tracking again. By the time the tracker has refocused the collectors, another cloud was blocking the sun. This experience showed an important difficulty one might expect with focusing collectors. During the November of 1977, the tracker malfunctioned and had to be replaced. In May, 1978, the tracking control panel was replaced, and data was collected for the different experiments.

Results of Experiments

1. Tube-in-Sheet Type Heat Exchanger. The heat exchanger was made 40" by 36" for 10 ft^2 of heated area. With this heat exchanger we experienced a contact resistance which produced contact temperature differences as shown in Table 4.1. The data was taken on May 15, 1978. The maximum value at 1400 hours (approximately half an hour after the solar noon) was 55.4°F while the collector fluid temperature was only 169.3°F. Of course, some contact temperature difference was expected due to the difficulty of maintaining good contact with a flat (not perfectly flat) steel plate to a somewhat uneven concrete surface. To reduce the contact resistance we introduced "Thermon" thermal cement between the heat exchanger plate and the surface of the bridge deck. The cement is water soluable and therefore can be easily removed. With this modification, the contact temperature difference was reduced to approximately 26°F as shown in Table 4.2 (the highest value from the data taken on October 13, 1977). This scheme is more acceptable, but the cement is expensive and may be too expensive to

TABLE 4.1

DATA MEASURED ON MAY 15, 1978, WITH NORTHRUP FOCUSING COLLECTOR

AND TUBE IN SHEET TYPE HEAT EXCHANGER

Time (h)	T_{avg}(°F)	ΔT(°F)	T_s(°F)	$T_{1/2}$(°F)	T_1(°F)	T_2(°F)	T_4(°F)	T_5(°F)	T_{amb}(°F)
09:30	104.9	31.5	73.4	72.5	72.5	72.5	71.6	71.6	72.5
10:00	116.2	35.6	80.6	78.8	77.0	75.2	71.6	71.6	74.8
10:30	132.4	46.4	86.0	83.3	80.6	77.9	73.4	72.5	79.7
11:00	141.4	49.1	92.3	89.2	85.8	83.3	76.1	75.2	81.0
11:30	149.5	52.5	97.0	93.2	89.6	85.0	77.9	76.1	82.4
12:00	154.9	52.7	102.2	97.7	93.4	88.7	80.6	79.0	84.2
12:30	160.3	53.6	106.7	102.2	97.7	92.3	83.3	82.0	88.0
13:00	-	-	-	-	-	-	-	-	-
13:30	166.6	52.7	113.9	109.4	104.9	99.5	89.6	86.9	89.6
14:00	169.3	55.4	113.9	112.1	107.6	102.2	92.3	89.6	91.4
14:30	168.4	50.0	118.4	113.9	109.4	104.0	93.2	90.5	89.6
15:00	168.4	48.2	120.2	115.7	111.2	105.8	95.0	92.3	89.6
15:30	168.9	46.0	122.9	117.5	113.9	108.0	97.7	94.1	88.7
16:00	168.4	43.7	124.7	119.3	115.7	110.3	99.5	96.8	88.7
16:30	168.4	41.9	126.5	122.0	117.5	113.0	102.2	98.6	88.7
17:00	168.1	39.8	128.3	123.8	119.3	114.8	104.0	100.4	87.8
17:30	166.7	37.5	129.2	125.2	121.1	115.7	105.8	102.2	86.0
18:00	161.2	32.0	129.2	125.6	122.0	117.5	107.6	104.0	85.6

Remarks: 1) Time indicates daylight saving of the central area.

2) T_s, $T_{1/2}$, T_1, T_2, T_4, and T_5 show the temperatures measured at the depth of surface, ½", 1", 2", 4" and 5". T_{avg} means the average temperature of heat exchanger.

3) Wind: 5-10 mph

4) Tracking Condition: very well

5) Clear sky all through the day.

TABLE 4.2

DATA MEASURED ON OCTOBER 13, 1977, TUBE-IN-SHEET

HEAT EXCHANGER WITH THERMAL CEMENT

Time (h)	T_{avg}(°F)	ΔT(°F)'	T_s(°F)	T_2(°F)	T_{amb}(°F)
08:45	84.2	- 7.2	91.4	91.4	46.0
09:15	115.7	17.1	98.6	91.4	50.0
09:45	127.9	22.1	105.8	93.2	53.0
10:15	136.9	24.8	112.1	97.7	55.0
10:45	144.5	26.1	118.4	104.0	57.0
11:15	151.7	26.1	125.6	107.6	60.0
11:45	157.1	24.3	132.8	111.2	64.0
12:15	162.5	26.1	136.4	116.6	68.0
12:45	166.6	25.7	140.9	120.2	73.0
13:15	170.2	26.6	143.6	122.9	77.0
13:45	172.0	23.9	148.1	125.6	80.0
14:15	172.0	23.0	149.0	129.2	80.0
14:45	173.3	22.5	150.8	131.9	79.5
15:15	173.8	20.3	153.5	134.6	79.0
15:45	176.0	20.7	155.3	136.4	79.0
16:15	176.9	19.8	157.1	138.2	79.0
16:45	177.4	18.5	158.9	140.9	78.5

Remarks: 1) Time indicates daylight saving time of central area.

2) Clear sky all through the day.

3) Solar collectors inclined at an angle of 23.88°.

use on an installation as large as a real bridge deck. Typical data taken with this heat exchanger is shown in Table 4.1 and Fig. 4.13. Also shown in the figures from 4.14 through 4.18 are the comparison with the analytical model which was assumed with various specific heat, effective surface area and the percentage of heat loss from the entire system. The analytical computer program was modified to simulate with the measured ambient temperatures and contact temperature differences. However, the assumed heat losses from the system must be incredibly high in order to force the temperature profiles of the experimental result and analytical results to be comparable. The effect of low efficiencies for the Northrup solar collectors will cause the same result as the high heat losses assumed in our analytical computer program. The former was later found to be more reasonable in our experimental program. The details will be discussed in the latter part of this chapter.

The highest temperature of the fluid only reached 169.3 °F. Also, due to the effect of thermal contact resistance, the highest surface temperature was 129.2 °F and the temperature at 2 inches depth was only about 118 °F after 8½ hours of continuous tracking period. In summary, the desired concrete slab temperatures were not achieved.

2. Modified Heat Exchanger of the First Type. Instead of putting fiberglass insulation on the top of the first type heat exhanger, a plexiglass cover was laid on top of it. The result is shown in Table 4.3 and Fig. 4.19. The maximum temperature of fluid was 177.4 °F which showed 8.1 °F increase. The maximum surface temperature and 2 inch temperature were 136.4 °F and 121.1 °F respectively after 7 hours tracking period. Somewhat higher temperatures than those shown in Table 4.3 could have been

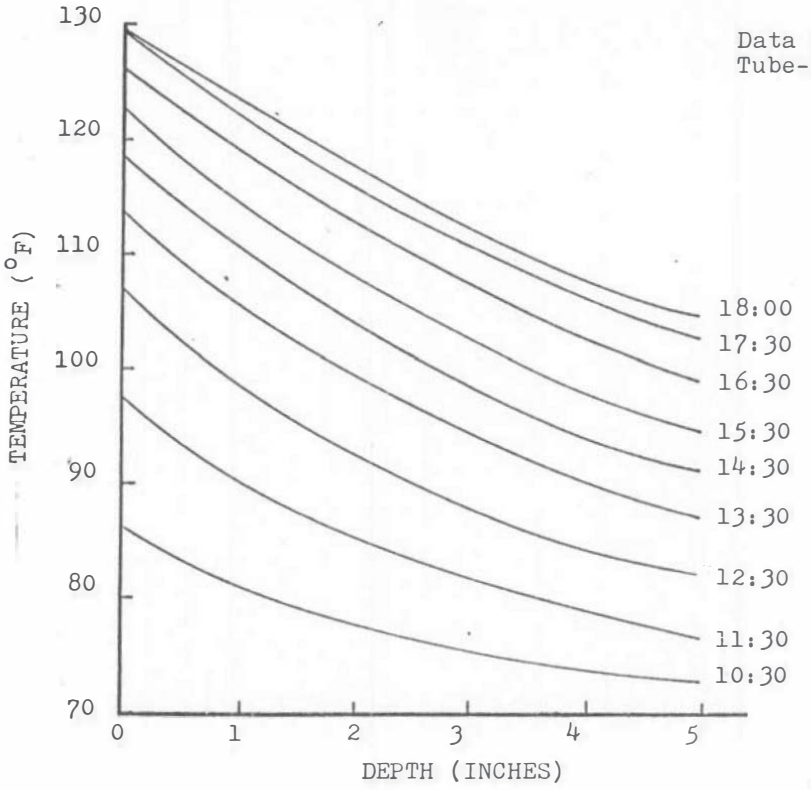

Fig. 4.13. Temperature distribution in the bridge deck with tube-in-sheet type heat exchanger.

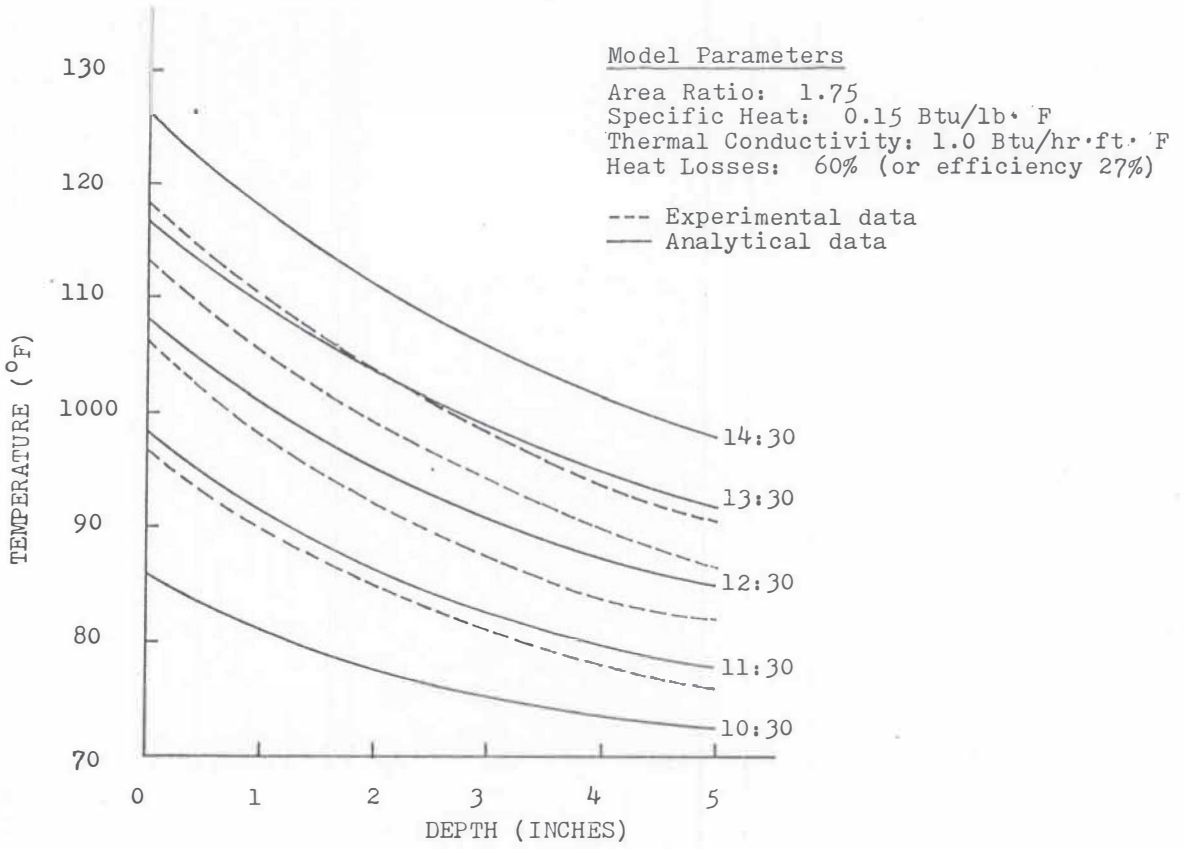

Fig. 4.14. Comparison of experimental data and analytical data (c_p=0.15 Btu/lb· F, Area Ratio = 1.75, Heat Losses = 60%)

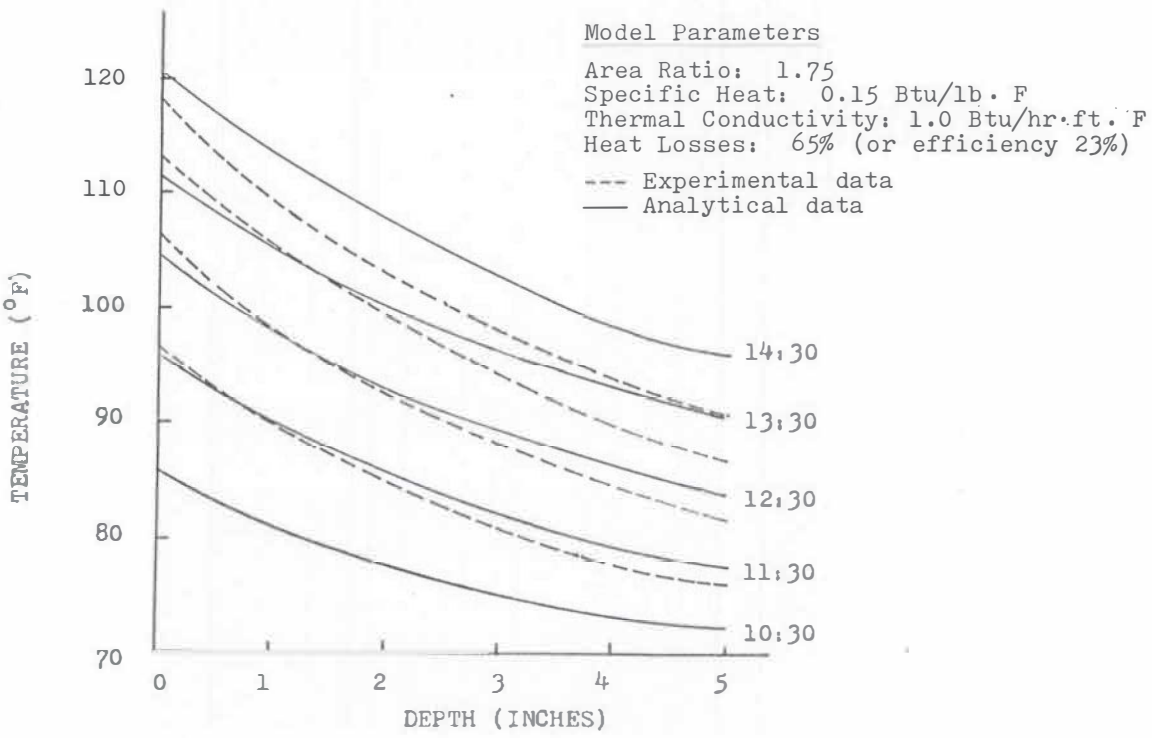

Fig. 4.15. Comparison of experimental data and analytical data (c_p=0.15 Btu/lb · F, Area Ratio=1.75, Heat Losses=65%)

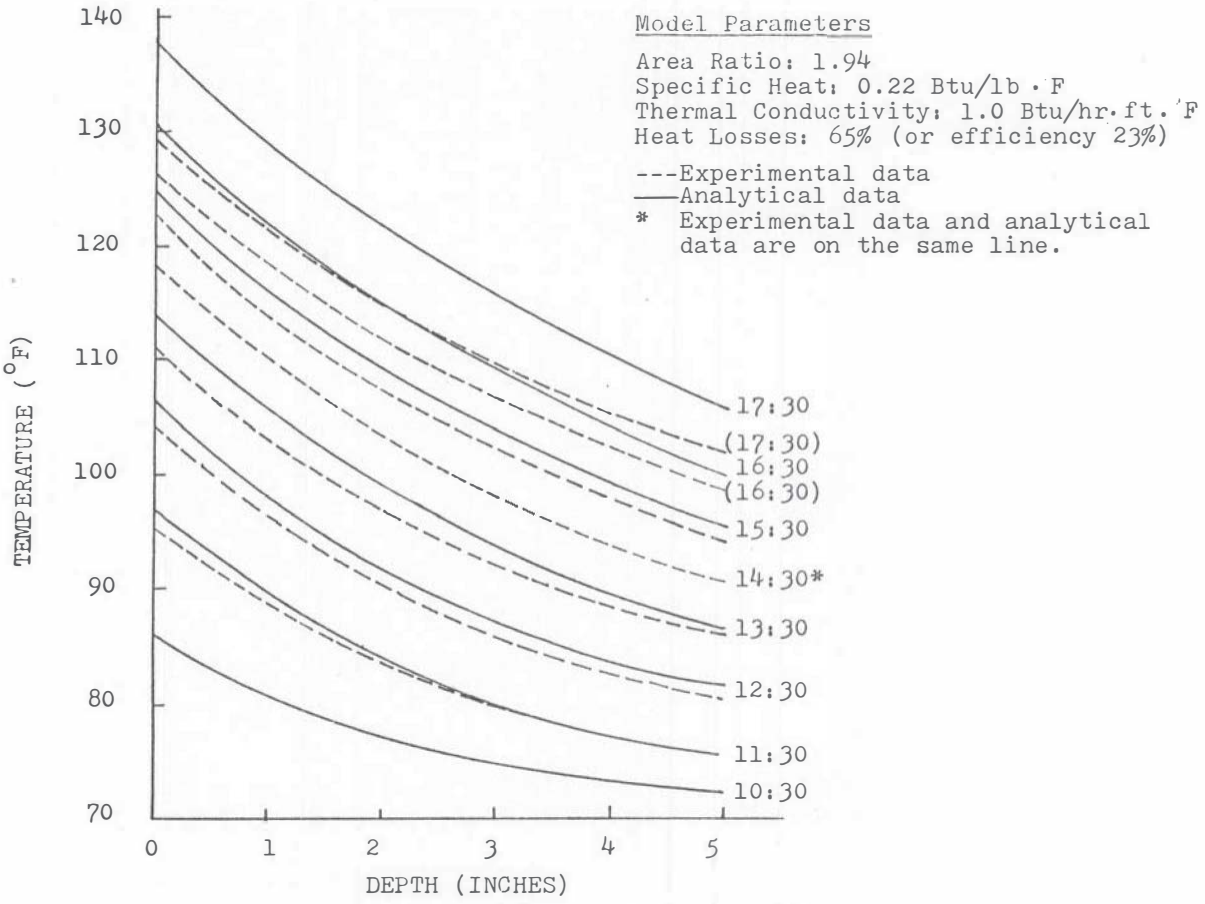

Fig. 4.16. Comparison of experimental data and analytical data (c_p= 0.22 Btu/lb· F, Area Ratio=1.94, Heat Losses = 65%)

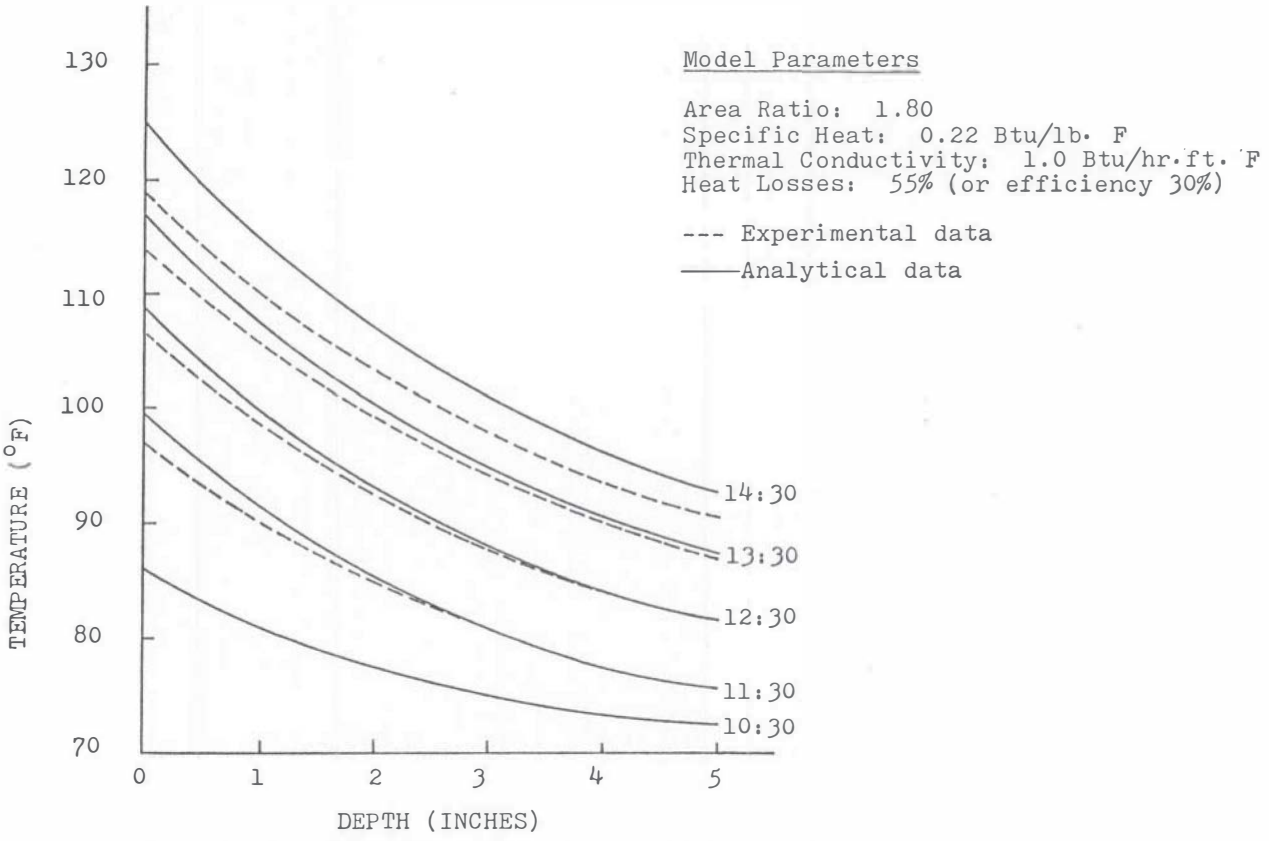

Fig. 4.17. Comparison of experimental data and analytical data (c_p = 0.22 Btu/lb. F, Area Ratio= 1.80, Heat Losses = 55%).

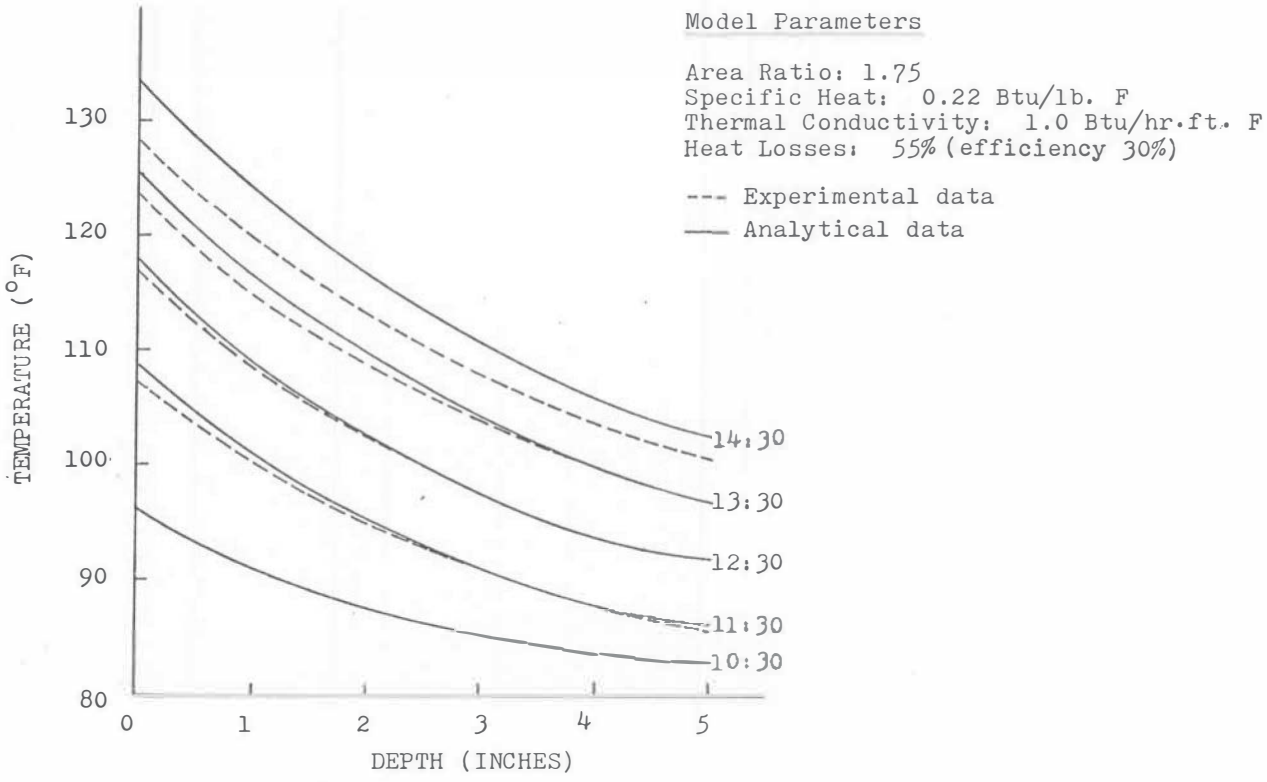

Fig. 4.18. Comparison of experimental data and analytical data. (c_p = 0.22 Btu/lb· F, Area Ratio=1.75, Heat Losses = 55%)

TABLE 4.3

DATA MEASURED ON JUNE 17, 1978, TUBE IN SHEET HEAT EXCHANGER WITH SINGLE COVER

Time (h)	T_{avg}(°F)	ΔT(°F)	T_s(°F)	$T_{½}$(°F)	T_1(°F)	T_2(°F)	T_4(°F)	T_5(°F)	T_{amb}(°F)
10:00	73.4	-18.0	91.4	89.6	86.9	83.3	77.9	77.0	83.5
10:30	106.7	15.3	91.4	89.6	87.8	85.1	79.3	78.8	84.0
11:00	136.6	38.9	97.7	95.0	91.4	86.9	80.6	79.7	85.0
11:30	153.1	47.3	105.8	100.9	96.8	91.0	82.9	81.5	86.0
12:00	160.7	49.0	111.7	106.7	102.2	95.5	86.0	84.2	87.0
12:30*	164.5	46.1	118.4	113.0	105.8	101.3	90.3	87.8	87.0
13:00	165.0	43.9	121.1	115.7	111.2	104.0	92.8	89.6	88.0
13:30	168.4	41.9	126.5	120.2	114.8	108.5	96.8	93.2	89.0
14:00	174.7	44.6	130.1	123.8	118.4	112.1	99.5	95.5	89.0
14:30	177.4	45.0	132.4	125.6	120.2	113.9	100.4	96.8	91.0
15:00	177.1	42.0	135.1	129.2	123.8	117.1	104.0	100.0	92.5
15:30	169.3	32.9	136.4	131.0	125.6	118.8	106.7	102.2	92.5
16:00**	150.1	15.9	134.2	130.1	126.1	121.1	109.4	104.9	92.0
16:30	155.8	22.1	133.7	129.2	125.6	121.1	109.9	105.8	92.0
17:00**	149.0	18.0	131.0	128.3	125.6	121.1	111.2	106.7	92.0

Remarks: 1) Time indicates daylight saving time of the central area.

2) T_s, $T_{½}$, T_1, T_2, T_4, and T_5 show the temperatures measured at the depth of surface, ½", 1", 2", 4" and 5". T_{avg} means the average temperature of heat exchanger.

3) Wind: 5-10 mph

4) Tracking Condition: * partly cloudy sky.
** off tracking.

5) Partly cloudy at 12:30, continuing throughout the afternoon.

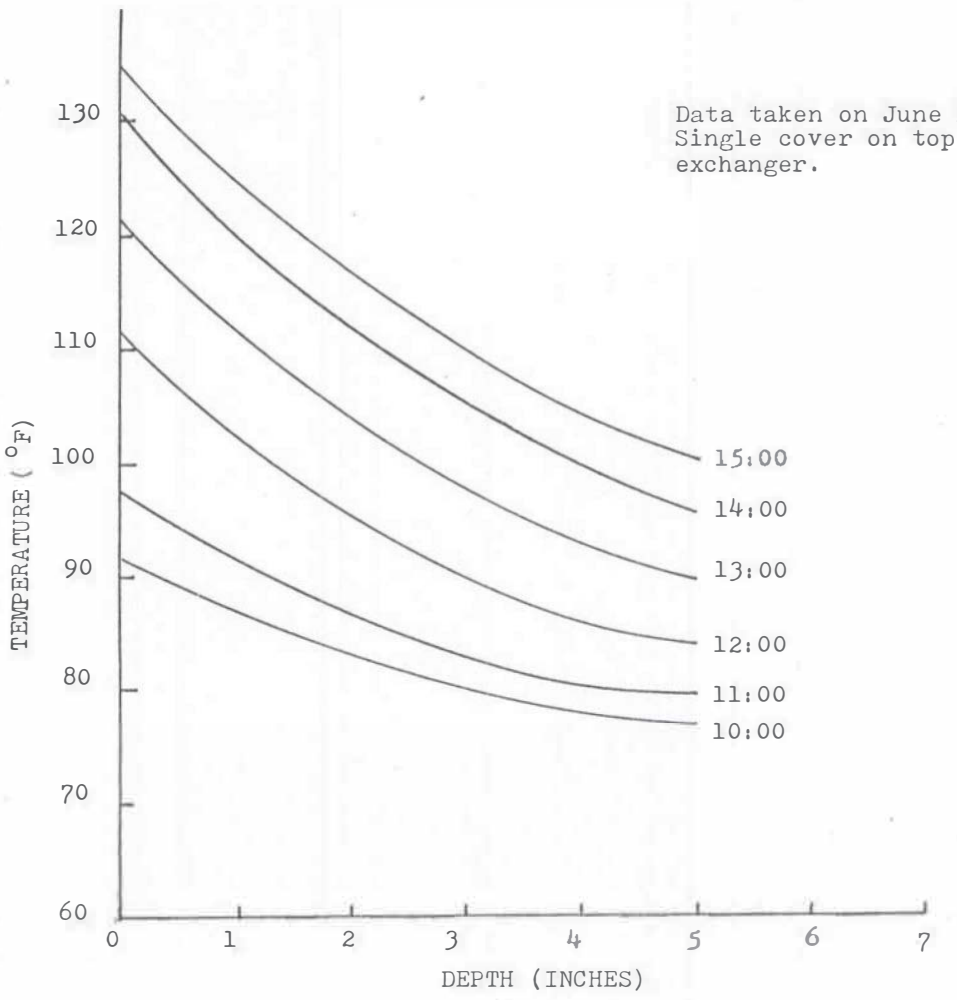

Fig. 4.19. Temperature distribution in the bridge deck with modified tube-in-sheet type heat exchanger.

achieved if we had not suffered the partly cloudy sky on June 17, 1978 which caused the off-tracking of both solar collectors. However, this scheme will still be faced with the large contact temperature differences like those faced with the previous heat exchanger.

3. Copper Tubes Embedded in Oil Type Heat Exchanger. In order to reduce the thermal contact resistance faced in the previous two types of heat exchanger, the type of heat exchanger as shown in Fig. 4.13 was evaluated. An aluminium sheet was laid on the surface of the bridge deck and a wooden frame was placed on top of the aluminium sheet, then, the aluminium sheet was folded to the frame. The internal region of the frame was then filled with Mobiltherm oil to a level approximately at the centerline of the copper tube heat transfer coils. These coils had oil from the collector circulated through them. The entire system was then covered with fiberglass insulation board.

Due to the fact that the concrete surface was uneven and the copper tube coils cannot be made on the same level, more than 5 gallons of oil was used. After this amount of oil was poured inside the frame, there are still several copper coils just barely touched with oil and some coils were completely embedded in the oil. The result of this scheme is shown in Table 4.4 and Fig. 4.20. This is also a negative result. The temperature profile of this scheme was worse than that of the first scheme. The contact resistance may be reduced to some degree but the additional mass of oil (approximately 32.5 lbm for 5 gallons of oil) in the heat exchanger will also absorb heat in order to be heated up. This disadvantage will reduce the effect of possibly reduced thermal contact resistance, and still cause the large temperature differences between the oil inside the coil and the slab surface.

TABLE 4.4

DATA MEASURED ON JUNE 25, 1978, WITH COPPER TUBES SUBMERGED IN THE OIL

TIME (h)	T_{avg}(°F)	ΔT(°F)	T_s(°F)	$T_{½}$(°F)	T_1(°F)	T_2(°F)	T_4(°F)	T_5(°F)	T_{amb}(°F)
08:30	86.7	7.0	79.7	79.7	79.7	79.7	78.4	77.9	81.0
09:00	106.3	24.8	81.5	81.1	80.6	79.7	78.4	77.9	82.0
09:30	125.2	40.5	84.7	84.2	82.4	80.6	78.8	78.4	83.0
10:00	131.5	42.8	88.7	87.4	85.6	82.9	79.3	78.8	84.0
10:30	139.8	47.5	92.3	90.5	88.7	85.1	80.6	79.7	85.5
11:00	146.8	51.8	95.0	94.1	91.4	87.8	81.5	81.1	87.5
11:30	153.8	55.2	98.6	96.8	94.1	90.1	83.3	82.4	89.0
12:00*	152.2	50.9	101.3	100.4	96.8	93.2	86.0	84.2	89.0
12:30	158.9	54.9	104.0	101.8	98.6	94.1	86.9	85.1	91.0
13:00	162.1	55.4	106.7	104.9	101.3	96.8	89.6	87.8	92.0
13:30	162.8	55.6	107.2	105.8	104.9	100.4	91.9	89.6	94.0
14:00**	156.3	45.1	111.2	109.0	105.8	102.2	93.2	92.3	94.0
14:30	157.1	44.1	113.0	109.4	107.6	103.6	95.0	90.5	94.5
15:00	161.6	47.2	114.4	111.2	108.3	104.0	95.9	93.7	95.0
15:30	166.4	49.8	116.6	113.0	109.4	105.8	96.8	95.9	96.0
16:00	167.6	48.3	119.3	115.7	113.0	108.6	100.4	98.2	96.0
16:30***	160.7	40.5	120.2	116.6	113.9	110.3	102.2	99.5	97.0

Remarks: 1) Time indicates daylight saving time of the central area.

2) T_s, $T_{½}$, T_1, T_2, T_4 and T_5 show the temperatures measured at the depth of surface, ½", 1", 2", 4" and 5" . T_{avg} means the average temperature of heat exchanger.

3) Wind velocity: 10-25 mph.

4) Tracking Condition:
   * right solar collector off tracking and being adjusted.
   ** strong wind caused collector off tracking.
   *** stop tracking.

5) Clear sky all through the day.

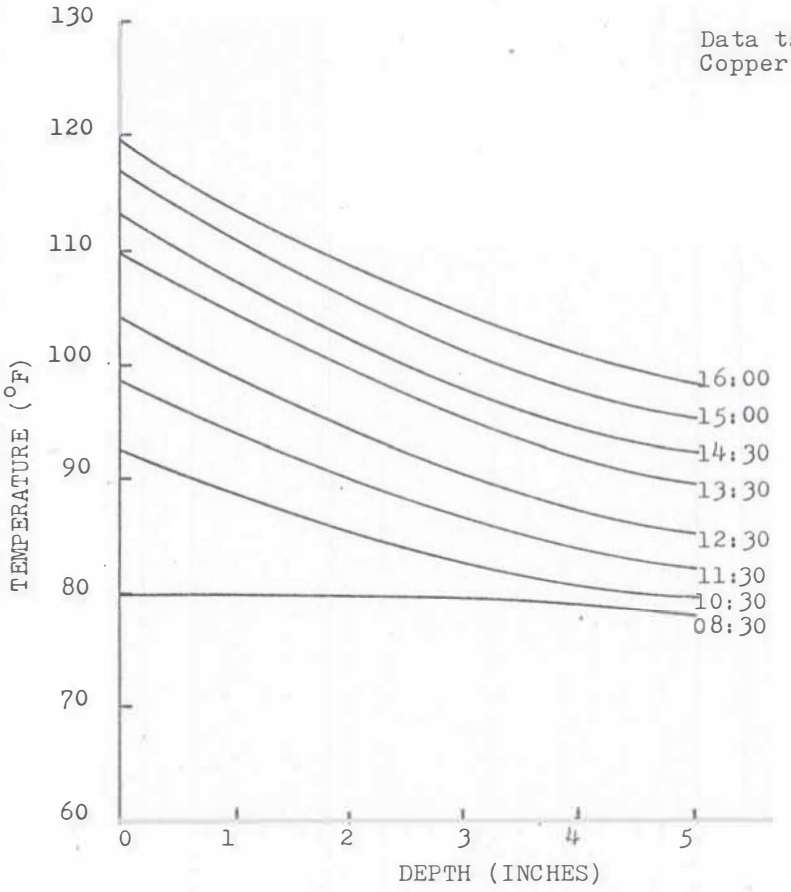

Fig. 4.20. Temperature distribution in the bridge deck with the oil embedded tube heat exchanger.

DISCUSSION

As previously mentioned, we experienced the following difficulties and problems which caused the temperature profiles of the experimental results to be much lower than the temperature profiles predicted from the analytical result:

1. Thermal Contact Resistance

The rough surface of the concrete slab, the slightly curved heat exchanger plate and welded square tubes, which are not welded continuously to the steel plate, caused the large contact temperature differences. Except the limited directly contacted spots, heat transfer is mainly by conduction and radiation through the air in between the two surfaces. The conductivity of the air is only $0.0181 \frac{Btu}{hr \cdot ft \cdot F}$ at 200 °F. No satisfactory theory is yet available to predict the thermal contact resistance [10]; thus, an experimental approach appears to be the only means to predict thermal contact resistance for practical purposes. The only way that the thermal contact resistance can be reduced is to insert a good thermal conductivity compound, like the Thermon thermal cement we used between the two surfaces, and between the square tubes and the steel plate.

2. High Heat Losses or Low Collector Efficiencies

In order to force the temperature profile of the analytical result to fit our experimental result, a 55% - 65% heat loss of the absorbed solar radiation was required. The effect of low efficiencies of the Northrup solar collectors would also cause the same result as the high heat losses assumed in our computer program. In the following, an analysis of the effect of heat loss in the system piping, one dimensional error, heat

loss from concrete slab is made. Also the solar collector efficiencies were modified to determine the main reason or cause for the low temperatures obtained experimentally.

(i) System Piping. The losses from the flow piping of the system for this size installation are disproportionately large. Steady state calculation was made with the assumed temperature difference between the fluid and the ambient air equal to 80 °F, the loss is about 300 Btu/hr which is approximately 10% of heat absorbed from the solar collector on the basis of 274 Btu/h · ft^2 average solar flux, 60% collector efficiency and 1.75 area ratio. The reason that we chose 1.75 area ratio was that we estimated about 10% deduction from the effective solar collector area should be made due to the effect of dust and shade to the solar collectors.

(ii) One-dimensional Error. The analytical study used was a one-dimensional transient model. For the 1200 ft^2 bridge simulation, this is reasonable, but for the 10 ft^2 heat exchanger the edge losses cannot be ignored. In our model, the edge area for conductive losses is about 8.5 ft^2 and the additional bridge surface is about 8.2 ft^2. Relative to the smaller model we have chosen, the area of heat losses is increased by almost a factor of two. This was one of the reasons the temperature profile was lower than expected. A study was made with two different sizes of plexiglass covers. The inside surface areas were 36" by 40" and 52" by 44" respectively. The bridge surface was blackened with commercial black paint. For each size of plexiglass cover used, its edges were well insulated. The results are shown in Table 4.5 and 4.6 and Fig. 4.21 to Fig. 4.23. A higher temperature profile was achieved with the larger cover, the reason for the higher temperatures were the higher initial temperature and the

TABLE 4.5

DATA MEASURED ON JUNE 30, 1978, BLACKENED TOP BRIDGE SURFACE WITH SINGLE COVER (COVER AREAS 40" x 36")

Time (h)	T_s(°F)	$T_{½}$(°F)	T_1(°F)	T_2(°F)	T_4(°F)	T_5(°F)	T_{amb}(°F)
09:45	96.8	93.2	90.5	86.9	81.5	79.7	86.0
10:00	101.3	97.7	94.1	89.6	83.3	82.0	87.0
10:30	105.8	101.3	97.7	92.8	85.1	83.3	87.0
11:00	112.6	107.6	103.1	97.3	87.8	86.0	89.5
11:30	117.5	112.6	108.1	101.3	90.5	88.7	91.0
12:00	121.1	115.7	111.2	104.9	93.2	91.0	92.0
12:30	127.4	122.0	116.6	109.4	97.7	94.1	92.5
13:00	132.8	127.0	122.0	113.9	100.4	97.7	93.0
13:30	136.4	130.1	125.2	117.1	103.6	100.4	94.5
14:00	140.0	133.7	128.8	120.7	106.7	103.6	94.5
14:30	143.6	137.3	132.8	124.7	110.3	106.7	94.5
15:00	145.0	139.1	134.2	126.5	112.1	108.5	95.0
15:30	146.3	140.9	136.4	129.2	114.8	111.2	95.0
16:00	146.3	141.8	137.3	130.1	116.6	113.0	95.0
16:30	145.9	141.8	138.2	131.5	118.4	113.9	95.0
17:00	144.5	141.4	137.8	131.9	119.3	114.8	94.0
17:30	142.3	140.0	136.4	131.9	119.8	115.7	94.0
18:00	140.0	137.3	135.1	131.0	120.7	116.6	94.0

Remarks:

1) Time indicates daylight saving time of central areas.

2) T_s, $T_{½}$, T_1, T_2, T_4, and T_5 show the temperatures measured at the depth of top bridge surface, ½", 1", 2", 4" and 5".

3) Sunrise: 6:15
   Sunset: 20:45

4) $(T_{amb})_{min}$ = 75 °F
   $(T_{amb})_{max}$ = 95 °F

5) Wind: 5-10 mph.

6) Clear sky all through the day.

TABLE 4.6

DATA MEASURED ON JULY 4, 1978, BLACKENED TOP BRIDGE SURFACE

WITH SINGLE COVER (COVER AREA 52" x 44")

Time (h)	T_s(°F)	$T_{½}$(°F)	T_1(°F)	T_2(°F)	T_4(°F)	T_5(°F)	T_{amb}(°F)
09:00	97.7	95.5	93.2	90.5	86.5	86.0	84.0
09:30	102.7	99.5	96.8	93.2	87.8	86.5	87.0
10:00	109.0	104.9	101.3	96.8	89.6	87.8	89.0
10:30	114.8	110.3	105.8	100.4	92.3	90.1	91.0
11:00	119.3	114.4	110.3	104.0	94.1	91.4	91.0
11:30	125.6	119.8	114.8	108.1	96.8	94.1	92.0
12:00	128.3	123.4	118.4	111.7	99.5	96.8	93.0
12:30	134.2	128.3	122.9	115.7	103.1	100.4	94.0
13:00	138.2	131.9	126.5	118.4	105.8	102.2	96.0
13:30	142.7	136.4	130.6	122.9	109.0	105.8	96.0
14:00	144.5	140.0	134.2	126.1	111.2	107.6	98.0
14:30	148.6	142.7	137.3	129.2	114.8	111.2	98.0
15:00	150.8	146.3	140.9	132.8	117.5	113.5	98.0
15:30	150.8	146.3	141.8	134.6	120.2	115.7	97.0
16:00	145.4	144.1	141.4	135.5	122.0	117.1	97.0
16:30	149.9	146.3	142.3	135.3	122.9	118.4	97.0
17:00	149.0	145.4	142.3	136.4	124.7	120.2	97.0
17:30	142.3	140.9	140.0	136.0	125.6	121.1	96.0

Remarks:

1) Time indicates daylight saving time of central areas.

2) T_s, $T_{½}$, T_1, T_2, T_4, and T_5 show the temperatures measured at the depth of top bridge surface, ½", 1", 2", 4", and 5".

3) Sunrise: 6:21
   Sunset: 20:49

4) $(T_{amb})_{min}$ = 74 °F
   $(T_{amb})_{max}$ = 98 °F

5) Wind: 5-10 mph

6) Scattered clouds from 15:30

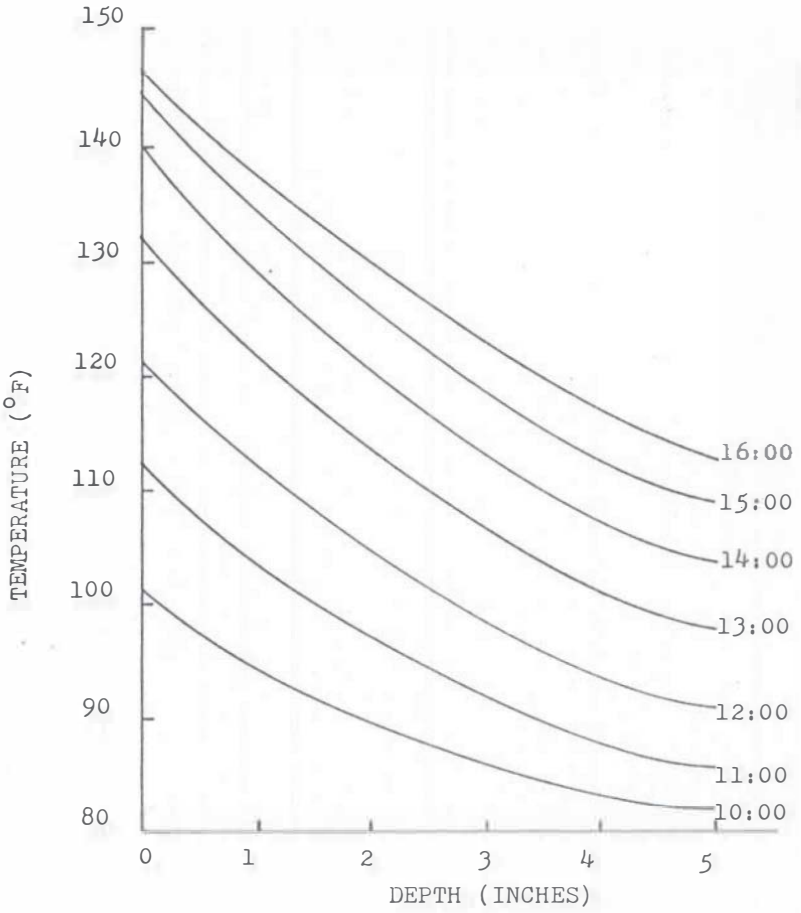

Fig. 4.21. Temperature distribution in the bridge deck with small plexiglass cover over the bridge surface.

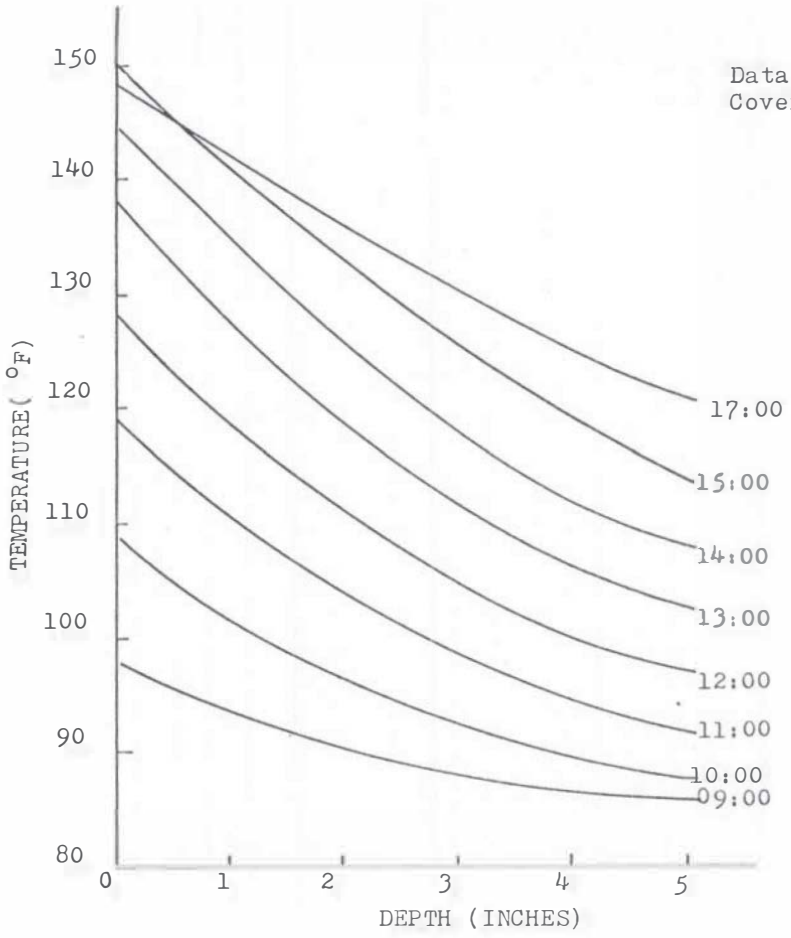

Fig. 4.22. Temperature distribution in the bridge deck with large plexiglass cover over the bridge surface.

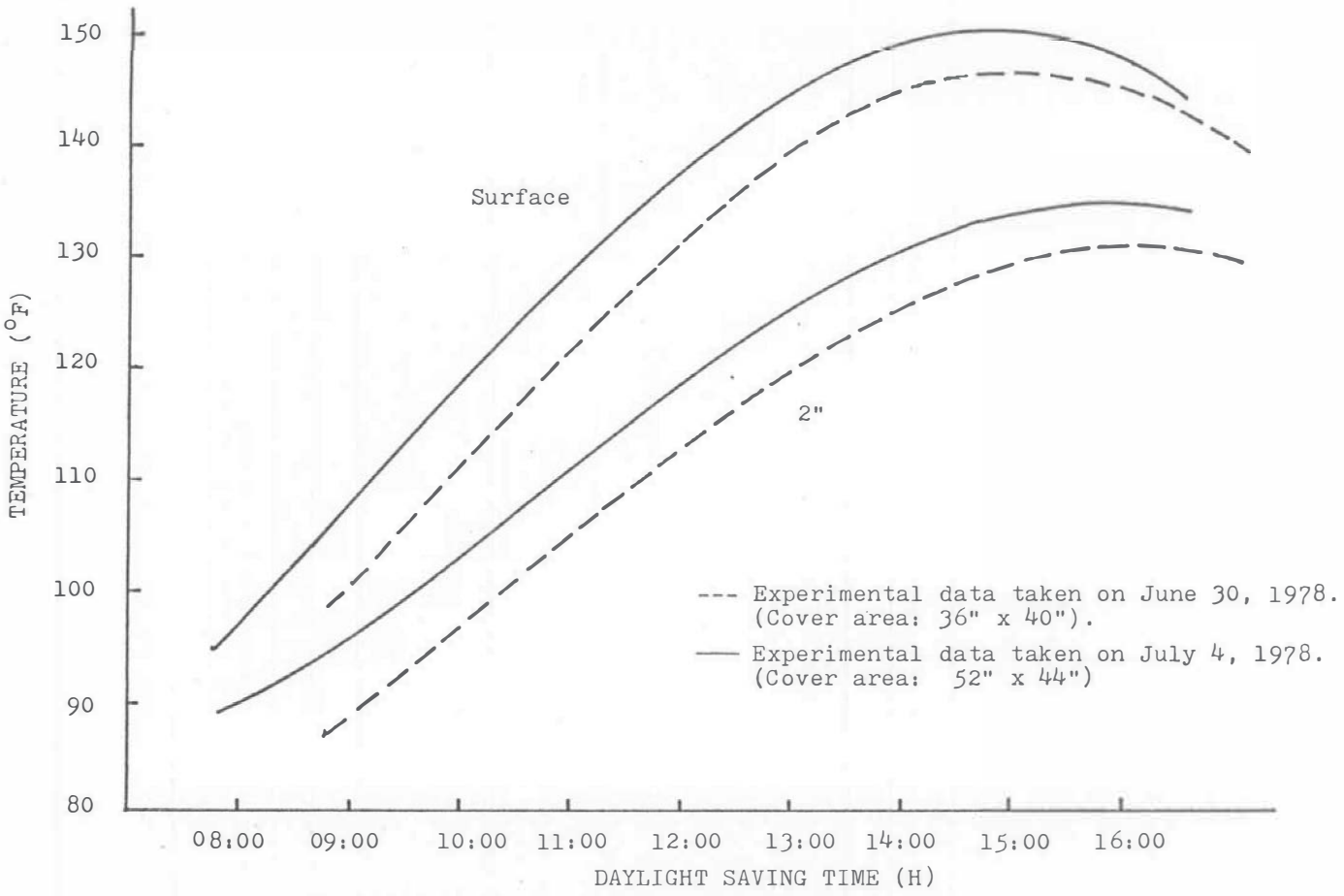

Fig. 4.23. Comparison of experimental data with different cover areas

larger area of the cover. The smaller heating area (smaller cover) has more bridge surface which is not exposed to solar heating. This of course would render the one dimensional analysis less valid for the smaller area since there would be a boundary condition variation over the bridge surface. In addition the smaller collector would collect less solar energy and therefore the average slab temperature would be lower. Thus the observed higher initial slab temperature for the larger collector. By comparison of these two temperature profiles, it may be observed that there are only small differences between the slopes of the temperature curves during the same time intervals. Therefore the one dimensional error is not the main factor explaining the 55% - 65% heat loss assumptions we made in our analytical results.

(iii) Edge Heat Losses from the Edge Insulation. The edges of this bridge model (57" x 46") were insulated with 1½" thick fiberglass sheet and 2" fiberglass board, then a thin plastic cover was covered and wrapped around by a rope to prevent the moisture or rain penetration. The edge temperatures at surface, 1 inch and 2 inches can be checked by the thermocouples embedded in the concrete (with the code letter B-S, B-1, and B-2) as shown in Table 4.7. They are only slightly above the ambient temperature and therefore the losses from the edges through the edge insulation can reasonably be neglected.

(iv) Top Heat Loss through the Top Insulation. A 1½ fiberglass sheet was placed on top of the heat exchanger and then was taped to the concrete slab to reduce the convective losses to a minimum. Afterward, three 2" thick-fiberglass sheet laid on top of each other to the top surface

TABLE 4.7

COMPARISON OF THE EDGE AND CENTER TEMPERATURES

Time	T_{C-S} (°F)	T_{B-S} (°F)	T_{C-1} (°F)	T_{B-1} (°F)	T_{C-2} (°F)	T_{B-2} (°F)	T_{amb} (°F)
10:00	101.3	79.7	94.1	78.8	89.6	78.8	87.0
10:30	105.8	81.5	97.7	80.6	92.8	80.6	87.0
11:00	112.6	82.9	103.1	82.4	97.3	82.4	89.5
11:30	117.5	85.1	108.1	84.2	101.3	84.2	91.0
12:00	121.1	86.5	111.2	86.0	104.9	86.0	92.0
12:30	127.4	89.2	116.6	89.2	109.4	88.7	92.5
13:00	132.8	91.4	122.0	91.0	113.9	90.5	93.0
13:30	136.4	93.2	125.2	93.2	117.1	93.2	94.5
14:00	140.0	95.0	128.8	95.0	120.7	94.1	94.5
14:30	143.6	97.3	132.8	97.3	124.7	96.8	94.5
15:00	145.0	99.5	134.2	98.6	126.5	98.6	95.0
15:30	146.3	100.9	136.4	100.4	129.2	100.4	95.0
16:00	146.3	102.7	137.2	102.2	130.1	101.3	95.0
16:30	145.9	104.0	138.2	104.0	131.5	103.1	95.0
17:00	144.5	104.9	137.8	104.9	131.9	104.0	94.0
17:30	142.3	105.8	136.4	105.8	131.9	104.9	94.0
18:00	140.0	106.7	135.1	106.3	131.0	105.4	94.0

Remark: 1) Time indicates daylight saving time of central area.

2) Letter C indicates the center location, Letter B indicates the bottom edge location. Subscripts S, 1, and 2 indicate surface, 1" and 2".

3) Data measured on June 30, 1978, blackened top bridge surface with single plexiglass cover (cover area 40" x 36").

of the above-mentioned fiberglass sheet to insure good insulation and to reduce the heat conduction from the top to the minimum. A calculation was also made with 100 °F temperature difference between the surface of heat exchanger and the exterior surface of fiberglass board. The heat loss through the top insulation is only about 50 Btu/hr, about 1.7% of the solar radiation absorbed from the solar collector (approximately 3000 Btu per h based on 274 Btu per $h \cdot ft^2$ averaging solar flux, 65% efficiency, 1.75 area ratio). In the actual case, the top surface of the insulation board will absorb heat from the solar radiation and therefore can reduce the possible heat loss from the top insulation to less than 50 Btu/hr. Hence, the loss through the top insulation is very small and may be considered negligible.

(v) Efficiency of Northrup Solar Collectors. Our analytical studies were based on the solar collector efficiency curve from the Northrup Commercial catalog as shown in Fig. 3.20. We linearized the efficiency curve to be a straight line, and programmed it in our computer program for the analytical studies. After the previous heat losses analysis, the only possibility that could have caused the high losses was the solar collector's lower efficiency than expected.

The effect of low efficiencies of the Northrup solar collectors will cause the same results as the high heat losses assumed in our analytical computer program. The program showed that during 9 hours tracking period, the solar collector will always have an efficiency higher than 60%. From our experimental data as shown in Table 4.8 we can calculate the average value of ΔT and S as follows:

TABLE 4.8

DATA MEASURED ON JUNE 25, 1978, TEMPERATURE DIFFERENCE BETWEEN INLET AND OUTLET END OF SOLAR COLLECTOR

Time (h)	T_{in}(°F)	T_{out}(°F)	ΔT(°F)	S(Btu/hr·ft^2)
08:30	86.0	86.5	0.5	250
09:00	106.7	108.1	1.4	-
09:30	124.7	126.5	1.8	268
10:00	131.5	135.1	3.6	-
10:30	136.4	140.9	4.5	278
11:00	142.7	145.4	2.7	-
11:30	153.5	154.4	0.9	284
12:00*	150.8	152.6	1.8	-
12:30	158.0	160.7	2.7	285
13:00	161.6	164.3	2.7	-
13:30	162.1	164.3	2.2	284
14:00**	151.7	156.2	4.5	-
14:30	154.4	157.1	2.7	278
15:00	159.8	163.4	3.6	-
15:30	165.2	167.0	1.8	268
16:00	167.5	169.3	1.8	-
16:30+	160.3	161.6	1.3	250

Remarks:
1) Time indicates daylight saving time of the central area.
2) T_{in} and T_{out} indicate the temperatures measured at the inlet end and the outlet end of the solar collector. $\Delta T = T_{out} - T_{in}$, S indicates the hourly solar insolation from [1].
3) Wind velocity: 10-25 mph.
4) Tracking Condition:
   * right solar collector off tracking and being adjusted
   ** strong wind caused collector off tracking.
   + stop tracking.
5) Clear sky all through the day.

$$(\Delta T)_{avg} = \sum_{i=1}^{n} \frac{(T_i + T_{i+1})}{2n} \quad , \quad n = 16$$

$$= 2.475\ ^{\circ}F$$

$$(S)_{avg} = \sum_{j=1}^{N} \frac{(S_j + S_{j+1})}{2\ N} \quad , \quad N = 8$$

$$= 274\ Btu/hr \cdot ft^2$$

where N = 8 hour intervals

n = 16 half hour intervals

The average efficiency of the solar collectors over the entire tracking period can be estimated as:

$$(\eta)_{avg} = mC_p(\Delta T)avg/A(S)avg$$

$$= 29\%$$

where

m = 3.3 gpm = 1288 lb/hr

A = 20 ft^2 (for area ratio = 2.0)

C_p = 0.5 Btu/lb· F (at 150 °F)

our data indicated that a reasonable efficiency for the Northrup solar collectors would be around 30% - 40% instead of 60%. Other people [11] have measured 60% efficiency for the Northrup, however, they are usually under controlled conditions and also they do not have the difficulties of strong wind, off-tracking etc., that we encountered.

With these focusing solar collectors, we experienced tracking difficulties due to intermittant cloud cover and strong wind etc. These are important factors that can cause low efficiency performance of solar collectors.

(vi) Burried Pipe Studies. In order to be able to better understand the limitations of the problem of heat transfer to the bridge deck, the Oklahoma Highway Department asked us to determine the transient temperature distribution in the bridge deck for the case when the heat exchanger tubes are located within the deck 2" below the top surface. The model we used was for 1/2" tubes located at 2" depth in the 8" slab and located on 6" centers. The cross-section studied is shown in figure 4-24 with the elements and nodes indicated. A finite element model was used to analyze the structure. The initial temperature of the bridge was assumed to be at 80°F which was also the ambient temperature. A thermal conductivity of 1 Btu/hr ft °F, density of 145 lb/ft^3 and specific heat of 0.28 Btu/hr °F were used. The tube temperature was assumed to be 205 F.

The results of this study are presented in Table 4-9 after a time of 3 hrs and 6 hrs. The temperature at node 55 is of particular interest. After 3 hrs, it has risen to 153 F and after 6 hrs it has risen to 173 F. Of course the model does not allow for any contact resistance and the bridge is treated as homogeneous; however, the results remain encouraging.

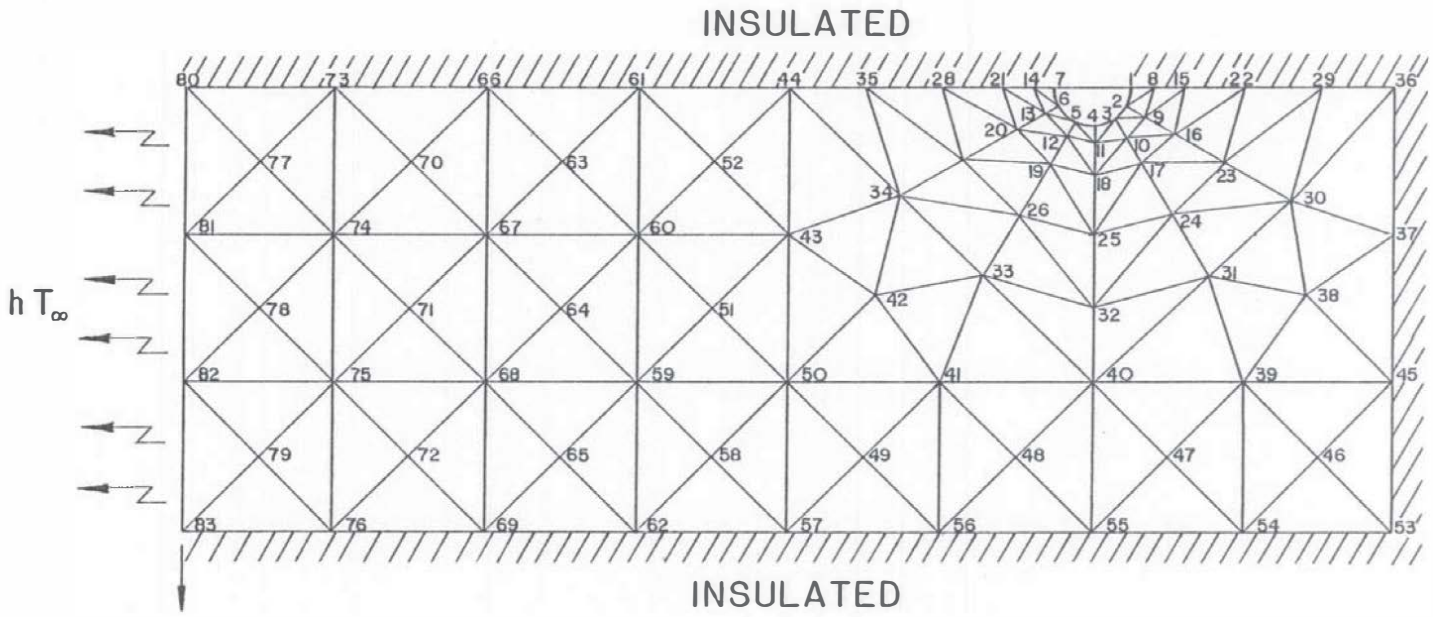

Figure 4-24 Bridge Cross-Section

Showing Finite Element Mesh

TABLE 4.9

TEMPERATURES FOR FINITE ELEMENT ANALYSIS OF BRIDGE
WITH BURRIED PIPE

TIME = 3.000

1.	0.20500D	03	2.	0.20500D	03	3.	0.20500D	03	4.	0.20500D	03	5.	0.20500D	03
7.	0.20500D	03	8.	0.19602D	03	9.	0.19562D	03	10.	0.19479D	03	11.	0.19408D	03
13.	0.19214D	03	14.	0.19106D	03	15.	0.18782D	03	16.	0.18732D	03	17.	0.18589D	03
19.	0.18184D	03	20.	0.18022D	03	21.	0.17955D	03	22.	0.17961D	03	23.	0.17836D	03
25.	0.17210D	03	26.	0.18806D	03	27.	0.16498D	03	28.	0.16387D	03	29.	0.17470D	03
31.	0.16831D	03	32.	0.18312D	03	33.	0.15882D	03	34.	0.15173D	03	35.	0.14985D	03
37.	0.16918D	03	38.	0.16664D	03	39.	0.16191D	03	40.	0.15759D	03	41.	0.14698D	03
43.	0.13876D	03	44.	0.13900D	03	45.	0.16260D	03	46.	0.16045D	03	47.	0.15756D	03
49.	0.13877D	03	50.	0.13333D	03	51.	0.12783D	03	52.	0.12973D	03	53.	0.15991D	03
55.	0.15335D	03	56.	0.14394D	03	57.	0.13191D	03	58.	0.12616D	03	59.	0.12054D	03
61.	0.12239D	03	62.	0.11996D	03	63.	0.11610D	03	64.	0.11547D	03	65.	0.11486D	03
67.	0.11054D	03	68.	0.11012D	03	69.	0.10991D	03	70.	0.10644D	03	71.	0.10622D	03
73.	0.10276D	03	74.	0.10268D	03	75.	0.10252D	03	76.	0.10244D	03	77.	0.10001D	03
79.	0.99824D	02	80.	0.97748D	02	81.	0.97705D	02	82.	0.97620D	02	83.	0.97577D	02

TIME = 6.000

1.	0.20500D	03	2.	0.20500D	03	3.	0.20500D	03	4.	0.20500D	03	5.	0.20500D	03
7.	0.20500D	03	8.	0.19953D	03	9.	0.19937D	03	10.	0.19876D	03	11.	0.19810D	03
13.	0.19649D	03	14.	0.19629D	03	15.	0.19506D	03	16.	0.19468D	03	17.	0.19356D	03
19.	0.19019D	03	20.	0.18879D	03	21.	0.18823D	03	22.	0.19038D	03	23.	0.18954D	03
25.	0.18462D	03	26.	0.18120D	03	27.	0.17846D	03	28.	0.17743D	03	29.	0.18777D	03
31.	0.18339D	03	32.	0.17916D	03	33.	0.17373D	03	34.	0.16918D	03	35.	0.16742D	03
37.	0.18458D	03	38.	0.18291D	03	39.	0.17984D	03	40.	0.17585D	03	41.	0.16714D	03
43.	0.15786D	03	44.	0.15921D	03	45.	0.18073D	03	46.	0.17930D	03	47.	0.17661D	03
49.	0.16069D	03	50.	0.15579D	03	51.	0.15063D	03	52.	0.15176D	03	53.	0.17914D	03
55.	0.17329D	03	56.	0.16531D	03	57.	0.15495D	03	58.	0.14963D	03	59.	0.14429D	03
61.	0.14539D	03	62.	0.14395D	03	63.	0.13947D	03	64.	0.13910D	03	65.	0.13874D	03
67.	0.13391D	03	68.	0.13366D	03	69.	0.13354D	03	70.	0.12906D	03	71.	0.12893D	03
73.	0.12441D	03	74.	0.12436D	03	75.	0.12427D	03	76.	0.12423D	03	77.	0.12019D	03
79.	0.12009D	03	80.	0.11622D	03	81.	0.11620D	03	82.	0.11615D	03	83.	0.11613D	03

CHAPTER V

CONCLUSIONS AND RECOMMENDATIONS

In this study we were not able to achieve the desired bridge deck temperatures nor were we able to achieve the temperatures predicted in the theoretical study. The analytical model gives the right trends but suffers from lack of accurate knowledge of the concrete properties and collector efficiency. In addition the model was based on a one dimensional slab with the entire top surface heated and under our test conditions this was not the case. The analytical flat plate study showed that with optimal property values we could achieve the desired bridge temperatures but that this was only optimally marginal and therefore not a viable alternative. The study was fraught with numerous experimental difficulties, many of which would always be faced with using this type collector and heat exchanger system. The difficulty of keeping the collectors tracking, the effect of intermittant cloud cover on collector performance and the estimated collector losses due to the high prevalent winds rendered the collector performance far below the values reported by others. By connecting the collector performance to the measured efficiency value for a typical day, the analytical model was shown to be quite reasonable. An anticipated difficulty which we were never able to overcome is the contact resistance between the heat exchanger and the bridge deck. While we did anticipate this difficulty it is fair to say that we did not anticipate the severity

of the problem. Preliminary studies of the effect of using buried pipes in the bridge deck did prove promising. An unknown contact resistance would be present in this case also but with good bonding it should be much less of a problem. Experiments conducted showed that the one dimensional assumption did not contribute greatly to the observed descrepency between theory and experiment. In addition to the problems mentioned, this study showed that the collectors we utilized may well require considerable maintenance.

Possible future studies which might be undertaken are:

1) The determination of the efficiency of the Northrup solar collector under Oklahoma operating conditions.
2) The scale of the study should be increased to minimize the losses and similar tests made.
3) The buried pipe study should be undertaken to determine if solar or conventional heating techniques can be used under these conditions to achieve the desire temperature.

REFERENCES

[1] Kreider, J. F. and Kreith, F., Solar Heating and Cooling:Engineering, Practical Design and Economics, McGraw Hill Book Company, New York, 1975, pp. 196-197.

[2] ASHRAE Handbook of Fundamentals, American Society of Heating, Refrigerating and Air-Conditioning Engineers, 1972, p. 389.

[3] McAdams, W. H., Heat Transmission, 3rd ed., MeGraw-Hill Book Company, New York, 1954, pp. 249-250.

[4] Swinbank, W. C., "Long-Wave Radiation from Clear Skies," Quarterly Journal of the Royal Meteorological Society, 1963, Vol. 89, pp. 339-348.

[5] Pell, K. M., Nydahl, J. E., Cundy, V., Twitchell, G., and Weber, M., "Thermal Response of Bridges." Transportation Research Records 576, 1976, pp. 5-16.

[6] Parker, J. D., Boggs, J. H., and Blick, E. F., Introduction to Fluid Mechanics and Heat Transfer, Addison-Wesley Publishing Company, Inc., Reading Massachuesetts, 1969, p. 587.

[7] Depuy, G. W., "Highway Applications of Concrete Polymer Materials," Transportation Research Records 542, 1975, p. 63.

[8] Duffie, J. A., and Beckman, W. A., Solar Energy Thermal Processes, Wiley Interscience, New York, 1974, pp. 108-137.

[9] Hottel, H. C. and Woertz, B. B., "Performance of Flat-Plate Solar-Heat Collectors," Trans. ASME, 1942, Vol. 64, pp. 91-104.

[10] Ozisik, N. M., Basic Heat Transfer, McGraw-Hill Book Company, New York, 1977, pp. 59-61.

[11] Jenkins, John P. and Hill, James E., "Testing of Water-Heating Collectors According to ASHRAE Standard 93-77", Proceedings of the International Solar Energy Society 1978 Meeting, SUN:Mankind's Future Source of Energy held in New Delhi, India, January 16-21, 1978.

APPENDIX A

Northrup Focusing Collector

Specifications

DIMENSIONS (std. size): 10'L x 1'W x 1.33'H
(3.05m x 0.305m x 0.406m)

EFFECTIVE COLLECTING AREA: 9.7 ft^2 per unit (0.901 m^2)

COLLECTOR WEIGHT: 95 lb per unit (43.1 kg)

ABSORBER MATERIAL: Copper

MAXIMUM OPERATING PRESSURE: 140 psia
(9.67 kgf-abs/cm^2)

TEST PRESSURE: 165 psia (11.6 kgf-abs/cm^2)

ABSORBER FLUID FLOW RATE: 0.4 gpm (1.51 ℓ/min)

PRESSURE DROP AT RATED FLOW: 0.2 psi (0.014 kgf/cm^2)
(Absorber Fluid:Water)

LENS LIFE: 20 years

LENS THICKNESS: 0.25 in. (0.635 cm)

LENS MATERIAL: DuPont Acrylic

TRACKING MOTOR: Rated Voltage - 120 v a c 60 Hz
Rated Current - 0.38 amp

TRACKING SPEED: 0.25°/min

DRIVE SPEED: 7.56°/min

COLLECTOR END FITTINGS: ¼" female NPT
(Rotating End Fittings included with Collector)
NOTE: SI units in parentheses.

APPENDIX B

```
C
C     THIS PROGRAM IS DESIGNED TO STUDY THE TEMPERATURE PROFILE OF THE
C     HIGHWAY BRIDGE WHERE ON TOP OF THE BRIDGE WILL BE HEATED WITH
C     NORTHRUP SOLAR COLLECTOR/HEAT EXCHANGER SYSTEM. THE RUNNING PERIOD
C     DESIGNED FOR THIS PROGRAM IS 9 HOURS TRACKING. I.E. FROM SOLAR
C     TIME 7:30 - 16:30. THE TEMPERATURE PROFILE WAS SOLVED WITH AN
C     EXPLICIT METHOD OF FINITE DIFFERENCE TECHNIQUE. THE GOVERNING
C     DIFFERENTIAL EQUATION WAS CONSIDERED AS AN ONE DIMENSIONAL
C     TRANSIENT HEAT CONDUCTION EQUATION.
C
C
C     VARIABLE AND CONSTANT NAMES FOR THE MAIN PROGRAM ARE.............
C
C     ALPHA    - PERCENTAGE OF HEAT LOSSES FROM THE SYSTEM
C     ANGCLN   - ANGLE OF INCLINATION (DEG)
C     AREA     - HEAT EXCHANGER AREA (SQ FT)
C     AREAC    - EFFECTIVE SOLAR COLLECTOR AREA (SQ FT)
C     CC       - CONVERGENCE CRITERIA OF EXPLICIT FINITE DIFFERENCING
C     DECK     - THICKNESS OF BRIDGE DECK (FT)
C     DEN      - DENSITY OF CONCRETE (LBM/CUFT)
C     DT       - TIME INCREMENT (HR)
C     DX       - GRID SPACING IN X DIMENSION (FT)
C     EFF      - SOLAR COLLECTOR EFFICIENCY
C     HC       - SPECIFIC HEAT OF CONCRETE (BTU/LBM/DEG. F)
C     HCV      - CONVECTIVE HEAT TRANSFER COEFFICIENT (BTU/HR/SQ FT/DEG F)
C     ND       - DAY OF THE YEAR
C     NT       - NUMBER OF THE TIME INTERVALS
C     NX       - NUMBER OF GRID SPACING
C     QL       - CONVECTIVE HEAT LOSS FROM THE BOTTOM (BTU)
C     QSOLAR   - SOLAR INSOLATION (BTU/SQ FT/HR)
C     QU       - SOLAR ENERGY ABSORBED FROM SOLAR COLLECTOR (BTU/HR)
C     RATIO    - EFFECTIVE SOLAR COLLECTOR AREA/HEAT EXCHANGER AREA
C     SLOPE    - ANGLE OF SOLAR COLLECTOR WITH HORIZONTAL (DEG)
C     SN       - HEAT RELEASED FROM HEAT EXCHANGER (BTU/HR)
C     SPH      - SPECIFIC HEAT OF THE LUMPED SYSTEM (BTU/LBM/DEG F)
C     T        - TEMPERATURES OF THE BRIDGE DECK (DEG F)
C     TAMB     - AMBIENT TEMPERATURE (DEG F)
C     TAVG     - AVERAGE TEMPERATURE OF THE LUMPED SYSTEM (DEG F)
C     TK       - THERMAL CONDUCTIVITY OF CONCRETE (BTU/HR/FT/DEG. F)
C     V        - WIND VELOCITY (FT/SEC)
C     XASS     - MASS OF THE LUMPED SYSTEM (LBM).
C     XLAT     - LATITUDE (DEG)
C
C     ***********************************************************************
      DIMENSION XTME(182),EFF(182),QSOLAR(182)
      DIMENSION QL(182),S(182),SN(182),DELT(182),Q(10),TOF(10),AMT(10)
      DIMENSION T(11,182),QS(182),TAMB(182),TAVG(182),QU(182)
C
C     THERMAL PROPERTIES OF THE CONCRETE SLAB
C
      DATA DEN,HC,TK/145.0,0.22,1.0/
C
C     MODEL PARAMETERS
C
      DATA AREA,ALPHA,RATIO,SPH,V,XASS/10.,0.45,1.75,0.155,7.3,120.0/
      DATA DECK/0.667/
C
C     INCIDENT ANGLE PARAMETERS
C
      DATA ND,SLOPE,XLAT/135,40.08,35.21/
C
      DATA NS,NT,NX/31,180,8/
      NX1=NX+1
      NT1=NT+1
      READ(5,300)(TOF (M),M=1,10)
  300 FORMAT (10F5.1)
      READ (5,301)(Q(N),N=1,5)
  301 FORMAT (5F10.1)
      READ (5,300) (AMT(J),J=1,9)
C
C     SET TEMPERATURES THROUGHOUT THE SLAB TO THE INITIAL VALUE
C
      READ (5,300)(T(I,NS),I=1,NX1)
C
C     INITIAL
C
      DELT(NS)=46.4
      TAVG(NS)=132.4
C
C     CALCULATE THE INCIDENT ANGLE OF SOLAR INSOLATION
C
      PI=3.141592
```

```
      ANGCLN=23.45*SIN(360.*(284.+ND)*PI/365./180.)*PI/180.
      CCANGT=COS((XLAT-SLOPE)*PI/180.)*COS(ANGCLN)+SIN((XLAT-SLOPE)*PI/1
     *80.)*SIN(ANGCLN)
C
CCC   CORRECTION OF THE NORMAL SOLAR INSOLATION
C
      QSOLAR(NS)=268.0 *CCANGT
      RUN=9.
      Z=NT
      DT=RUN/Z
      Z2=NX
      DX=DECK/Z2
      AREAC=AREA*RATIO
      ALPHA=ALPHA*DT
C
CCC   INTEGRATION OF THE INITIAL TEMPERATURE PROFILE IN THE SLAB BY
CCC   TRAPEZOIDAL RULE
C
      NT2=NT+2
      DO 2 I=NS,NT2
    2 QS(I)=0.0
      DO 3 J=2,NX
    3 QS(NS)=QS(NS)+T(J,NS)*DX
      QS(NS)=QS(NS)+(T(1,NS)+T(NX1,NS))*DX/2.
      CC=(TK*DT)/(DEN*HC*DX*DX)
C
CCC   CHECK FOR CONVERGENCE
C
      IF (CC.GT.0.5) GO TO 80
C
CCC   CALCULATE AMBIENT TEMPERATURE
C
      TIME=0.0
      DO 4 I=1,NT1
      TIME = TIME+DT
      CALL AMBT (TIME,I,AMT,TAMB)
    4 CONTINUE
C
CCC   CALCULATE THE CONVECTIVE COEFFICIENT
C
       HCV=1.+0.204*V
C
CCC   CALCULATE THE COLLECTOR EFFICIENCY
C
      XIME (NS)=(NS-1)/20.
      DO 6 I=NS,NT1
      T(1,I)=TAVG(I)- DELT(I)
      K=I+1
      XIME(K)=XIME(I)+DT
      CALL SOLAR(XIME,K,CCANGT,QSOLAR,Q)
      PARAM=(TAVG(I)-TAMB(I))/QSOLAR(I)
      EFF(I)=(81.65-54.82*PARAM)/100.
C
CCC   HEAT ABSORBED FROM SOLAR COLLECTOR (BTU/HR)
C
      QU(I)=EFF(I)*QSOLAR(I)*AREAC
C
CCC   CALCULATION OF BRIDGE DECK TEMPERATURES AND HEAT LOSSES
C
   11 N1=NX+1
      T(N1,K)=T(N1,I)+2.*CC*(T(NX,I)-T(N1,I))+(2.*HCV*DT/(DEN*HC*DX))*(T
     1AMB(I)-T(N1,I))
      DO 5 J=2,NX
      J1=J-1
      J2=J+1
      T(J,K)=T(J,I)+CC*(T(J1,I)-2.*T(J,I)+T(J2,I))
    5 QS(K)=QS(K)+T(J,I)*DX
      QS(K)=QS(K)+(T(1,I)+T(N1,I))*DX/2.
      S(K)=(QS(K)-QS(I))*DEN*HC*AREA
      CALL DELTM (XIME,K,DELT,TDF)
C
CCC   CONVECTIVE HEAT TRANSFER FROM THE BOTTOM OF BRIDGE (BTU/HR)
C
      QL(K)= HCV*(T(N1 ,I)-TAMB(I))*AREA*DT
C
CCC   HEAT RELEASED FROM HEAT EXCHANGER TO HEAT THE BRIDGE (BTU/HR)
C
      SN(I)=(S(K)+QL(K))/DT
C
CCC   CALCULATE THE AVERAGE TEMPERATURE OF
CCC   THE SOLAR COLLECTOR/HEAT EXCHANGER SYSTEM
C
      TAVG(K)=TAVG(I)+(ALPHA*QU(I)-SN(I)*DT)/(XASS*SPH)
    6 CONTINUE
    8 CONTINUE
C
C     ********************************************************
      DO 7 I=31,181,10
```

```
      WRITE (6,112) XIME(I),EFF(I)
      WRITE(6,113)
      WRITE(6,104)QSOLAR(I),SN(I),QU(I)
      WRITE(6,111)
   77 WRITE(6,78)(T(J1,I),J1=1,NX1)
    7 WRITE(6,102)TAVG(I)
  102 FORMAT(F10.4)
   78 FORMAT(9F10.4)
  111 FORMAT(1H0,'SURFACE   1 INCH    2 INCHES  3 INCHES  4 INCHES  5 IN
     1CHES  6 INCHES  7 INCHES  8 INCHES')
  112 FORMAT (/,20X,'TIME = ',F5.2,15X,'EFFICIENCY = ',F7.4,/)
  113 FORMAT(1H0,'SOLAR FLUX      HEAT TO BRIDGE      HEAT ABSORBED')
  104 FORMAT(3F14.3)
      GO TO 81
   80 WRITE (6,105) CC
  105 FORMAT(/,2X,'NO CONVERGENCE, CC = ',F5.2)
   81 CONTINUE
C     ******************************************************
C
      STOP
      END
      SUBROUTINE SOLAR(XIME,K,COANGT,QSOLAR,Q)
C
C     THIS SUBROUTINE WAS DESIGNED TO CACULATE THE NORMAL SOLAR INSOLATION
C     AT EACH TIME INTERVAL BY KNOWING THE HOURLY SOLAR INSOLATION
C     FROM LITERATURES
C
      DIMENSION QSOLAR(182),Q(10),XIME(182)
      TIME=XIME(K)
      IF (K.GE.20)GO TO 21
      QSOLAR(K)=Q(1)+(Q(2)-Q(1))*TIME
      GO TO 10
   21 IF (K.GE.40)GO TO 22
      QSOLAR(K)=Q(2)+(Q(3)-Q(2))*(TIME-1. )
      GO TO 10
   22 IF(K.GE.60)GO TO 23
      QSOLAR(K)=Q(3)+(Q(4)-Q(3))*(TIME-2. )
      GO TO 10
   23 IF(K.GE.80)GO TO 24
      QSOLAR(K)=Q(4)+(Q(5)-Q(4))*(TIME-3. )
      GO TO 10
   24 IF(K.GE.100)GO TO 25
      QSOLAR(K)=Q(5)
      GO TO 10
   25 IF(K.GE.120)GO TO 26
      QSOLAR(K)=Q(5)+(Q(4)-Q(5))*(TIME-5. )
      GO TO 10
   26 IF(K.GE.140)GO TO 27
      QSOLAR(K)=Q(4)+(Q(3)-Q(4))*(TIME-6. )
      GO TO 10
   27 IF(K.GE.160)GO TO 28
      QSOLAR(K)=Q(3)+(Q(2)-Q(3))*(TIME-7. )
      GO TO 10
   28 QSOLAR(K)=Q(2)+(Q(1)-Q(2))*(TIME-8. )
   10 QSOLAR(K)=QSOLAR(K)*COANGT
      RETURN
      END
      SUBROUTINE AMBT(TIME,I,AMT,TAMB)
C
C     THIS SUBROUTINE WAS DESIGNED TO CALCULATE THE AMBIENT TEMPERATURE AT
C     EACH TIME INTERVAL BY KNOWING THE HOURLY AMBIENT TEMPERATURES FROM
C     THE EXPERIMENTAL MEASUREMENT OF A CERTAIN DAY
C
      DIMENSION AMT(10),TAMB(182)
      IF (I.GE.20) GO TO 91
      TAMB(I)=AMT(1) + (AMT(2)-AMT(1))*TIME
      GO TO 90
   91 IF (I.GE.40) GO TO 92
      TAMB(I) = AMT(2) + (AMT(3)-AMT(2))*(TIME-1.0)
      GO TO 90
   92 IF (I.GE.60) GO TO 93
      TAMB(I)=AMT(3)+(AMT(4)-AMT(3))*(TIME-2.0)
      GO TO 90
   93 IF (I.GE.80) GO TO 94
      TAMB(I)=AMT(4)+(AMT(5)-AMT(4))*(TIME-3.0)
      GO TO 90
   94 IF (I.GE.100) GO TO 95
      TAMB(I)=AMT(5)+(AMT(6)-AMT(5))*(TIME-4.0)
      GO TO 90
   95 IF (I.GE.120) GO TO 96
      TAMB(I)=AMT(6)+(AMT(7)-AMT(6))*(TIME-5.0)
      GO TO 90
   96 IF (I.GE.140) GO TO 97
      TAMB(I)=AMT(7)+(AMT(8)-AMT(7))*(TIME-6.0 )
      GO TO 90
   97 IF (I.GE.160) GO TO 98
      TAMB(I)=AMT(8)+(AMT(9)-AMT(8))*(TIME-7.0)
      GO TO 90
```

```
   98 TAMB(1)=AMT(9)
   90 RETURN
      END
      SUBROUTINE CELTM (XIME,K,DELT,TOF)
C
C     THIS SUBROUTINE WAS DESIGNED TO CALCULATE THE CONTACT TEMPERATURE
C     DIFFERENCE AT EACH TIME INTERVAL BY KNOWING THE HOURLY CONTACT
C     TEMPERATURE DIFFERENCES FROM THE EXPERIMENTAL MEASUREMENT OF A CERTAIN DAY
C
      DIMENSION DELT(182),TOF(10),XIME(182)
      TIME=XIME(K)
      IF (K.GE.20) GO TO 31
      DELT(K)=TOF(1)+(TOF(2)-TOF(1))*TIME
      GO TO 30
   31 IF (K.GE.40) GO TO 32
      DELT(K)=TOF(2)+(TOF(3)-TOF(2))*(TIME-1.0)
      GO TO 30
   32 IF (K.GE.60) GO TO 33
      DELT(K)=TOF(3)+(TOF(4)-TOF(3))*(TIME-2.0)
      GO TO 30
   33 IF (K.GE.80) GO TO 34
      DELT(K)=TOF(4)+(TOF(5)-TOF(4))*(TIME-3.0)
      GO TO 30
   34 IF (K.GE.100) GO TO 35
      DELT(K)=TOF(5)+(TOF(6)-TOF(5))*(TIME-4.0)
      GO TO 30
   35 IF (K.GE.120) GO TO 36
      DELT(K)=TOF(6)+(TOF(7)-TOF(6))*(TIME-5.0)
      GO TO 30
   36 IF (K.GE.140) GO TO 37
      DELT(K)=TOF(7)+(TOF(8)-TOF(7))*(TIME-6.0)
      GO TO 30
   37 IF (K.GE.160) GO TO 38
      DELT(K)=TOF(8)+(TOF(9)-TOF(8))*(TIME-7.0)
      GO TO 30
   38 DELT(K)=TOF(9)+(TOF(10)-TOF(9))*(TIME-8.0)
   30 RETURN
      END
$EXEC
 31.5 35.6 49.1 52.7 53.6 55.4 48.2 43.7 39.8 32.0
    250.0      266.0      278.0      284.0      285.0
 72.5 79.7 82.4 88.0 90.5 89.6 88.7 88.7 86.0
 86.0 80.6 77.9 75.6 73.4 72.5 72.0 72.0 73.0
```

APPENDIX C

```
C
C     THIS PROGRAM IS DESIGNED TO STUDY THE THERMAL RESPONSES OF THE
C     CONCRETE BRIDGE DECK FOR 36 HOURS WITH DIFFERENT TOP SURFACE BOUNDARY
C     CONDITIONS AS: (1) BLACKENED TOP BRIDGE SURFACE WITHOUT GLASS COVER.
C     (2) BLACKENED TOP BRIDGE SURFACE WITH SINGLE GLASS COVER.
C     (3) BLACKENED TOP BRIDGE SURFACE WITH DOUBLE GLASS COVER.
C
C
C     VARIABLE AND CONSTANT NAMES FOR THE MAIN PROGRAM ARE.............
C
C     A1        -  ANGLE OF INCIDENCE (RADIAN)
C     A2        -  ANGLE OF REFRACTION (RADIAN)
C     ALPHA     -  ABSORPTANCE OF CONCRETE.
C     BHCV      -  CONVECTIVE HEAT TRANSFER COEFFICIENT OF BOTTOM SIDE OF THE
C                  BRIDGE. (BTU/HR/SQFT/DEG F)
C     CC        -  CONVERGENCE CRITERIA OF EXPLICIT FINITE DIFFERENCING.
C     D         -  DEGREES OF INCLINATION FROM THE HORIZONTAL SURFACE (DEGREE)
C     DEN       -  DENSITY OF CONCRETE (LBM/CUFT)
C     DL        -  THICKNESS OF BRIDGE DECK (FT)
C     DRFL      -  DIFFUSE REFLECTANCE
C     DT        -  TIME INCREMENT (HOUR)
C     DU        -  DUST FACTOR
C     DX        -  GRID SPACING IN X DIMENSION (FT)
C     E         -  EMITTANCE OF CONCRETE
C     EG        -  EMITTANCE OF GLASS
C     HC        -  SPECIFIC HEAT OF CONCRETE (BTU/LBM/DEG F)
C     HCV       -  CONVECTIVE HEAT TRANSFER COEFFICIENT AT THE TOP SURFACE OF
C                  BRIDGE (BTU/HR/SQFT/DEG F)
C     ID        -  IDENTIFICATION FOR DIFFERENT TOP SURFACE BOUNDARY CONDITIONS
C                  -1 INDICATES TOP SURFACE WITHOUT COVER
C                  0 INDICATES TOP SURFACE WITH SINGLE COVER
C                  1 INDICATES TOP SURFACE WITH DOUBLE COVERS
C     NG        -  NUMBER OF GLASS COVER
C     NT        -  NUMBER OF TIME INTERVALS
C     NX        -  NUMBER OF GRID SPACING
C     Q         -  PEAK SOLAR INSOLATION AT SOLAR NOON (BTU/SQFT/HR)
C     QC        -  HEAT TRANSFERRED BY CONVECTION (BTU/SQFT/HR)
C     QR        -  HEAT TRANSFERRED BY RADIATION (BTU/SQFT/HR)
C     QS        -  HEAT ABSORBED BY THE BRIDGE TOP SURFACE (BTU/SQFT/HR)
C     RFL       -  REFLECTANCE OF GLASS COVER OR COVERS
C     RFL1      -  REFLECTANCE OF THE FIRST COMPONENT OF POLARIZATION
C     RFL2      -  REFLECTANCE OF THE SECOND COMPONENT OF POLARIZATION
C     RN        -  REFRACTIVE INDEX OF THE GLASS
C     S         -  NET SOLAR FLUX ABSORBED BY THE TOP BRIDGE SURFACE (BTU/SQFT/HR)
C     SH        -  SHADE FACTOR
C     SIGM      -  STEFAN-BOLTZMANN CONSTANT (BTU/HR/SQFT/R4)
C     SIGM1     -  STEFAN-BOLTZMANN CONSTANT (W/M2/K4)
C     T         -  TEMPERATURES OF THE BRIDGE DECK (DEG F)
C     TA,TAMB   -  AMBIENT TEMPERATURE (DEG F)
C     TAO       -  TOTAL TRANSMITTANCE ALLOWING FOR BOTH REFLECTION AND ABSORPTION
C     TAOA      -  TRASMITTANCE CONSIDERING ONLY ABSORPTION
C     TAOR      -  TRANSMITTANCE CONSIDERING ONLY REFLECTION
C     TB        -  BOTTOM SURFACE TEMPERATURE OF BRIDGE DECK (DEG F)
C     TBC       -  TOP SURFACE TEMPERATURE OF BRIDGE DECK (DEG F)
C     TH        -  EFFECTIVE SKY TEMPERATURE (DEG R)
C     TI        -  INITIAL TEMPERATURES OF THE CONCRETE SLAB (DEG F)
C     TK        -  THERMAL CONDUCTIVITY OF CONCRETE (BTU/HR/FT/DEG F)
C     TPR       -  TOP SURFACE TEMPERATURE (DEG R)
C     TPR1      -  TOP SURFACE TEMPERATURE (DEG K)
C     TR        -  AMBIENT TEMPERATURE (DEG R)
C     TR1       -  AMBIENT TEMPERATURE (DEG K)
C     UL        -  OVERALL HEAT TRANSFER COEFFICIENT OF THE HORIZONTAL SURFACE
C                  (BTU/HR/SQFT/DEG F)
C     US        -  OVERALL HEAT TRANSFER COEFFICIENT AT 45 DEG SURFACE
C                  (BTU/HR/SQFT/DEG F)
C     V         -  WIND VELOCITY (M/SEC)
C     W         -  ANGULAR FREQUENCY OF SOLAR HEAT FLUX VARIATION FOR A
C                  TWELVE HOUR DAY (RADIAN/HR)
C
C*********************************************************************
C
      DIMENSION T(9,901),TAMB(900)
C
C     THERMAL PROPERTIES OF THE CONCRETE SLAB
C
      DATA DEN,HC,TK/145.,.22,1.0/
C
C     MODEL PARAMETERS
C
      DATA NX,DL,DT,TI,C,V/8,.667,.04,85,.310,3.353/
      ID=1
      PI=3.141592
      NT1=900
      W=PI/12.
      DX=DL/NX
```

```
      N1=NX+1
      DX2=DX*DX
C
CCC   CHECK FOR CONVERGENCE
C
      CC=(TK*DT)/(DEN*HC*DX2)
      IF (CC.GT.0.5) GO TO 44
C
CCC   SET ALL TEMPERATURES TO THE INITIAL VALUES
C
      DO 1 I=1,N1
    1 T(I,1)=TI
C
CCC   INITIALS
C
      S=0.
      TIME=0.
      THETA=0.
      TB=TI
      TBC=TI
      WRITE(6,100)DX
C
CCC   PRINT ONLY THE HOURLY VALUE
C
      IC=0
      L=25
      DO 55 I=1,NT1
    3 IF(IC.GE.L)GO TO 7
      IC=IC+1
      TIME=TIME+DT
      THETA=W*TIME
      THETA1=W*(TIME-3.)
      GO TO 42
    7 WRITE(6,101)TIME
      PRINT 15,THETA
      PRINT 20,S
      IF (ID.GT.-1) GO TO 5
      GO TO 4
    5 CONTINUE
      PRINT 13,TAC
      PRINT 16,UL
    4 WRITE(6,102)(T(J1,I),J1=1,N1)
      PRINT 12
      IC=0
      GO TO 3
C
CC CALCULATE AMBIENT TEMPERATURE
C
   42 TD=10.*SIN(THETA1)
      TA=TD+85.
      TAMB(I)=TA
      TR=TA+460.
      TPR=TBC+460.
C
CCC   CALCULATE THE TOP AND BOTTOM BRIDGE CONVECTIVE HEAT TRANSFER COEF
C
      HCV=(5.7+3.8*V)*0.1761
      BHCV=HCV/2.
      IF(ID)30,40,40
   30 CALL BNDRY1 (HCV,TBC,TA,TPR,Q,THETA,S)
      GO TO 50
   40 CALL BNDRY2 (HCV,TBC,TA,TPR,TR,Q,THETA,TIME,IC,W,S,UL,TAO)
   50 CONTINUE
      K=I+1
C
CCC   CALCULATION OF THE TOP SURFACE TEMPERATURE
C
      T(1,K)=TBC+2.*CC*(T(2,I)-TBC)+2.*DT*S/(DEN*HC*DX)
      TBC=T(1,K)
C
CCC   CALCULATION OF THE BOTTOM SURFACE TEMPERATURE
C
      T(N1,K)=TB+2.*CC*(T(NX,I)-TB)+(2.*BHCV*DT/(DEN*HC*DX))*(TA-TB)
      TB=T(N1,K)
C
CCC   CALCULATION OF TEMPERATURES AT DEPTHS
C
      DO 2 J=2,NX
    2 T(J,K)=T(J,I)+CC*(T(J-1,I)-2.*T(J,I)+T(J+1,I))
   55 CONTINUE
   44 CONTINUE
C ***************************************************************************
   12 FORMAT('0')
   13 FORMAT('-','TRANSMITTANCE OF GLASS COVERS =',F8.4)
   15 FORMAT('-','THETA=',F8.4)
   16 FORMAT('-','OVERALL COEF.=',F8.4)
   20 FORMAT('-','NET HEAT FLUX=',F10.3)
  100 FORMAT('-','INTERVAL WIDTH=',F8.4)
  101 FORMAT('-','TIME=',F8.3)
  102 FORMAT('-','TEMPERATURE AT GRID POINTS='/'-',12(2X,F6.2))
      STOP
      END
C ***************************************************************************
```

```
      SUBROUTINE BNDRY1(HCV,TBC,TA,TPR,Q,THETA,S)
C
C     THIS SUBROUTINE IS DESIGNED TO CALCULATE THE NET HEAT FLUX ABSORBED
C     BY THE TOP SURFACE WITHOUT GLASS COVER ON THE SURFACE
C
C
C     THERMAL RADIATION PROPERTIES
C
      DATA E,SIGM ,ALPHA/0.94,0.1714E-8,0.94/
      QC=HCV*(TBC-TA)
      TH=0.0411*(TA+460.)**1.5
      QR=E*SIGM*(TPR**4.-TH**4.)
      QS=ALPHA*Q* SIN(THETA)
      IF(QS)80,80,95
   80 QS=0.0
   95 CONTINUE
C
C     CALCULATE THE NET FLUX
C
      S=QS-QR-QC
      RETURN
      END
      SUBROUTINE BNDRY2 (HCV,TBC,TA,TPR,TR,Q,THETA,TIME,ID,W,S,UL,TAO)
C
C     THIS SUBROUTINE IS DESIGNED TO CALCULATE THE NET HEAT FLUX ABSORBED
C     BY THE TOP SURFACE WITH ONE AND TWO GLASS COVERS RESPECTIVELY
C     ON THE SURFACE
C
C
C     THERMAL RADIATION PROPERTIES
C
      DATA E,SIGM1,ALPHA/0.94,5.6697E-8,0.94/
      D=0.
      IF (ID.EQ.0) GO TO 81
      NG=2
      DRFL=0.24
      GO TO 82
   81 CONTINUE
      NG=1
      DRFL=0.16
   82 CONTINUE
      DU=0.02
      SH=0.03
      IF(SIN(THETA))31,31,25
   31 TAO=0.0
      GO TO 8
   25 A1=ABS(W*(6.-TIME))
      A2=ARSIN(SIN(A1)/1.526)
      IF(A1)6,9,6
C
C     CALCULATION OF THE POLARIZED REFLECTANCE COMPONENTS
C
    6 RFL1=((SIN(A2-A1))**2)/((SIN(A2+A1))**2)
      RFL2=((TAN(A2-A1))**2)/((TAN(A2+A1))**2)
      RFL=0.5*(RFL1+RFL2)
      GO TO 11
C
C     CALCULATION OF NORMAL REFLECTANCE
C
C
C     TAOR IS THE FRACTION ENTERING THE GLASS     TAOA IS THE ABSORBED FRACTION
C     ACCOUNT FOR THE RADIATION REFLECTED FROM THE UNDER SIDE OF THE GLASS
C
      TAOR=(1.-RFL)/(1.+(2.*NG-1.)*RFL)
      GO TO 10
    9 RFL=((RN-1.)/(RN+1.))**2
   11 TAOR1=(1.-RFL1)/(1.+(2.*NG-1.)*RFL1)
      TAOR2=(1.-RFL2)/(1.+(2.*NG-1.)*RFL2)
   10 CONTINUE
      TAOR=0.5*(TAOR1+TAOR2)
      TAOA=EXP(-NG*0.037/COS(A2))
      TAO=TAOR*TAOA
    8 CONTINUE
      TAOAPH=TAO*ALPHA/(1.-(1.-ALPHA)*DRFL)
      QS=Q*SIN(THETA)
C
C     EFFECT OF SHADING AND DUST
C
      QS=TAOAPH*QS*(1.-DU)*(1.-SH)
      EG=0.88
      HCV=HCV/(0.1761)
      TPR1=TPR/1.8
      TR1=TR/1.8
```

```
      SIGMA=5.6697E-8
      F=(1.-0.04*HCV+0.0005*HCV*HCV)*(1.+0.058*NG)
      US=(NG/((344./TPR1)*((TPR-TR)/(NG+F))**.31)+1./HCV)**(-1.)+SIGMA*(
     1TPR1+TR1)*(TPR1**2-TR1**2)/((E+0.0425*NG*(1.-E))**(-1.)+((2.*NG+F-
     21.)/EG)-NG)
C
C     CORRECTION FOR TILT OTHER THAN 45 DEGREES
C
      UL=US*(1.-(D-45.)*(0.00259-0.00144*E))
C
C   CONVERSION TO BRITISH UNITS
C
      UL=UL*.1761
      QL=UL*(TBC-TA)
C   ENSURE SOLAR FLUX IS NEVER LESS THAN ZERO
      IF(QS)60,60,65
   60 QS=0.0
   65 CONTINUE
C
C  CALCULATE THE NET FLUX
C
      S=QS-QL
      RETURN
      END
$EXEC
```